



Entergy Nuclear Northeast
Entergy Nuclear Operations, Inc.
James A. FitzPatrick NPP
P.O. Box 110
Lycoming, NY 13093
Tel 315-342-3840

Chris M. Adner
Licensing Manager - JAF

JAFP-13-0035
April 17, 2013

United States Nuclear Regulatory Commission
Attn: Document Control Desk
Washington, D.C. 20555

Subject: Response to Request for Additional Information Core for Plate Rim Hold Down Bolting, Plant Specific Analysis and Inspection Plan, License Renewal Commitment #23
James A. FitzPatrick Nuclear Power Plant
Docket No. 50-333
License No. DPR-59

- References:
1. Letter, Entergy to USNRC, "James A. FitzPatrick Nuclear Power Plant, License Renewal Application," JAFP-06-0109, dated July 31, 2006
 2. Letter, USNRC to Entergy, "Safety Evaluation Report Related to the License Renewal of James A. FitzPatrick Nuclear Power Plant," NUREG-1905, dated April, 2008
 3. Letter, Entergy to USNRC, "Deviation from BWRVIP-25 Inspection Requirements," JAFP-11-0043, dated March 30, 2011
 4. Letter, Entergy to USNRC, "Core Plate Rim Hold Down Bolting, Plant Specific Analysis and Inspection Plan, License Renewal Commitment #23," JAFP-12-0122, dated September 28, 2012

Dear Sir or Madam:

On July 31, 2006, Entergy Nuclear Operations, Inc. (ENO) submitted the License Renewal Application (LRA) for the James A. FitzPatrick Nuclear Power Plant (JAF) [Reference 1]. After subsequent requests for additional information (RAI) the Nuclear Regulatory Commission (NRC) issued a Safety Evaluation Report [Reference 2]. On March 30, 2011, JAF submitted a letter [Reference 3] for a deviation from BWRVIP-25 inspection requirements. On September 28, 2012, JAF submitted a response [Reference 4] to commitment #23 of Reference 2. On January 25 and February 14, 2013, JAF received a RAI from the NRC staff via email. A follow-up teleconference with the staff on February 19 clarified the RAI.

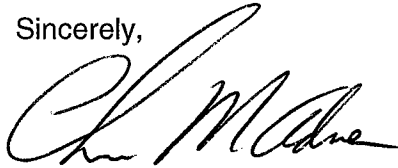
The Attachment in this letter provides a response to the RAI. Enclosure 1 contains the documents requested by the RAI. Enclosure 2 contains the proprietary version to Structural Integrity (SI) File No. 1101291.303 (JAF-CALC-12-00015) with Affidavit.

There are no new commitments made in this letter.

Enclosure 2 to this letter contains Proprietary Information that should be withheld from public disclosure per 10 CFR 2.390. When separated from Enclosure 2 there are no withholding criteria.

Questions concerning this submittal may be addressed to Mr. Mark Dooley, Programs & Components Engineering Manager, at 315-349-6529.

Sincerely,



Chris M. Adner
Licensing Manager - JAF

CA/mh

Attachment: Responses to Request for Additional Information Questions
Enclosure: 1) Documents Requested by the Request for Additional Information
2) SI File No. 1101291.303 (JAF-CALC-12-00015) (Proprietary \w Affidavit)

cc:

Regional Administrator, Region I
U. S. Nuclear Regulatory Commission
2100 Renaissance Boulevard, Suite 100
King of Prussia, PA 19406-2713

Resident Inspector's Office
U.S. Nuclear Regulatory Commission
James A. FitzPatrick Nuclear Power Plant
P.O. Box 136
Lycoming, NY 13093

Mr. Mohan Thadani, Senior Project Manager
Plant Licensing Branch I-1
Division of Operating Reactor Licensing
Office of Nuclear Reactor Regulation
U.S. Nuclear Regulatory Commission
Washington, DC 20555-0001

Ms. Bridget Frymire
New York State Department of Public Service
3 Empire State Plaza, 10th Floor
Albany, NY 12223

Mr. Francis J. Murray Jr., President
New York State Energy and Research Development Authority
17 Columbia Circle
Albany, NY 12203-6399

Enclosure 2 to this letter contains Proprietary Information that should be withheld from public disclosure per 10 CFR 2.390. When separated from Enclosure 2 there are no withholding criteria.

JAFP-13-0035

Attachment

Responses to Request for Additional Information Questions

(2 Pages)

Responses to Request for Additional Information Questions

Request for Additional Information (RAI) No. 1

BWRVIP-25, in the discussion of visual examination (VT) as an inspection option in Section 3.2.2.2, states:

The critical number of bolts is plant-specific (dependent on plant geometry, number of bolts, and location of bolts intact, and loading conditions). The conservative example of the analysis in Appendix A shows that about 80% of the bolts at the allowable stress would react with the applied load. A distributed inspection sample of 50% of the bolts, with none cracked, assures the integrity of 80% of the bolts with very high confidence. Therefore, inspection of 50% of the bolts is recommended. If cracking is detected in any of these first 50%, the remaining 50% should be inspected.

Based on the above, the NRC staff requests the following information:

Considering the effectiveness of the VT-3 examination at detecting cracked or broken bolts, does the percentage of the bolts previously sampled at JAF support demonstration that the required number of bolts is intact, assuming no failed bolts are found in the sample? Provide a statistical argument or analysis similar to that provided in BWRVIP-25, Section 3.2.2.2. Include the details of the statistical calculation.

JAF Response to RAI No. 1

BWRVIP-25 in Section 3.2.2.2 states, “once the first VT inspection is completed, a reinspection schedule should be developed, based on plant-specific analyses which consider plant geometry, number of bolts, loading conditions, and inspection experience. Note that good inspection results combined with the good operating experience of BWR bolts and the degree of redundancy of the hold down bolts may justify elimination of any reinspection.”

JAF has a total of 72 core plate hold down bolts. JAF has performed multiple inspections of these bolts as documented in SEP-RVI-004, JAF Reactor Vessel Internals (RVI) Inspection Program Plan, Rev. 1 and JAF-RPT-13-00002, James A. FitzPatrick NPP RFO-20 In vessel Visual Inspection (IVVI) Final Report, Rev 0. These inspections are summarized below:

Year	Refuel Outage	Number of Bolts Inspected	Inspection Method	Results
1994/1995	RO11	20	VT-1	No relevant indications noted
1998	RO13	72	VT-3	No relevant indications noted
2008	RO18	33	VT-1	No relevant indications noted
2012	RO20	10	VT-1	No relevant indications noted

BWRVIP-25 recommends inspection of 50% of the hold down bolts. JAF performed a baseline inspection of 100% of the core plate bolts in 1998 and found no relevant indications. Since 100% of the core plate bolts at JAF were inspected, no statistical evaluation is required to validate the “very high confidence level” associated with the BWRVIP-25 recommendation for inspection of 50% of the bolts. Subsequent to this baseline inspection, Entergy performed two additional inspections of the core plate bolting. Both subsequent examinations showed no signs of degradation.

BWRVIP-25 states that once the first VT inspection is completed, a reinspection schedule should be developed, based on plant-specific analyses which consider plant geometry, number of bolts, loading conditions, and inspection experience.

JAF has performed a plant specific evaluation that includes consideration of known degradation mechanisms, relaxation of bolt preload over a 60 year operating life, flaw tolerance of the hold down bolts, and the minimum number of bolts required to prevent horizontal displacement. Based on this evaluation, the results of the four previous hold down bolt inspections, and satisfactory operating experience at operating BWR plants, JAF concludes that no further inspection of the bolts is required during the period of extended operation. Per the teleconference discussions with the NRC on February 19, 2013, in lieu of a statistical argument or analysis, the Technical Basis for this conclusion is developed in references 3, 4, 5, 6, and 7 of JAF-RPT-12-00009 Rev. 0. Copies of these documents are provided in the Enclosure to this letter.

RAI No. 2

Sections 2.1 and 2.2 of the submittal document the conclusions of evaluations performed in order to determine the susceptibility of the JAF core bolts to degradation mechanisms and the relaxation of core bolt preload over 60 years of operation.

These sections heavily reference calculations performed by Structural Integrity Associates (SIA) and Transware to substantiate the conclusions and information presented in these sections.

As critical information required to review the submittal is only referenced in the submittal, and is contained in the references supplied there, the staff requests that references 3, 4, and 15 of JAF-RPT-12-00009 Rev. 0, "Proposed Core Bolt Inspection Protocol and Technical Basis," be provided in their entirety.

JAF Response to RAI No. 2

References 3, 4, and 15 documents requested are contained in the Enclosure to this letter.

RAI No. 3

Section 2.3 of the submittal documents a core plate bolt fracture mechanics evaluation performed in support of the submittal. This section heavily references calculations and details contained in Reference 5 of the submittal. As critical information required to review the submittal is only referenced in the submittal, and is contained in the reference supplied there, the staff requests that reference 5 of JAF-RPT-12-00009 Rev. 0, "Proposed Core Bolt Inspection Protocol and Technical Basis," be provided in its entirety

JAF Response to RAI No. 3

Reference 5 document request is contained in the Enclosure to this letter.

In addition, based on the phone conversation with the NRC on February 19, 2013, JAF is also providing References 6, 7, and 24 of JAF-RPT-12-00009 Rev 0 in the Enclosure to this letter.

JAFP-13-0035

Enclosure 1

**Documents Requested by the
Request for Additional Information**

Table of Contents

JAF-RPT-12-00009 Reference table	Vendor Document ID	JAF Document ID	Description
3	1101291.301	JAF-CALC-12-00013	Core Plate Bolt Degradation Susceptibility Evaluation.
4	1101291.302	JAF-CALC-12-00014	Core Plate Bolt Preload Relaxation.
5	1101291.303	JAF-CALC-12-00015	Core Plate Bolt Fracture Mechanics Evaluation (non-proprietary w/ affidavit)
6	1101291.304	JAF-CALC-12-00016	Minimum Required Number of Core Plate Bolts
7	1101291.305	JAF-CALC-12-00017	Minimum Required Number of Core Plate Bolts – Consideration of Aligner Brackets.
24	1101291.306	JAF-CALC-12-00018	Recommendations for a Core Plate Bolt Inspection Protocol
15	ENT-JAF-001-R-001	JAF-RPT-12-00006	James A. Fitzpatrick Core Support Plate Rim Bolt Fluence Evaluation at End of Cycle 20, 32 EFPY and 54 EFPY

<input type="checkbox"/> ANO-1	<input type="checkbox"/> ANO-2	<input type="checkbox"/> GGNS	<input type="checkbox"/> IP-2	<input type="checkbox"/> IP-3	<input type="checkbox"/> PLP
<input checked="" type="checkbox"/> JAF	<input type="checkbox"/> PNPS	<input type="checkbox"/> RBS	<input type="checkbox"/> VY	<input type="checkbox"/> W3	
<input type="checkbox"/> NP-GGNS-3	<input type="checkbox"/> NP-RBS-3				
CALCULATION COVER PAGE		⁽¹⁾ EC # 36003		⁽²⁾ Page 1 of <u>18</u>	
⁽³⁾ Design Basis Calc. <input checked="" type="checkbox"/> YES <input type="checkbox"/> NO			⁽⁴⁾ <input checked="" type="checkbox"/> CALCULATION <input type="checkbox"/> EC Markup		
⁽⁵⁾ Calculation No: JAF-CALC-12-00013				⁽⁶⁾ Revision: 0	
⁽⁷⁾ Title: Core Plate Bolt Degradation Susceptibility Evaluation (SIA File No. 1101291.301 Rev 0)				⁽⁸⁾ Editorial <input type="checkbox"/> YES <input checked="" type="checkbox"/> NO	
⁽⁹⁾ System(s): 02-1 Reactor Vessel		⁽¹⁰⁾ Review Org (Department): DE - Civil			
⁽¹¹⁾ Safety Class: <input checked="" type="checkbox"/> Safety / Quality Related <input type="checkbox"/> Augmented Quality Program <input type="checkbox"/> Non-Safety Related		⁽¹²⁾ Component/Equipment/Structure Type/Number:			
		02V-1			
⁽¹³⁾ Document Type: DCAL					
⁽¹⁴⁾ Keywords (Description/Topical Codes): Core Plate Bolt					
REVIEWS					
⁽¹⁵⁾ Name/Signature/Date <u>Structural Integrity Associates</u> Responsible Engineer		⁽¹⁶⁾ Name/Signature/Date <u>R. Casella / R Casella 9/10/12</u> <input type="checkbox"/> Design Verifier <input checked="" type="checkbox"/> Reviewer <input type="checkbox"/> Comments Attached		⁽¹⁷⁾ Name/Signature/Date <u>G. Foster SEE AS</u> <u>EC 36003</u> Supervisor/Approval <input type="checkbox"/> Comments Attached	

CALCULATION REFERENCE SHEET	CALCULATION NO: <u>JAF-CALC-12-00013</u> REVISION: <u>0</u>																																										
I. EC Markups Incorporated (N/A to NP calculations) N/A 1. 2. 3. 4. 5.																																											
II. Relationships:	<table border="1" style="width: 100%; border-collapse: collapse; text-align: center;"> <thead> <tr> <th style="width: 30%;"></th> <th style="width: 8%;">Sht</th> <th style="width: 8%;">Rev</th> <th style="width: 12%;">Input Doc</th> <th style="width: 12%;">Output Doc</th> <th style="width: 12%;">Impact Y/N</th> <th style="width: 18%;">Tracking No.</th> </tr> </thead> <tbody> <tr> <td>1.</td> <td></td> <td></td> <td><input type="checkbox"/></td> <td><input type="checkbox"/></td> <td></td> <td></td> </tr> <tr> <td>2.</td> <td></td> <td></td> <td><input type="checkbox"/></td> <td><input type="checkbox"/></td> <td></td> <td></td> </tr> <tr> <td>3.</td> <td></td> <td></td> <td><input type="checkbox"/></td> <td><input type="checkbox"/></td> <td></td> <td></td> </tr> <tr> <td>4.</td> <td></td> <td></td> <td><input type="checkbox"/></td> <td><input type="checkbox"/></td> <td></td> <td></td> </tr> <tr> <td>5.</td> <td></td> <td></td> <td><input type="checkbox"/></td> <td><input type="checkbox"/></td> <td></td> <td></td> </tr> </tbody> </table>		Sht	Rev	Input Doc	Output Doc	Impact Y/N	Tracking No.	1.			<input type="checkbox"/>	<input type="checkbox"/>			2.			<input type="checkbox"/>	<input type="checkbox"/>			3.			<input type="checkbox"/>	<input type="checkbox"/>			4.			<input type="checkbox"/>	<input type="checkbox"/>			5.			<input type="checkbox"/>	<input type="checkbox"/>		
	Sht	Rev	Input Doc	Output Doc	Impact Y/N	Tracking No.																																					
1.			<input type="checkbox"/>	<input type="checkbox"/>																																							
2.			<input type="checkbox"/>	<input type="checkbox"/>																																							
3.			<input type="checkbox"/>	<input type="checkbox"/>																																							
4.			<input type="checkbox"/>	<input type="checkbox"/>																																							
5.			<input type="checkbox"/>	<input type="checkbox"/>																																							
III. CROSS REFERENCES: See body of calculation. 1. 2. 3. 4. 5.																																											
IV. SOFTWARE USED: Title: <u>None</u> Version/Release: _____ Disk/CD No. _____																																											
V. DISK/CDS INCLUDED: Title: <u>N/A</u> Version/Release _____ Disk/CD No. _____																																											
VI. OTHER CHANGES: None																																											

Revision	Record of Revision
0	Initial issue.



Structural Integrity Associates, Inc.®

CALCULATION PACKAGE

File No.: 1101291.301

Project No.: 1101291

Quality Program: Nuclear Commercial

PROJECT NAME:

JAF Core Plate Bolt Evaluation

CONTRACT NO.:

10340564

CLIENT:

Entergy Nuclear

PLANT:

James A. Fitzpatrick Nuclear Plant

CALCULATION TITLE:

Core Plate Bolt Degradation Susceptibility Evaluation

NOTE: This document references vendor proprietary information. Such information is identified with -2xxP SI Project File numbers in the list of references. Any such references and the associated information in this document where those references are used are identified so that this information can be treated in accordance with applicable vendor proprietary agreements.



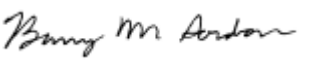

Document Revision	Affected Pages	Revision Description	Project Manager Approval Signature & Date	Preparer(s) & Checker(s) Signatures & Date
0	1 - 15	Initial Issue	 D. V. Sommerville 7/15/2012	<p><u>Responsible Engineers</u></p>  C. Oberembt 7/15/2012  B. Gordon 7/15/2012 <p><u>Responsible Verifier</u></p>  T. Giannuzzi 7/15/2012

Table of Contents

1.0	INTRODUCTION	3
2.0	TECHNICAL APPROACH	3
	2.1.1 <i>Method for IGSCC Susceptibility Evaluation</i>	3
	2.1.2 <i>Method for IASCC Susceptibility Evaluation</i>	4
	2.1.3 <i>Method for Fatigue Susceptibility Evaluation</i>	4
3.0	DESIGN INPUTS.....	5
4.0	ASSUMPTIONS.....	9
5.0	SUSCEPTIBILITY EVALUATION.....	9
	5.1 IGSCC Susceptibility.....	9
	5.2 IASCC Susceptibility.....	11
	5.3 Fatigue Crack Initiation and Propagation Susceptibility	12
	5.4 Operating Experience	13
6.0	CONCLUSIONS	13
7.0	REFERENCES	14

List of Tables

Table 3-1:	Material Properties	6
Table 3-2:	JAF Historical Water Chemistry.....	7
Table 5-1:	JAF Core Plate Bolt Inspection Summary	13

1.0 INTRODUCTION

The James A. Fitzpatrick (JAF) nuclear power plant license renewal commitment number 23 [1, Attachment 1] states that Entergy will either install core plate wedges at JAF prior to the period of extended operation or complete a plant specific analysis to develop and justify a core plate bolt inspection plan. The inspection plan must include acceptance criteria that meet the requirements of BWRVIP-25 [2].

An evaluation of the susceptibility of the JAF core plate bolts to the degradation mechanisms known to affect Boiling Water Reactor (BWR) internals is needed to support the development of an inspection protocol. This document contains an evaluation to assess the relative degree to which the JAF core plate bolts are susceptible to intergranular stress corrosion cracking (IGSCC), irradiation assisted stress corrosion cracking (IASCC), and fatigue from both system cycling and flow induced vibration (FIV).

2.0 TECHNICAL APPROACH

This section of the calculation package contains a description of the technical approach used for the susceptibility evaluations. Known degradation mechanisms affecting BWR internals include:

- IGSCC
- IASCC
- Thermal fatigue (system cycling)
- Flow induced vibration fatigue

Although these mechanisms were considered during preparation of BWRVIP-25 [2], for completeness, each of these degradation mechanisms will be addressed in this document as well. A literature review was conducted to identify relevant data, both recent and historical, regarding the susceptibility of Type 304 stainless steel (SS) bolts to IGSCC and IASCC. Additionally, a review of relevant operating experience was conducted to ensure that the fleet operating experience was appropriately considered in the evaluation. Susceptibility to thermal and FIV fatigue was assessed by review of the plant design documentation and startup test vibration report, as discussed below.

2.1.1 Method for IGSCC Susceptibility Evaluation

As stated in BWRVIP-25 [2] and Reference [3], the occurrence of IGSCC is dependent on the simultaneous presence of an aggressive environment, a susceptible material, and a tensile stress. Each of these necessary components for IGSCC is addressed in this evaluation by specific consideration of the following factors:

- Environment
 - The JAF plant specific water chemistry history was evaluated to assess the environmental conditions in the vicinity of the core plate bolts.
 - The effects of the expected crevice conditions at the thread roots and at the thread to nut interfaces were considered.



- The effect of the protective coating provided by the anti-seize lubricant applied during initial assembly was evaluated.
- Material
 - The material type and bolt manufacturing process were reviewed with a focus on the issues of material susceptibility, fabrication induced sensitization and fabrication induced cold work.
- Stress
 - The design function of the core plate bolts requires that they be subject to a tensile stress; this stress level is evaluated further in Section 5.1 of this calculation.

2.1.2 Method for IASCC Susceptibility Evaluation

The susceptibility of the core plate bolts to IASCC is dependent on the cumulative neutron fluence received by the bolt material, the local environment, including radiolysis effects on the environment, and the presence of a tensile stress. An important note regarding IASCC is that a material is initially non-susceptible then becomes susceptible over time due to the effects of accumulated neutron fluence. The effect of a “threshold” neutron fluence (i.e. the fluence below which IASCC initiation would not be expected to occur,) and a comparison to the predicted neutron fluence at the bolt locations is evaluated herein.

2.1.3 Method for Fatigue Susceptibility Evaluation

The significance of system cycling on the potential for corrosion fatigue crack initiation and propagation in the core plate bolting is assessed by review of:

- The design transients defined on the Reactor Pressure Vessel (RPV) thermal cycle diagram (TCD) [4],
- The reported fatigue results for reactor internals documented in the plant Updated Final Safety Analysis Report (UFSAR) [5].

The significance of FIV on the potential for fatigue crack initiation and propagation or fretting of the core plate bolting is assessed by review of:

- Available vibration data from the startup vibration test report [6] and the UFSAR [5].
- Industry Inspection and Evaluation guidelines [2],
- Relevant operating experience.

3.0 DESIGN INPUTS

The design inputs used in the susceptibility evaluation are discussed in this section.

The core plate bolt material, geometry, preload, and thread lubricant inputs are listed below:

- Bolt material: Type 304 stainless steel in accordance with ASTM A-193, Grade B-8 [6, 7]
- Bolt nominal diameter: 1.125 inches [6, 8]
- Bolt tensile area: 0.856 in² [9]
- Bolt thread form: 1 1/8-12UNF-2A [6, 8]
- Bolt length (between nuts): 21.813 inches (minimum) [8]
- Preload torque: 330 ± 25 ft-lbs [6]
- Thread lubricant: D50YP5B [10]
- Torque Coefficient (nut factor): 0.18 [12]

The lubricant D50YP5B corresponds to “Thread Lubricant FELPRO N5000” [11, Appendix F]. FELPRO N5000 is currently manufactured by Henkel Corporation under the name Loctite N-5000, and is a high purity (e.g. lowest practical levels of halogens, sulfur, chlorides and heavy metals) nickel based anti-seize lubricant [12].

The torque coefficient or nut factor for Loctite N-5000 used with Type 304 SS bolts was experimentally determined to be 0.18 [12].

The temperatures and pressures in different regions of the JAF RPV are taken from the RPV TCD [4]. The core plate is located below the core, which corresponds to either the bottom of Region B or the top of Region C [4]. Both regions are considered and the bounding service conditions are summarized as follows:

- RPV normal operating pressure: 1040 psig [4]
- Regions B and C normal operating temperature: 527°F [4]
- Region B maximum temperature: 551°F [4]

Material properties for Type 304 SS are taken from the ASME Boiler & Pressure Vessel Code [13] and are listed in Table 3-1 below.

Table 3-1: Material Properties

Material Property	Temperature	
	70°F	550°F
Allowable Stress, S_m (ksi)	20	16
Yield Strength, S_y (ksi)	30	17.75
Young's Modulus, E (ksi)	27400	25700

Bounding fluence values, $E > 1$ MeV, for the core support plate are taken from Reference [14] at 27.7 Effective Full Power Years (EFPY) (end of operating cycle 20), 32 EFPY and at 54 EFPY, and are listed below:

- 27.7 EFPY: 1.25×10^{20} n/cm²
- 32 EFPY: 1.36×10^{20} n/cm²
- 54 EFPY: 1.93×10^{20} n/cm²

These bounding fluence values are representative of the location of the core plate bolts as discussed in Reference [14].

Water chemistry inputs are taken from References [6, 15, and 16]. Estimated average reactor water conductivity and the electrochemical corrosion potential (ECP) for stainless steel core plate bolts, referenced to a standard hydrogen electrode (SHE), are summarized for each year of operation in Table 3-2 below.

Table 3-2: JAF Historical Water Chemistry

Year	Est. Avg. Rx Water Conductivity, ($\mu\text{S}/\text{cm}$)	ECP at Core Plate Bolts (mV[SHE])
1975	1.315	+200
1976	0.485	+200
1977	0.998	+200
1978	0.793	+200
1979	1.103	+200
1980	2.053	+200
1981	0.796	+200
1982	0.507	+200
1983	0.540	+200
1984	0.230	+200
1985	0.389	+200
1986	0.115	+200
1987	0.342	+200
1988	0.427	+200
1989	0.125, HWC-L ¹ , Jan. 1989, 0.3 ppm	+200
1990	0.255, HWC increased to 0.35 ppm	+200
1991	0.171	+200
1992	S/D	+200
1993	0.100	+200
1994	0.095	+200
1995	0.074, HWC increased to 0.5 ppm	-50 to -100
1996	0.071	-50 to -100

Table 3-2: JAF Historical Water Chemistry (continued)

Year	Est. Avg. Rx Water Conductivity, ($\mu\text{S}/\text{cm}$)	ECP at Core Plate Bolts (mV[SHE])
1997	0.066	-50 to -100
1998	0.067	-50 to -100
1999	0.085, NMCA ² , Nov. 1999, HWC down to 0.2 ppm	Jan. - Nov. +200 Nov. - Dec. < -230
2000	0.095, HWC increased to 0.25 ppm	< -230
2001	0.069	< -230
2002	0.09	< -400
2003	0.09	< -400
2004	0.1 (NMCA reapplication Sept. 2004)	< -400
2005	0.10	< -400
2006	0.11	< -400
2007	0.11	< -400
2008	0.14 (chronic condenser in-leakage)	< -400
2009	0.17 (chronic condenser in-leakage)	< -400
2010	0.15 (chronic condenser in-leakage)	< -400
2011	0.11 (OLNC Aug. 2011)	< -400
2012	TBD (OLNC reapplication April 2012)	
2012 - 2035 ⁴	< 0.1	< -400

¹ low hydrogen water chemistry (HWC)

² noble metals chemical addition (NMCA)

³ on-line noble chemistry (OLNC)

⁴ The water chemistry values for 2012 – 2035 are assumed as described in Section 4.0, Assumption 3.



4.0 ASSUMPTIONS

The following assumptions are used in this evaluation:

1. The JAF core plate bolt threads are assumed to be machined (i.e. cut) onto the stud. This is a reasonable assumption based on the manufacturing information contained in Reference [8] that states that at least 180° of the imperfect thread form be removed and that the surface is to be honed. Cutting would most likely leave an imperfect thread form and would result in greater surface roughness compared to rolling. Additionally, this assumption is considered conservative because machined threads are expected to provide a greater stress concentration at the thread root compared to rolled threads [17, pg. 51-12].
2. Bolt tensile area is assumed constant. There will be some reduction in area based on the Poisson effect when loading the core plate bolts; however, this reduction in area is assumed negligible. This assumption is justified because the Poisson ratio for stainless steels is approximately 0.30 [17, pg. 46-4] and the axial elongation due to strain is small. The reduction in diameter will be very small.
3. The water chemistry values for 2012 through 2035 (end of period of extended operation) are assumed based on input provided by JAF in Reference [16], and are considered reasonable based on the water chemistry history from 2002 through 2011.

5.0 SUSCEPTIBILITY EVALUATION

The degree of susceptibility of the core plate bolts to the identified material degradation mechanisms (IGSCC, IASCC and fatigue) is discussed in this section.

5.1 IGSCC Susceptibility

Type 304 SS can be susceptible to IGSCC in the light water reactor (LWR) environment [2]. Austenitic stainless steels, of which Type 304 SS is an example, are resistant to general corrosion due to the relatively high level of chromium (~18 wt.%) that forms a passive oxide layer at the surface [18, pg. 6-29]. However, passive alloys like stainless steel are susceptible to localized forms of corrosion such as pitting corrosion and stress corrosion cracking. Austenitic stainless steels, such as Type 304 SS, can become susceptible to IGSCC due to sensitization caused by depletion of chromium adjacent to grain boundaries through the formation of chromium carbides when subjected to a sensitizing heat treatment between approximately 900°F and 1500°F [3], or through welding. The effects of cold work (e.g. machining, rolling, grinding, cutting, etc.) can significantly increase the IGSCC susceptibility of Type 304 SS by itself or by enhancing the kinetics of the sensitization reactions [3, 19].

The core plate bolts were fabricated from solution heat treated descaled Type 304 SS [7]. Therefore, the material is not considered to be thermally sensitized. The threads are conservatively assumed to be machined, as described in Assumption 1. The machining process will impart some level of cold work; however, the purchase specification [7] requires that any components that receive cold work, other than specified pipe bending operations, be solution annealed after cold working. The honing process described in Reference [8] would provide a smooth matte finish with little additional cold work.

The core plate bolts are subject to tensile stress due to preload and potential applied loads from the core plate. The preload can be calculated using the following equation [17, pg. 51-12]:

$$T = K \cdot D \cdot F \quad (1)$$

Where: T = Installation torque, ft-lbs
 K = Torque coefficient
 D = Bolt diameter, ft
 F = Tensile force, lbs

Rearranging Eq. (1) to solve for F and using the inputs from Section 3.0 (T=330 ft-lbs, K=0.18, and D=1.125 inches) results in a tensile force of 19,556 lbf. The effective bolt stress is calculated based on the following equation [17]:

$$\sigma = F / A \quad (2)$$

Where: σ = Bolt stress, psi
 A = Tensile stress area, in²

The calculated bolt stress $\sigma = 19,556 / 0.856 = 22,845$ psi. This represents the tensile stress in the bolt due to preload. The stress concentration effect at the root of the threads could result in near yield stresses at these locations at ambient temperature. The calculated bolt stress is presented here since the presence of a tensile stress is a prerequisite for IGSCC. It should be noted that the effect of increased temperature during operation may result in permanent deformation due to yielding. It is also recognized that relaxation of the bolt preload may occur over time due to thermal relaxation, creep and radiation relaxation. The effects of temperature and preload relaxation will be evaluated in a subsequent calculation.

The JAF water chemistry environment can be evaluated based on historical water chemistry data. The ECP of stainless steel at the core plate bolt location and reactor water conductivity are of particular interest. Literature supports an IGSCC initiation “threshold” ECP, in the BWR environment, of -230 mV[SHE] in high purity water (i.e. < 0.15 μ S/cm) [3]. While, values of ECP below this threshold are representative of environments which are unlikely to support IGSCC initiation, crack growth can still occur below -230 mV[SHE]. A summary of the historical water chemistry for JAF is shown in Table 3-2..

The nature of threaded fasteners provides a possible crevice condition that will locally produce more aggressive water chemistry due to the effects of the ECP difference between the exterior of the crevice and the interior of the crevice [20]. However, HWC, which is effective at this location, will greatly reduce this corrosion potential difference driven effect.

An anti-seize lubricant was used during the installation of the core plate bolts. Anti-seize lubricants are used to provide a barrier between the contacting metal surfaces of fasteners and also the environment. Protecting the metal surfaces from the environment is intended to prevent corrosion and subsequently prevent seizing of the contacting surfaces. The manufacturer of Loctite N-5000 provides information



that suggests this particular anti-seize prevents SCC during service [12]. Additional bases for this claim could not be found in literature, and there are no known studies relating to the stability of anti-seize lubricants in LWR environments. However, the presence of a high purity anti-seize could provide some benefit against IGSCC if it acts as a barrier separating the stainless steel from the environment. The lubricant would be expected to be more likely to remain effective early in life, which is also the time that the environment, based on water chemistry, was most aggressive. With time, the lubricant effectiveness is potentially deteriorating, but the water chemistry has improved significantly.

The Type 304 SS bolts are not sensitized, but may have some amount of cold work do to thread cutting. The effects of cold working are expected to be relieved due to the required solution annealing following cold working. Honing of the nut and bolt mating surfaces to a matte finish reduces surface roughness that may help to improve IGSCC resistance by removing fine grooves (micro-crevices) from the surface, but is a small source of cold work. Significant tensile stresses (greater than 50% yield strength) are present in the core plate bolts due to design preload and the geometric stress concentration contributed by the thread form. Prior to November of 1999 the ECP values at the core plate bolts were greater than -230 mV[SHE]. Since November of 1999, the ECP values have been significantly less than -230 mV[SHE]. The presence of an anti-seize lubricant in the bolt threads may provide some additional protection from the LWR environment.

The core plate bolts may be susceptible to IGSCC due to possible cold work, the presence of a significant tensile stress, and an environment, early in plant operation, that would be more supportive of IGSCC. However, the probability of cracking is considered low since the material is not thermally sensitized since it was purchased to a specification requiring solution annealing following cold work, has a smooth surface finish, the environment has been mitigated, and a protective barrier may exist due to the presence of an anti-seize lubricant.

5.2 IASCC Susceptibility

Austenitic stainless steels are susceptible to IASCC in the LWR environment [20, 21 and 22]. As discussed in Reference [21] and summarized here:

IASCC can be categorized into radiation effects on the water chemistry (radiolysis) and on the material properties. The cracking response to changes in water chemistry is similar for both irradiated and un-irradiated materials. In both cases, there is a steep increase in IASCC kinetics with a rise in the ECP above approximately 100 mV[SHE]. At high ECP, the crack growth rate also increases sharply as impurities (especially chloride and sulfate) are added to pure water in either the irradiated or un-irradiated cases. In post-irradiation tests, the dominant radiation-related factors are microstructural and micro-chemical changes, which can be responsible for “threshold-like” behavior in much the same way as ECP, impurities, degree of sensitization, stress, temperature, etc. Other radiation phenomena, like radiation creep relaxation and differential swelling, could also have “persistent” effects. The effects of radiation rapidly (in seconds) achieve a dynamic equilibrium in water, primarily because of the high mobility of species in water. In metals, dynamic equilibrium is achieved – if ever – only after many displacements per atom (dpa), typically requiring years of exposure. While both radiation induced segregation (RIS) and radiation hardening (and the associated microstructural development) asymptotically approach a dynamic equilibrium, other factors (e.g., RIS of Si, or precipitate formation or dissolution) may become important. Yet data on



post-irradiation slow strain rate tests (SSRT) on stainless steels show that there is a distinct (although not invariant) “threshold” fluence at which IASCC is observed under LWR conditions. Because this “threshold” occurs at a fraction to several dpa depending on the stress, water chemistry, etc., in-situ effects (ECP, conductivity, temperature) may be important, but only “persistent” radiation effects (microstructural and micro-chemical changes) can be responsible for the “threshold-like” behavior vs. fluence in post-irradiation tests.

The Reference [21] test results suggest that a “threshold” fluence of 5×10^{20} n/cm² and 2×10^{21} n/cm² for “highly” and “lower” stressed components in the BWR NWC environments, respectively. For components exposed to HWC characterized by a lower ECP, the “threshold” fluence may be approximately 3×10^{21} n/cm² [21]. The core plate bolts can be considered a highly stressed component for this evaluation. During the first 14 years of operation, JAF operated at NWC conditions; therefore, the corresponding fluence “threshold” value is 5×10^{20} n/cm². This value for fluence “threshold” is also supported by and consistent with References [20, 22]. The bounding fluence values from Reference [14] indicate that the fluence “threshold” will not be exceeded prior to 54 EFPY. Additionally, after the introduction of HWC in 1989, the fluence “threshold” value may be much higher due to the associated reduction in SS ECP.

The JAF core support bolts are not considered to be susceptible to IASCC.

5.3 Fatigue Crack Initiation and Propagation Susceptibility

To be thorough, susceptibility of the core plate bolts to fatigue caused by system thermal transients and FIV should be considered. Additionally, since the core plate bolts reside in an aqueous environment, environmentally-assisted fatigue (EAF) should be considered. From the RPV TCD [4], there are few thermal transients that would be expected to affect the core plate bolts based on the cycle definitions given for Regions B and C. The startup and shutdown events occur under quasi-uniform heating and cooling, since the heat-up and cool-down rates are 100 °F/hr or less, and would not be expected to contribute to fatigue of the bolting. The improper start of cold recirc loop event would not affect the core plate bolt location, because reverse flow through the recirculation outlet nozzle would occur outside of the shroud. The loss of feedwater pumps event and the sudden start of pump in cold recirc loop event could possibly induce thermal transients on the core plate bolts, but the effect is expected to be small due to the limited numbers of defined cycles.

FIV was not identified as an issue for the core plate bolts in the JAF Updated Final Safety Analysis Report (UFSAR) [5, Section 3.3.6] or in the startup vibration test report [6]. Additionally, fatigue is not identified in BWRVIP-25 [2] as a degradation mechanism of concern for the core plate bolts. As long as the bolted joint has sufficient preload to resist the normal operating ΔP across the core plate then there will be no leakage flow passing through the bolt hole which could cause FIV and consequent fretting wear or fatigue accumulation. This will be demonstrated in the subsequent calculations that quantify residual preload and sum the applied loads.

Due to the low probability of significant fatigue loading/cycling and the lack of evidence that FIV is an issue at JAF or elsewhere in the fleet, thermal and FIV induced fatigue/EAF are not considered to be a relevant degradation mechanism for the core plate bolts.

5.4 Operating Experience

Many US plants, including JAF and Vermont Yankee (VY) have inspected their core plate bolts using visual inspections from above the bolts, and no obvious signs of degradation have been found [6, 23, 24, and 25]. A summary of the JAF inspections to date is provided in Table 5-1 below. While these examinations would not have been able to detect cracking in the threaded regions of the bolting, failures of the keepers and rotation of the bolting, caused by gross failures over the past 30+ years of operation, would have been observable. Additionally, as stated in Reference [24], and supported by BWRVIP-25 [2], no failures of core plate bolts have been observed in the US BWR fleet.

Table 5-1: JAF Core Plate Bolt Inspection Summary

Outage	No. of Bolts	Method	Results
RO11	20	VT-1	No indications requiring evaluation
RO13	72	VT-3	No indications requiring evaluation
RO18	33	VT-1	No indications requiring evaluation

6.0 CONCLUSIONS

This evaluation supports the following conclusions:

1. The core plate bolts are potentially susceptible to IGSCC due to possible cold work and the presence of a significant tensile stress. In particular, the environment present early in plant operation would support IGSCC. However, the probability of cracking is considered low since the material is not thermally sensitized, was purchased to a specification requiring solution annealing following cold work, has a smooth surface finish, and the environment has been mitigated with the introduction of HWC and NMCA/OLNC. Furthermore, visual examinations performed in the US BWR fleet, including at JAF, suggest that the operating experience has been excellent to date.
2. The core plate bolts are not considered susceptible to IASCC since the expected fluence at the core plate bolt location is below the relevant “threshold” value for IASCC considering the material type and water chemistry.
3. The core plate bolts are not considered susceptible to degradation by thermal fatigue or FIV due to the absence of sufficient fatigue loading and cycles, the lack of evidence of FIV following the startup vibration testing, and the lack of industry evidence of FIV degradation of the core plate bolts.

7.0 REFERENCES

1. ADAMS Accession No. ML071060390, “James A. Fitzpatrick, License Renewal Application, Amendment 9.”
2. EPRI TR-107284, BWR Vessel and Internals Project, BWR Core Plate Inspection and Flaw Evaluation Guidelines (BWRVIP-25), December 1996, SI File No. BWRVIP-01-225P (**EPRI Proprietary Information**).
3. IAEA Nuclear Energy Series, No. NP-T-3.13, “Stress Corrosion Cracking in Light Water Reactors: Good Practices and Lessons Learned,” International Atomic Energy Agency, 2011, SI File No. 1101291.221.
4. General Electric Drawing No. 729E762, Revision 2, “Reactor Thermal Cycles,” SI File No. 0800846.202.
5. James A. Fitzpatrick Nuclear Power Plant, Updated Final Safety Analysis Report (UFSAR), Docket No. 50-333, SI File No. 0900777.202.
6. SI Project No. 1101291, Design Input Request, Revision 3, SI File No. 1101291.200.
7. GE Document No. 21A1056, “Standard Requirements for Miscellaneous Piping and Hardware (Reactor Internals),” SI File No. 1101291.210.
8. GE Drawing No. 158B7234, “Stud,” SI File No. 1101291.201.
9. Portland Bolt & Manufacturing Company, Thread Pitch Chart, SI File No. 1200362.221.
10. Email from Priit Okas (Entergy) to Dick Matson (SI), Nov. 04 2002, 5:46 PM, “FW: Bolt Torque,” SI File No. EPRI-179-207.
11. ADAMS Accession No. ML091110498, Vermont Yankee Nuclear Power Station, AP 0319, Revision 20, “I&C Surveillance, Preventive and Corrective Maintenance Program.”
12. Henkel Technical Data Sheet, “Loctite N-5000 High Purity Anti-Seize,” SI File No. 1101291.221.
13. ASME Boiler and Pressure Vessel Code, Section III, Rules for Construction of Nuclear Vessels, 1965 Edition with 1966 Winter Addenda.
14. TransWare Enterprises Document No. ENT-JAF-001-R-001, Revision 0, “James A. Fitzpatrick Core Support Plate Rim Bolt Fluence Evaluation at End of Cycle 20, 32 EFPY and 54 EFPY,” June 2012, SI File No. 1101291.203.
15. Email from Bob Carter (EPRI) to Dick Mattson (SI), Aug. 08 2002, 2:49 PM, “FW: Requested info for JAF-Core plate bolts,” SI File No. EPRI-179-207.
16. Email from M. Rose (JAF) to D. Sommerville (SI), March 19, 2012, 7:18 AM, “FW: Emailing: Item 4-1 EPRI-179-207-2 water chem,” SI File No. 1101291.202.
17. M. R. Lindeburg, Mechanical Engineering Reference Manual, 10th Ed., Professional Publications, Inc., 1998, SI File No. 1101291.221.

18. E. A. Avallone, T. Baumeister III, A. M. Sadegh, Mark's Standard Handbook for Mechanical Engineers, 11th Ed., McGraw-Hill, 2007, SI File No. 1101291.221.
19. G. M. Gordon and R. E. Blood, "Reactor Structural Materials Environmental Exposure Program," Nuclear Metallurgy Volume Nineteen, Symposium on Materials Performance in Operating Nuclear Systems, 1973, SI File No. 1101291.221.
20. H. Hanninen and I. Aho-Mantila, "Environment-Sensitive Cracking of Reactor Internals," Proceedings of the Third International Symposium on Environmental Degradation of Materials in Nuclear Power Systems – Water Reactors, The Metallurgical Society, 1988, SI File No. 1101291.221.
21. G. S. Was, J. T. Busby and P. L. Andresen, "Effect of Irradiation on Stress Corrosion Cracking and Corrosion in Light Water Reactors," ASM Handbook Volume 13C, Corrosion: Environments and Industries, A. D. Cramer and B. S. Covino, Jr. Eds, ASM, Metals Park, OH, 2006, p 386, SI File No. 1101291.221.
22. T. R. Allen and J. T. Busby, "Radiation Damage Concerns for Extended Light Water Service," JOM Journal of the Minerals, Metals and Materials Society, Volume 61, Number 7, July 2009, pgs 29-34, SI File No. 1101291.221.
23. James A. Fitzpatrick ICD No. JAF-ICD-03-00014, Revision 0, "JAF-IVVI Program-Technical Justification, Alternate Technique for Inspection of Vessel Internals Core Plate Rim Hold-down Bolts (BWRVIP-25)," SI File No. 1101291.204.
24. ADAMS Accession No. ML120760152, "Safety Evaluation by the Office of Nuclear Reactor Regulation Core Plate Hold Down Bolt Inspection Plan and Analysis Entergy Nuclear Operations, Inc. Vermont Yankee Nuclear Power Station Docket No. 50-271," SI File No. 1101291.211.
25. James A. Fitzpatrick Program Section No. SEP-RVI-004, Revision 0, Appendix F, "Core Plate," SI File No. 1101291.204.

<input type="checkbox"/> ANO-1	<input type="checkbox"/> ANO-2	<input type="checkbox"/> GGNS	<input type="checkbox"/> IP-2	<input type="checkbox"/> IP-3	<input type="checkbox"/> PLP
<input checked="" type="checkbox"/> JAF	<input type="checkbox"/> PNPS	<input type="checkbox"/> RBS	<input type="checkbox"/> VY	<input type="checkbox"/> W3	
<input type="checkbox"/> NP-GGNS-3	<input type="checkbox"/> NP-RBS-3				
CALCULATION COVER PAGE		⁽¹⁾ EC # <u>36003</u>		⁽²⁾ Page 1 of <u>23</u>	
⁽³⁾ Design Basis Calc. <input checked="" type="checkbox"/> YES <input type="checkbox"/> NO			⁽⁴⁾ <input checked="" type="checkbox"/> CALCULATION <input type="checkbox"/> EC Markup		
⁽⁵⁾ Calculation No: JAF-CALC-12-00014				⁽⁶⁾ Revision: 0	
⁽⁷⁾ Title: Core Plate Bolt Preload Relaxation (SIA File No. 1101291.302 Rev 0)				⁽⁸⁾ Editorial <input type="checkbox"/> YES <input checked="" type="checkbox"/> NO	
⁽⁹⁾ System(s): 02-1 Reactor Vessel		⁽¹⁰⁾ Review Org (Department): DE - Civil			
⁽¹¹⁾ Safety Class: <input checked="" type="checkbox"/> Safety / Quality Related <input type="checkbox"/> Augmented Quality Program <input type="checkbox"/> Non-Safety Related		⁽¹²⁾ Component/Equipment/Structure Type/Number:			
		02V-1			
⁽¹³⁾ Document Type: DCAL					
⁽¹⁴⁾ Keywords (Description/Topical Codes): Core Plate Bolt					
REVIEWS					
⁽¹⁵⁾ Name/Signature/Date <u>Structural Integrity Associates</u> Responsible Engineer		⁽¹⁶⁾ Name/Signature/Date <u>R. Casella / R Casella 9/10/12</u> <input type="checkbox"/> Design Verifier <input checked="" type="checkbox"/> Reviewer <input type="checkbox"/> Comments Attached		⁽¹⁷⁾ Name/Signature/Date <u>G. Foster / See AS EC 36003</u> Supervisor/Approval <input type="checkbox"/> Comments Attached	

CALCULATION REFERENCE SHEET	CALCULATION NO: <u>JAF-CALC-12-00014</u> REVISION: <u>0</u>																																										
I. EC Markups Incorporated (N/A to NP calculations) N/A 1. 2. 3. 4. 5.																																											
II. Relationships:	<table border="1" style="width: 100%; border-collapse: collapse;"> <thead> <tr> <th style="width: 35%;"></th> <th style="width: 8%;">Sht</th> <th style="width: 8%;">Rev</th> <th style="width: 12%;">Input Doc</th> <th style="width: 12%;">Output Doc</th> <th style="width: 10%;">Impact Y/N</th> <th style="width: 15%;">Tracking No.</th> </tr> </thead> <tbody> <tr> <td>1. JAF-CALC-12-00013</td> <td></td> <td>0</td> <td style="text-align: center;"><input checked="" type="checkbox"/></td> <td style="text-align: center;"><input type="checkbox"/></td> <td></td> <td></td> </tr> <tr> <td>2.</td> <td></td> <td></td> <td style="text-align: center;"><input type="checkbox"/></td> <td style="text-align: center;"><input type="checkbox"/></td> <td></td> <td></td> </tr> <tr> <td>3.</td> <td></td> <td></td> <td style="text-align: center;"><input type="checkbox"/></td> <td style="text-align: center;"><input type="checkbox"/></td> <td></td> <td></td> </tr> <tr> <td>4.</td> <td></td> <td></td> <td style="text-align: center;"><input type="checkbox"/></td> <td style="text-align: center;"><input type="checkbox"/></td> <td></td> <td></td> </tr> <tr> <td>5.</td> <td></td> <td></td> <td style="text-align: center;"><input type="checkbox"/></td> <td style="text-align: center;"><input type="checkbox"/></td> <td></td> <td></td> </tr> </tbody> </table>		Sht	Rev	Input Doc	Output Doc	Impact Y/N	Tracking No.	1. JAF-CALC-12-00013		0	<input checked="" type="checkbox"/>	<input type="checkbox"/>			2.			<input type="checkbox"/>	<input type="checkbox"/>			3.			<input type="checkbox"/>	<input type="checkbox"/>			4.			<input type="checkbox"/>	<input type="checkbox"/>			5.			<input type="checkbox"/>	<input type="checkbox"/>		
	Sht	Rev	Input Doc	Output Doc	Impact Y/N	Tracking No.																																					
1. JAF-CALC-12-00013		0	<input checked="" type="checkbox"/>	<input type="checkbox"/>																																							
2.			<input type="checkbox"/>	<input type="checkbox"/>																																							
3.			<input type="checkbox"/>	<input type="checkbox"/>																																							
4.			<input type="checkbox"/>	<input type="checkbox"/>																																							
5.			<input type="checkbox"/>	<input type="checkbox"/>																																							
III. CROSS REFERENCES: See body of calculation. 1. 2. 3. 4. 5.																																											
IV. SOFTWARE USED: Title: <u>None</u> Version/Release: <u> </u> Disk/CD No. <u> </u>																																											
V. DISK/CDS INCLUDED: Title: <u>N/A</u> Version/Release <u> </u> Disk/CD No. <u> </u>																																											
VI. OTHER CHANGES: None																																											

Revision	Record of Revision
0	Initial issue.



Structural Integrity Associates, Inc.®

CALCULATION PACKAGE

File No.: 1101291.302

Project No.: 1101291

Quality Program: Nuclear Commercial

PROJECT NAME:

JAF Core Plate Bolt Evaluation

CONTRACT NO.:

10340564

CLIENT:

Entergy Nuclear

PLANT:

James A. Fitzpatrick Nuclear Power Plant

CALCULATION TITLE:

Core Plate Bolt Preload Relaxation

NOTE: This document references vendor proprietary information. Such information is identified with -2xxP SI Project File numbers in the list of references. Any such references and the associated information in this document where those references are used are identified so that this information can be treated in accordance with applicable vendor proprietary agreements.



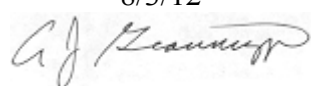

Document Revision	Affected Pages	Revision Description	Project Manager Approval Signature & Date	Preparer(s) & Checker(s) Signatures & Date
0	1 - 13 A-1 - A-7	Initial Issue	 D. V. Sommerville 8/3/12	<p><u>Responsible Engineers</u></p>  C. Oberembt 8/3/12  T. Giannuzzi 8/3/12 <p><u>Responsible Verifier</u></p>  H. Gustin 8/3/12



Table of Contents

1.0 INTRODUCTION 3

2.0 TECHNICAL APPROACH 3

 2.1 Thermal Relaxation 3

 2.2 Stress Relaxation 4

 2.3 Radiation Relaxation 4

3.0 DESIGN INPUTS 5

4.0 ASSUMPTIONS 6

5.0 CALCULATIONS 6

 5.1 Thermal Relaxation 6

 5.2 Stress Relaxation 8

 5.3 Radiation Relaxation 10

6.0 RESULTS 11

7.0 CONCLUSIONS 12

8.0 REFERENCES 12

APPENDIX A JUSTIFICATION FOR USING AVERAGE FLUENCE A-1

List of Figures

Figure 5-1: General Stress-Strain Curve for Type 304 SS, with Annotations 7

Figure 5-2: Stress Relaxation as a Function of Applied Load, with Annotations 9

Figure 5-3: Remaining Preload as a Function of Fluence, with Annotations 10

List of Tables

Table 3-1: Material Properties 5

Table 3-2: Adjusted Maximum Average Fluence Values 5

Table 6-1: Summary of Results 11

1.0 INTRODUCTION

The James A. Fitzpatrick (JAF) nuclear power plant license renewal commitment number 23 [1, Attachment 1] states that JAF will either install core plate wedges prior to the period of extended operation or complete a plant specific analysis to develop and justify a core plate bolt inspection plan. The inspection plan must include acceptance criteria which meet the requirements of BWRVIP-25 [2].

An evaluation of the loss of core plate bolt preload is needed to support the development of an inspection protocol. This document contains an evaluation to assess the loss of preload in the JAF core plate bolts due to potential mechanisms including thermal relaxation, stress relaxation, and radiation relaxation. These results will be used to determine the minimum required number of core plate bolts in subsequent calculations.

2.0 TECHNICAL APPROACH

This section contains a description of the technical approach used for the loss of preload calculations for the Type 304 stainless steel (SS) core plate bolts at JAF. A literature review was conducted to identify information regarding the relevant mechanisms of preload reduction and the associated analysis methods. The following mechanisms were identified as relevant to the JAF core plate bolts [3, 4, 5, 6, 7, 8 and 9]:

- Thermal Relaxation
- Stress Relaxation
- Radiation Relaxation

In this evaluation the term “thermal relaxation” will be used to describe the loss of preload associated with thermal effects on temperature dependent material properties. These effects will contribute to the reduction in preload at operating temperatures. See Section 2.1 for details.

The methods used to calculate the predicted loss of preload for each of the mechanisms identified above are described below.

2.1 Thermal Relaxation

Thermal relaxation occurs due to thermal effects on temperature dependent material properties and can result in both a temporary (i.e. recoverable) reduction in preload due to a change in the modulus of elasticity and a permanent loss of preload due to a change in the yield strength and consequent yielding of the material at an elevated temperature. For this evaluation, the elevated temperature is taken as the operating temperature. As temperature increases, both the modulus of elasticity and the yield strength of Type 304 SS decrease [10]; thus, both effects are considered here.

The loss of stiffness due to the decrease in the modulus of elasticity causes a consequent loss of preload force, and can be represented by the following equation [11, pgs. 483-484]:

$$F_2 = F_1 * (E_2 / E_1) \quad (1)$$

Where:

F_2	=	Preload at elevated temperature, lbf
F_1	=	Preload at installation temperature, lbf
E_2	=	Modulus of elasticity at elevated temperature, ksi
E_1	=	Modulus of elasticity at installation temperature, ksi

The potential for yielding exists if the stress in the bolt, at an elevated temperature, is greater than the yield stress for the material at that temperature. This effect is evaluated by comparing the remaining (i.e. at operating temperature) preload stress in the bolt, factored as shown in Eq. (1), to the yield stress at the elevated temperature. If the remaining preload stress is greater than the yield strength, additional analysis will be performed using representative stress-strain curves for Type 304 SS. If the remaining preload stress is less than the yield stress, the reduction in preload will be evaluated using Eq. (1).

The stress-strain curve will be used by identifying the strain due to the preload stress at room temperature and determining the equivalent stress for constant strain on an elevated temperature curve representing the operating temperature. If stress-strain curves are used, the effects of both the reduction in modulus and yielding are inherently accounted for.

2.2 Stress Relaxation

Stress relaxation occurs due to a creep mechanism in the material [3, 8]. Stress relaxation is evaluated based on the temperature, stress, and time of operation. The potential relaxation effects of both primary and secondary creep are assessed for Type 304 SS, through evaluation of available information.

2.3 Radiation Relaxation

Radiation relaxation, also referred to as irradiation creep, is a fluence (time) dependent deformation process which affects stainless steels in the light water reactor (LWR) environment [3, 4, 5, 6, 7]. Fluence for energy > 0.1 MeV is considered for the evaluation of radiation relaxation. This is consistent with the approach in Reference [3], and is conservative compared to the use of fluence values for energy > 1.0 MeV as applied in References [6, 7 and 8]. The maximum value of average fluence, along the loaded length of the core plate bolts, for all bolts around the core plate, is used to calculate the relaxation along each bolt. Additional justification for using the average fluence is included in Appendix A of this calculation. Using the maximum average fluence is bounding for all other azimuthal locations. Radiation relaxation is evaluated utilizing the different methodologies presented in References [3, 6, 8] and by comparing the results to develop a reasonable and bounding loss of preload.

3.0 DESIGN INPUTS

The design inputs used in the relaxation calculations are discussed in this section.

The temperatures and pressures in different regions of the JAF reactor pressure vessel (RPV) are taken from the RPV thermal cycle diagram (TCD) [12]. The core plate is located below the core, which corresponds to either the bottom of Region B or the top of Region C [12]. Both regions are considered and the bounding service conditions are summarized as follows:

- Normal operating RPV pressure = 1040 psig [12]
- Normal operating temperature in Regions B and C = 527°F [12]
- Maximum temperature in Region B = 551°F [12]

Material properties for Type 304 SS are taken from the ASME Boiler & Pressure Vessel Code [10] and are listed in Table 3-1 below. Representative stress-strain curves for Type 304 SS are taken from Reference [13, pg. 183, Figure SS.042].

Table 3-1: Material Properties

Material Property	Temperature	
	70 °F	550 °F
Yield Strength, S_y (ksi)	30	17.75
Young's Modulus, E (ksi)	27,400	25,700

Initial bolt preload and stress are evaluated in Reference [14], and are taken as:

- Initial Preload = 19,556 lbf at 70 °F
- Initial Stress = 22,845 psi at 70 °F

Maximum average fluence values for the JAF core plate bolts are taken from Reference [15]. Based on the guidance from Reference [15], the fluence values are adjusted to account for bias and uncertainty. The adjusted maximum average fluence values are listed in Table 3-2 below, for select Effective Full Power Years (EFPY). End of Cycle (EOC) 20 is equivalent to 27.7 EFPY.

Table 3-2: Adjusted Maximum Average Fluence Values

EFPY	Average Fluence (n/cm^2), $E > 0.1$ MeV
27.7 (EOC 20)	2.63E+19
32	2.88E+19
54	4.24E+19



4.0 ASSUMPTIONS

The following assumptions were used in this evaluation:

1. Bolt tensile area is assumed constant. There will be some reduction in area based on the Poisson effect when loading the core plate bolts; however, this reduction in area is negligible. This is justified because the Poisson ratio for stainless steels is approximately 0.30 [16, pg. 46-4] and the axial elongation due to initial preload strain is approximately 0.021 in. as shown in Appendix A. Therefore, the reduction in diameter will be approximately 0.006 in., which is very small (less than 1%).
2. A maximum average fluence value along the length the core plate bolts is used. This value corresponds to the peak azimuthal location as described in Reference [15]. An average value is appropriate because it more accurately represents the effects of radiation relaxation along the length of a core plate bolt compared to the use of a bounding peak fluence value, since the relaxation will occur over the length of the entire bolt. The loss of preload associated with radiation relaxation is a general effect on the preload stress in the bolt cross section. Detailed justification of this approach is provided in Appendix A. The result of a numerical integration of discrete displacements, due to radiation relaxation, along the length of the core plate bolt is within 2% normalized difference of the result obtained using the average value.
3. A conversion factor for displacements per atom (dpa) to n/cm^2 of $1 \text{ dpa} = 6.5 \times 10^{20} \text{ n/cm}^2$ is assumed. This value is consistent with the value from Reference [8, pg. H-12], and is appropriate for the LWR neutron spectra. It is recognized that the conversion from dpa to n/cm^2 is not exact and that a range of values are present in the literature. However, this value is also consistent with, and slightly more conservative than, the value reported in Reference [17].
4. Representative stress-strain curves generated at multiple temperatures for Type 304 SS can be used to accurately estimate the effect of temperature on strain. Since the ASME Code does not contain stress-strain curves, an atlas of stress-strain curves [13] will be used. Curves in Reference [13] represent the general elastic-plastic behavior of Type 304 SS. The use of representative/general stress-strain curves is appropriate to represent the average behavior of all of the core plate bolts with respect to determining a percent loss of preload.

5.0 CALCULATIONS

The loss of preload calculations, for the relevant degradation mechanisms, are developed and discussed in this section.

5.1 Thermal Relaxation

The value of (E_2 / E_1) from Eq. (1) can be considered a scaling ratio for the retained preload force or stress after thermal relaxation. Using the inputs from Section 3.0, this scaling ratio is evaluated as:

$$25,550 / 28,300 = 0.903$$

Multiplying this value by 100% provides a value of 90.3% retained preload, which corresponds to a 9.7% loss of preload due to the change in the modulus of elasticity. Taking the initial preload stress

given in Section 3.0 (22,845 psi), the remaining preload stress after increasing the temperature to 550°F is evaluated as:

$$22,845 * (0.903) = 20,629 \text{ psi}$$

Comparing this value to the yield stress at 550°F indicates that the core plate bolts may be expected to yield during the first power ascension in plant life. Since the stress in the bolts is displacement controlled, once yielding occurs the stress is not expected to exceed yield again upon subsequent heat-ups. Therefore, ratcheting is not expected to occur. To account for the potential effect of yielding on the reduction in preload, a second approach for evaluating thermal relaxation is used. General stress-strain curves for Type 304 SS at room and elevated temperatures are provided in Reference [13, pg. 183, Figure SS.042], and are replicated in Figure 5-1, with annotations, below.

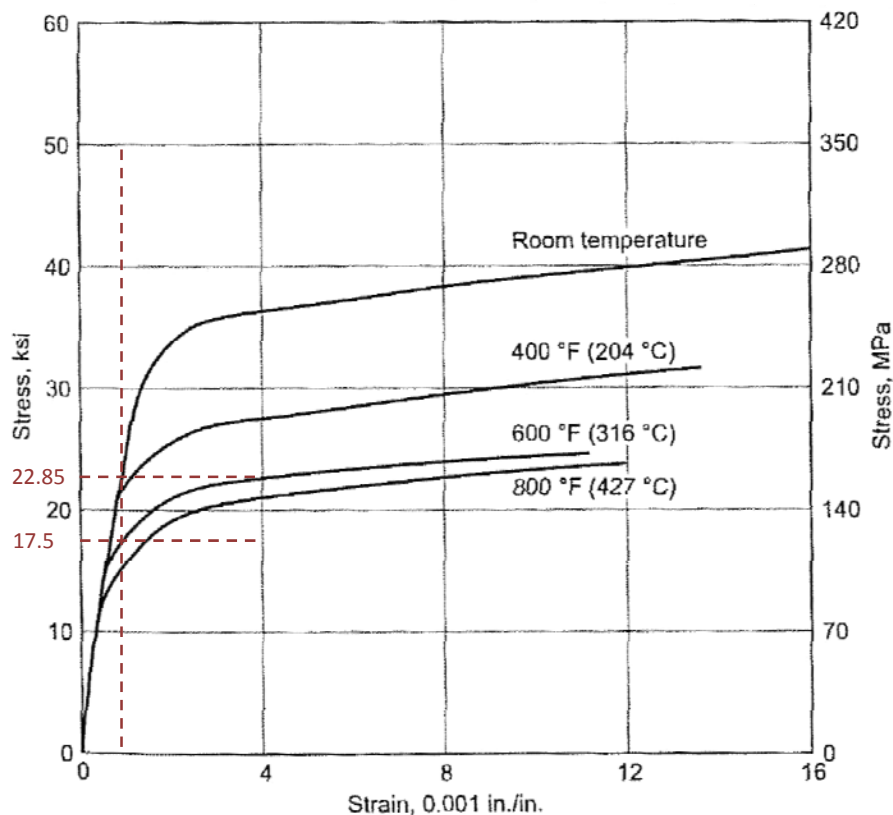


Figure 5-1: General Stress-Strain Curve for Type 304 SS, with Annotations [13]

To evaluate the thermal relaxation, the initial preload stress value of 22,845 psi is located on the room temperature (~70 °F) curve in Figure 5-1, and a constant strain line is drawn. The stress-strain curve for 600 °F from Reference [13, pg. 183, Figure SS.042] is used to approximate the behavior of Type 304 SS at 550 °F. This is appropriate because a curve for 550 °F is not provided, and using a slightly higher temperature curve is conservative in regards to determining the loss of preload. The intersection of the



constant strain line and the 600 °F curve provides an estimate of the preload stress after thermal relaxation. From Figure 5-1, the approximate preload stress, after thermal relaxation, is taken as 17,500 psi. This value corresponds to a 23.4% reduction in preload due to thermal relaxation, and accounts for both the reduction in modulus and the effect of yielding.

5.2 Stress Relaxation

Creep deformation of metals occurs in three stages: primary creep, secondary creep and tertiary creep [18, pg. 31]. For the core plate bolts, primary creep is most relevant, and further stages of creep (i.e. secondary and tertiary) are considered negligible [3, 8]. Secondary (steady state) creep is typically considered a high temperature phenomenon, and the temperatures in an operating BWR (approximately 550 °F [12]) are generally regarded to be outside of the secondary creep regime. This is supported by the approximate value given in Reference [19, pg. 228] for the lower limit of elevated-temperature behavior for austenitic steels of 1000 °F. Additionally, References [5, 8, 18] state that creep (secondary creep) becomes a consideration at approximately 35-50% of the melting temperature. Since secondary creep is negligible, tertiary creep is also negligible. However, at lower temperatures, stress relaxation does occur, and is the result of primary creep.

Reference [3, Figure 6] provides an average curve for relaxation stress due to primary creep as a function of applied load for Type 304 SS. This curve is shown in Figure 5-2, with annotations, below.

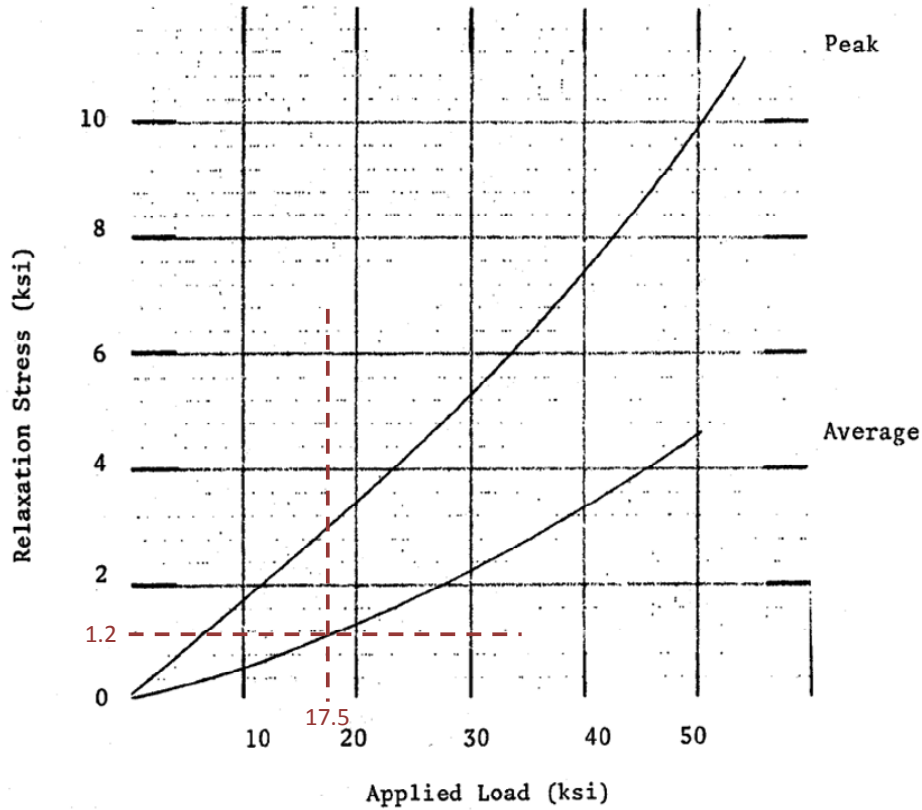


Figure 5-2: Stress Relaxation as a Function of Applied Load, with Annotations [3]

After thermal relaxation, the remaining preload stress is 17,500 psi. Taking 17,500 psi as the initial preload which will be affected by primary creep and considering the average curve in Figure 5-2, gives a relaxation stress of approximately 1,200 psi. This value corresponds to a 6.8% additional reduction in preload due to stress relaxation. The value of 6.8% will be used in this evaluation.

In this evaluation, the thermal relaxation occurs over a short time scale (first heat-up); therefore, the primary creep affects the preload after thermal relaxation has occurred. Further, since this evaluation considers primary creep for all core plate bolts it is more appropriate to evaluate the average primary creep relaxation and apply this to all core plate bolts than to assume the maximum creep relaxation occurs for all core plate bolts.

5.3 Radiation Relaxation

The period of extended operation for JAF extends to 60 years (54 EFPY) [1]. References [3, 6, 8] provide methods and guidance for evaluating the loss of bolt preload caused by radiation relaxation due to accumulated fluence over the life of a plant.

Reference [3, Figure 10] provides an average curve for retained elastic tensile stress as a function of neutron fluence based on an initial preload stress of 20 ksi and Type 304 SS material. This curve is shown in Figure 5-3, with annotations, below.

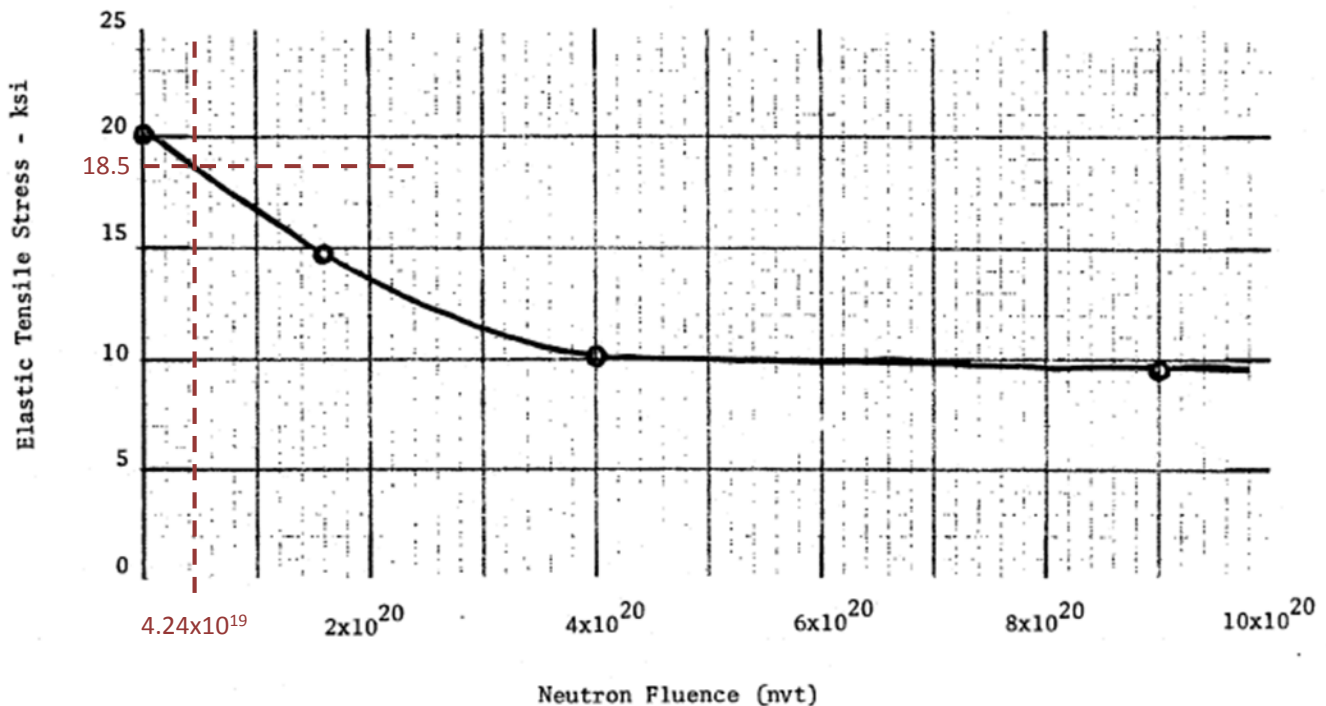


Figure 5-3: Remaining Preload as a Function of Fluence, with Annotations [3]

Using the maximum average fluence at 54 EFPY of $4.24\text{E}+19$ n/cm², from Table 3-2, a relaxed preload stress of 18.5 ksi is obtained. This corresponds to a 7.5% reduction in preload from 20 ksi.

References [6, 7] provide methods for calculating the retained preload in Type 304L SS, which may not directly correlate to Type 304 SS; however, these methods will provide an engineering estimate of radiation relaxation. Reference [6] is considered to be more applicable to the JAF core plate bolts based on the fluence values, and is used here. Using Reference [6, Eq. 4], which is consistent with Reference [8, Eq. H-1], the modulus of elasticity at 550°F, the maximum average fluence for the JAF core plate bolts, and the tabulated coefficients for Type 304L SS from Reference [6, Table IV], a 3% reduction in preload is calculated. It should be noted that the irradiation-enhanced transient creep is ignored in this evaluation and this value should be considered a lower bound.

Reference [8, Figure H-7] provides test data for percent remaining preload stress as a function of fluence (in dpa). Using the lower bound curve for all test data and the maximum average fluence for the JAF core plate bolts, the corresponding remaining preload stress is approximately 50%. The lower bound curve is not representative of Type 304 SS, as it includes data for all materials in the study. Using an upper bound curve for all test data the remaining preload stress is approximately 96%, but this value is considered non-conservative because it does not represent the average behavior of Type 304 SS. Using an average or best fit curve (approximated as linear in the fluence range of interest) for the solution annealed Type 304 SS in uniaxial tension test data, the corresponding remaining preload stress is approximately 93.2% as shown in Appendix A. The use of the uniaxial tension test data is considered appropriate for the evaluation of a bolt in tension, and bounds the average behavior for the solution annealed Type 304 SS bent-beam data. This value corresponds well (i.e. within 0.2 % relaxation) with the value obtained using the methods of Reference [3] and Figure 5-3, above.

The range of average preload stress reduction due to radiation relaxation is approximately 3-8%. For this evaluation, the value of 8% will be used.

6.0 RESULTS

The results for the thermal, stress and radiation relaxation evaluations are summarized in Table 6-1 below.

Table 6-1: Summary of Results

Mechanism	Reduction in Preload	Remaining Preload (lbf)
Thermal Relaxation	23.4%	14980
Stress Relaxation	6.8%	13961
Radiation Relaxation	8.0%	12844
Total at 54 EFPY	34.3%	12844

The effects of the three different relaxation mechanisms are such that they occur in an order. Thermal relaxation happens upon first going to power, then stress relaxation occurs over a short period of time at temperature, and radiation relaxation occurs over an extended period of time. Therefore, the total equivalent percent reduction in preload is calculated as follows:

$$\text{Total \%} = 1 - (1 - 0.234) * (1 - 0.068) * (1 - 0.08) = 34.3\%$$

7.0 CONCLUSIONS

The results of this evaluation are used in additional analyses to determine the minimum number of required bolts and to support development of a core plate bolt inspection plan. This evaluation supports the following conclusions:

1. Thermal relaxation is sensitive to the elastic-plastic behavior of Type 304 SS at elevated temperatures.
2. Secondary creep is not a concern for stress relaxation in Type 304 SS core plate bolts at JAF.
3. Limited test data for radiation relaxation of Type 304 SS exists, and a conservative value should be used.
4. The total equivalent reduction in preload at 54 EFPY is evaluated as 34.3% of initial preload, which corresponds to a remaining preload of 12,844 lbf.

8.0 REFERENCES

1. James A. Fitzpatrick Nuclear Plant License Renewal Application, Amendment 9, ADAMS Accession No. ML071060390.
2. EPRI TR-107284, BWR Vessel and Internals Project, BWR Core Plate Inspection and Flaw Evaluation Guidelines (BWRVIP-25), December 1996, SI File No. BWRVIP-01-225P (**EPRI Proprietary Information**).
3. General Electric Document No. NEDE 13334, Class II, "A Study of Stress Relaxation in AISI 304 Stainless Steel," April 1973, SI File No. EPRI-179-202.
4. General Electric Document No. NEDO 24282, Class I, "Stress Relaxation of Austenitic Stainless Steels at 290°C," August 1980, SI File No. EPRI-179-202.
5. T. R. Allen and J. T. Busby, "Radiation Damage Concerns for Extended Light Water Service," JOM Journal of the Minerals, Metals and Materials Society, Volume 61, Number 7, July 2009, pgs 29-34, SI File No. 1101291.221.
6. J. P. Foster and T. M. Karlsen, "Irradiation Creep and Irradiation Stress Relaxation of 316 and 304L Stainless Steel," 14th International Conference on Environmental Degradation of Materials in Nuclear Power Systems – Water Reactors, August 2009, SI File No. 1101291.221.
7. J.P. Foster and T. M. Karlsen, "Irradiation Creep and Irradiation Stress Relaxation of 316 and 304L Stainless Steels in Thermal and Fast Neutron Spectrum Reactors," 15th International Conference on Environmental Degradation of Materials in Nuclear Power Systems – Water Reactors, August 2011, SI File No. 1101291.221.
8. Materials Reliability Program: *PWR Internals Material Aging Degradation Mechanism Screening and Threshold Values (MRP-175)*. EPRI, Palo Alto, CA: 2005. 1012081.
9. MRP, Technical Basis Document Concerning Irradiation Induced Stress Relaxation and Void Swelling in PWR RV Internals Components (MRP-50), EPRI, Palo Alto, CA: 2001. 1000970.

10. ASME Boiler and Pressure Vessel Code, Section III, Rules for Construction of Nuclear Vessels, 1965 Edition with 1966 Winter Addenda.
11. J. H. Bickford, “An Introduction to the Design and Behavior of Bolted Joints,” CRC Press, Taylor & Francis Group, 3rd Edition, 1995, SI File no. 1101291.221.
12. General Electric Drawing No. 729E762, Revision 2, “Reactor Thermal Cycles,” SI File No. 0800846.202.
13. Atlas of Stress-Strain Curves, 2nd Edition, ASM International, SI File No. 1101291.221.
14. SI Calculation No. 1101291.301, Revision 0, “Core Plate Bolt Degradation Susceptibility Evaluation.”
15. TransWare Enterprises Document No. ENT-JAF-001-R-001, Revision 0, “James A. Fitzpatrick Core Support Plate Rim Bolt Fluence Evaluation at End of Cycle 20, 32 EFPY and 54 EFPY,” June 2012, SI File No. 1101291.203.
16. M. R. Lindeburg, Mechanical Engineering Reference Manual, 10th Ed., Professional Publications, Inc., 1998, SI File No. 1101291.221.
17. NRC SER, “Safety Evaluation by the Office of Nuclear Reactor Regulation Core Plate Hold Down Bolt Inspection Plan and Analysis Entergy Nuclear Operations, Inc. Vermont Yankee Nuclear Power Station Docket No. 50-271,” ADAMS Accession No. ML120760152, SI File No. 1101291.211.
18. A. Saxena, “Nonlinear Fracture Mechanics for Engineers,” CRC Press, LLC, 1998, SI File No. 1101291.221.
19. D. J. Wolpi, “Understanding How Components Fail,” 2nd Ed., ASM International, 2000, SI File No. 1101291.221.

APPENDIX A

JUSTIFICATION FOR USING AVERAGE FLUENCE

Objective

This Appendix provides justification for the use of an average fluence value over the length of the core plate bolts to determine the loss of preload associated with radiation relaxation.

Methodology

A numerical integration method is used to evaluate the total radiation relaxation by summing the contribution of discrete increments over the length of the core plate bolt. Fluence data over the length of the core plate bolt is provided at discrete increments along the length [15]. A lost preload is determined for each increment based on the fluence (converted to dpa based on $1 \text{ dpa} = 6.5 \times 10^{20} \text{ n/cm}^2$) and the methods presented in Reference [8] and discussed in Section 5.3 of this calculation. An associated value of displacement is calculated for each increment based on the modulus of elasticity, the effective tensile area, the lost preload force, and the increment length using the equation:

$$\Delta L = (P * L) / (A * E) \quad (\text{A-1})$$

Where:	ΔL	=	Displacement, in
	L	=	Increment length, in
	P	=	Lost preload, lbf
	A	=	Effective bolt tensile area, in ²
	E	=	Modulus of elasticity, psi

The total displacement is calculating by summing all of the discrete displacements over the entire length. Using the total displacement, the overall length (taken as the sum of the incremental lengths), and rearranging Eq. A-1 to solve for P, a total lost preload is calculated. This value is compared to the lost preload calculated using the average fluence value.

Inputs and Assumptions

Inputs are taken from Section 3.0 of this calculation. Material properties at 70 °F are used to perform all calculations. The results are not sensitive to temperature dependent material properties, but consistent values must be used. The effective bolt tensile area is assumed to be constant.

Calculations

The remaining preload used in this Appendix is determined by taking an estimated average or best fit curve of the “Joseph, Solution Annealed Type 304 uniaxial tension, <100 °F” data from Reference [8, Figure H-7]. This curve is approximated as linear for this evaluation. This is appropriate for low fluence values based on the general shape of the data and the lower bound curve, and is conservative for high fluence values. Since Reference [8] is a proprietary document, the figure is not shown here; however, the formula for the linear best fit curve used in this evaluation is as follows:

$$y = -1.14 * x + 100\% \quad (A-2)$$

Using the initial preload of 19,556 lbf and Eq. A-1, the initial displacement due to preload is calculated as 0.02143 in. Detailed calculations are tabulated on the following pages.

Results

The results are summarized in the following table:

Method	Result	Value	Units
Numerical Integration	Total Integrated Displacement	0.001468	in
	Calculated Lost Preload	1340	lbf
	% Lost Preload	6.850%	
Average Fluence	Calculated Lost Preload	1317	lbf
	% Lost Preload	6.734%	

Absolute Difference Between Methods	0.117%
% Difference Between Methods	1.7%

Conclusions

The results of the percent loss of preload calculated by both numerical integration and the use of the average fluence along the bolt length agree very well. The percent difference, taken with respect to the numerical integration result, is less than 2% (absolute difference less than 0.2% relaxation).

The use of an average fluence value is acceptable for evaluating radiation relaxation in core plate bolts.

Tabulated Calculations
Inputs

Eff. Area 0.856 in²
 E1 27400000 psi
 Load 19556 lbf

Calculated Displacements

Initial ΔL (Preload) 0.021428355 in
 Relaxed ΔL (Total) 0.001467936 in
 Ratio 0.068504378

Inches from Top	Fluence (n/cm ²) at EOC 20	Fluence (n/cm ²) at 32 EFPY	Fluence (n/cm ²) at 54 EFPY	Fluence (dpa) at 54 EFPY	Remaining Preload (%)	Lost Preload (lbf)	ΔL
0	1.78E+20	1.96E+20	2.88E+20	4.43E-01	49%	9878	0.00E+00
0.4	1.58E+20	1.74E+20	2.56E+20	3.94E-01	55%	8780	1.68E-04
0.8	1.41E+20	1.55E+20	2.27E+20	3.49E-01	60%	7786	1.50E-04
1.2	1.25E+20	1.37E+20	2.01E+20	3.09E-01	65%	6894	1.33E-04
1.6	1.11E+20	1.22E+20	1.79E+20	2.75E-01	69%	6139	1.18E-04
2	9.82E+19	1.08E+20	1.59E+20	2.45E-01	72%	5453	1.05E-04
2.4	8.72E+19	9.59E+19	1.41E+20	2.17E-01	75%	4836	9.30E-05
2.8	7.74E+19	8.51E+19	1.25E+20	1.92E-01	78%	4287	8.25E-05
3.2	6.87E+19	7.55E+19	1.11E+20	1.71E-01	81%	3807	7.31E-05
3.6	6.42E+19	7.06E+19	1.04E+20	1.60E-01	82%	3567	6.49E-05
4	5.61E+19	6.17E+19	9.06E+19	1.39E-01	84%	3107	6.08E-05
4.3	4.90E+19	5.39E+19	7.92E+19	1.22E-01	86%	2716	3.97E-05
4.7	4.28E+19	4.71E+19	6.92E+19	1.06E-01	88%	2373	4.63E-05
5.1	3.74E+19	4.12E+19	6.05E+19	9.31E-02	89%	2075	4.05E-05
5.5	3.27E+19	3.60E+19	5.28E+19	8.12E-02	91%	1811	3.54E-05
5.9	2.64E+19	2.90E+19	4.25E+19	6.54E-02	93%	1458	3.09E-05
6.3	2.35E+19	2.58E+19	3.79E+19	5.83E-02	93%	1300	2.49E-05

6.7	2.09E+19	2.30E+19	3.37E+19	5.18E-02	94%	1156	2.22E-05
7.1	1.86E+19	2.05E+19	3.01E+19	4.63E-02	95%	1032	1.97E-05
7.5	1.66E+19	1.82E+19	2.68E+19	4.12E-02	95%	919	1.76E-05
7.9	1.48E+19	1.62E+19	2.38E+19	3.66E-02	96%	816	1.57E-05
8.3	1.31E+19	1.45E+19	2.12E+19	3.26E-02	96%	727	1.39E-05
8.7	1.17E+19	1.29E+19	1.89E+19	2.91E-02	97%	648	1.24E-05
9.1	1.04E+19	1.15E+19	1.68E+19	2.58E-02	97%	576	1.11E-05
9.5	9.29E+18	1.02E+19	1.50E+19	2.31E-02	97%	514	9.83E-06
9.9	8.27E+18	9.10E+18	1.34E+19	2.06E-02	98%	460	8.77E-06
10.3	7.37E+18	8.10E+18	1.19E+19	1.83E-02	98%	408	7.84E-06
10.7	6.56E+18	7.22E+18	1.06E+19	1.63E-02	98%	364	6.96E-06
11.1	5.84E+18	6.43E+18	9.43E+18	1.45E-02	98%	323	6.20E-06
11.5	5.20E+18	5.72E+18	8.40E+18	1.29E-02	99%	288	5.52E-06
11.9	4.63E+18	5.10E+18	7.48E+18	1.15E-02	99%	257	4.91E-06
12.3	4.13E+18	4.54E+18	6.66E+18	1.02E-02	99%	228	4.38E-06
12.7	3.68E+18	4.04E+18	5.93E+18	9.12E-03	99%	203	3.90E-06
13	3.27E+18	3.60E+18	5.28E+18	8.12E-03	99%	181	2.60E-06
13.4	2.91E+18	3.21E+18	4.71E+18	7.25E-03	99%	162	3.09E-06
13.8	2.60E+18	2.86E+18	4.19E+18	6.45E-03	99%	144	2.76E-06
14.2	2.31E+18	2.54E+18	3.73E+18	5.74E-03	99%	128	2.45E-06
14.6	2.06E+18	2.26E+18	3.32E+18	5.11E-03	99%	114	2.18E-06
15	1.83E+18	2.02E+18	2.96E+18	4.55E-03	99%	102	1.94E-06
15.4	1.63E+18	1.80E+18	2.64E+18	4.06E-03	100%	91	1.73E-06
15.8	1.45E+18	1.60E+18	2.35E+18	3.62E-03	100%	81	1.54E-06
16.2	1.30E+18	1.42E+18	2.09E+18	3.22E-03	100%	72	1.37E-06
16.6	1.15E+18	1.27E+18	1.86E+18	2.86E-03	100%	64	1.22E-06
17	1.03E+18	1.13E+18	1.66E+18	2.55E-03	100%	57	1.09E-06

17.4	9.15E+17	1.01E+18	1.48E+18	2.28E-03	100%	51	9.71E-07
17.8	8.15E+17	8.96E+17	1.32E+18	2.03E-03	100%	45	8.66E-07
18.2	7.26E+17	7.98E+17	1.17E+18	1.80E-03	100%	40	7.72E-07
18.6	6.46E+17	7.11E+17	1.04E+18	1.60E-03	100%	36	6.84E-07
19	5.75E+17	6.33E+17	9.29E+17	1.43E-03	100%	32	6.08E-07
19.4	5.13E+17	5.64E+17	8.27E+17	1.27E-03	100%	28	5.43E-07
19.8	7.18E+17	7.90E+17	1.16E+18	1.78E-03	100%	40	4.84E-07
20.2	6.36E+17	7.00E+17	1.03E+18	1.58E-03	100%	35	6.79E-07
20.6	5.64E+17	6.20E+17	9.10E+17	1.40E-03	100%	31	6.02E-07
21	5.00E+17	5.50E+17	8.07E+17	1.24E-03	100%	28	5.32E-07
21.4	4.43E+17	4.87E+17	7.15E+17	1.10E-03	100%	25	4.72E-07
21.7	3.93E+17	4.32E+17	6.34E+17	9.75E-04	100%	22	3.14E-07
22.1	3.48E+17	3.83E+17	5.62E+17	8.65E-04	100%	19	3.71E-07
22.5	3.08E+17	3.39E+17	4.98E+17	7.66E-04	100%	17	3.29E-07
22.9	2.73E+17	3.01E+17	4.41E+17	6.78E-04	100%	15	2.91E-07
23.3	2.42E+17	2.66E+17	3.91E+17	6.02E-04	100%	13	2.58E-07
23.7	2.15E+17	2.36E+17	3.47E+17	5.34E-04	100%	12	2.29E-07
24.1	1.90E+17	2.09E+17	3.07E+17	4.72E-04	100%	11	2.03E-07
24.5	1.69E+17	1.85E+17	2.72E+17	4.18E-04	100%	9	1.80E-07
24.9	1.49E+17	1.64E+17	2.41E+17	3.71E-04	100%	8	1.59E-07
25.3	1.32E+17	1.46E+17	2.14E+17	3.29E-04	100%	7	1.41E-07
25.7	1.17E+17	1.29E+17	1.89E+17	2.91E-04	100%	6	1.25E-07

Average	2.38E+19	2.61E+19	3.84E+19	5.91E-02	93.266%	1317
----------------	-----------------	-----------------	-----------------	-----------------	----------------	-------------

Total ΔL	0.001467936
Total Strain	5.71181E-05

Stress	1565.036929
Load	1339.671611
% of Preload	6.850%

Using Average Fluence, % of Preload	6.734%
-------------------------------------	--------

% Difference, Normalized to Integrated	1.7%
--	------

NEIL WILMSHURST
Vice President and
Chief Nuclear Officer

April 8, 2013

Document Control Desk
Office of Nuclear Reactor Regulation
U.S. Nuclear Regulatory Commission
Washington, DC 20555-0001

Subject: Request for Withholding of the following Proprietary Information Included in:

“Core Plate Bolt Fracture Mechanics Evaluation” SI File No. 1101291.303

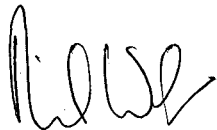
To Whom It May Concern:

This is a request under 10 C.F.R. §2.390(a)(4) that the U.S. Nuclear Regulatory Commission (“NRC”) withhold from public disclosure the report identified in the enclosed Affidavit consisting of the proprietary information owned by Electric Power Research Institute, Inc. (“EPRI”) identified in the attached report. Proprietary and non-proprietary versions of the Report and the Affidavit in support of this request are enclosed.

EPRI desires to disclose the Report in confidence to assist the NRC review of the enclosed submittal to the NRC by Entergy. The Report is not to be divulged to anyone outside of the NRC or to any of its contractors, nor shall any copies be made of the Report provided herein. EPRI welcomes any discussions and/or questions relating to the information enclosed.

If you have any questions about the legal aspects of this request for withholding, please do not hesitate to contact me at (704) 704-595-2732. Questions on the content of the Report should be directed to Andy McGehee of EPRI at (704) 502-6440.

Sincerely,



Attachment(s)

c: Sheldon Stuchell, NRC (sheldon.stuchell@nrc.gov)

AFFIDAVIT

RE: Request for Withholding of the Following Proprietary Information Included In:
"Core Plate Bolt Fracture Mechanics Evaluation" SI File No. 1101291.303

I, Neil Wilmshurst, being duly sworn, depose and state as follows:

I am the Vice President and Chief Nuclear Officer at Electric Power Research Institute, Inc. whose principal office is located at 3420 Hillview Avenue, Palo Alto, California ("EPRI") and I have been specifically delegated responsibility for the above-listed report that contains EPRI Proprietary Information that is sought under this Affidavit to be withheld "Proprietary Information". I am authorized to apply to the U.S. Nuclear Regulatory Commission ("NRC") for the withholding of the Proprietary Information on behalf of EPRI.

EPRI requests that the Report be withheld from the public on the following bases:

Withholding Based Upon Privileged And Confidential Trade Secrets Or Commercial Or Financial Information:

a. The Report is owned by EPRI and has been held in confidence by EPRI. All entities accepting copies of the Report do so subject to written agreements imposing an obligation upon the recipient to maintain the confidentiality of the Report. The Report is disclosed only to parties who agree, in writing, to preserve the confidentiality thereof.

b. EPRI considers the Report contained therein to constitute trade secrets of EPRI. As such, EPRI holds the Information in confidence and disclosure thereof is strictly limited to individuals and entities who have agreed, in writing, to maintain the confidentiality of the Information. EPRI made a substantial economic investment to develop the Report and, by prohibiting public disclosure, EPRI derives an economic benefit in the form of licensing royalties and other additional fees from the confidential nature of the Report. If the Report were publicly available to consultants and/or other businesses providing services in the electric and/or nuclear power industry, they would be able to use the Report for their own commercial benefit and profit and without expending the substantial economic resources required of EPRI to develop the Report.

c. EPRI's classification of the Report as trade secrets is justified by the Uniform Trade Secrets Act which California adopted in 1984 and a version of which has been adopted by over forty states. The California Uniform Trade Secrets Act, California Civil Code §§3426 – 3426.11, defines a "trade secret" as follows:

"Trade secret" means information, including a formula, pattern, compilation, program device, method, technique, or process, that:

(1) Derives independent economic value, actual or potential, from not being generally known to the public or to other persons who can obtain economic value from its disclosure or use; and

(2) Is the subject of efforts that are reasonable under the circumstances to maintain its secrecy."

d. The Report contained therein are not generally known or available to the public. EPRI developed the Information only after making a determination that the Report was not available from public sources. EPRI made a substantial investment of both money and employee hours in the development of the Report. EPRI was required to devote these resources and effort to derive the Report. As a result of such effort and cost, both in terms of dollars spent and dedicated employee time, the Report is highly valuable to EPRI.

e. A public disclosure of the Report would be highly likely to cause substantial harm to EPRI's competitive position and the ability of EPRI to license the Report both domestically and internationally. The Report can only be acquired and/or duplicated by others using an equivalent investment of time and effort.

I have read the foregoing and the matters stated herein are true and correct to the best of my knowledge, information and belief. I make this affidavit under penalty of perjury under the laws of the United States of America and under the laws of the State of California.

Executed at 1300 W WT Harris Blvd being the premises and place of business of Electric Power Research Institute, Inc.

Date: 4-8-2013.
Neil Wilmshurst
Neil Wilmshurst

(State of North Carolina)
(County of Mecklenburg)

Subscribed and sworn to (or affirmed) before me on this 8th day of April, 2013, by Neil Wilmshurst, proved to me on the basis of satisfactory evidence to be the person(s) who appeared before me.

Signature Deborah H. Rouse (Seal)

My Commission Expires 2nd day of April, 2016.

<input type="checkbox"/> ANO-1	<input type="checkbox"/> ANO-2	<input type="checkbox"/> GGNS	<input type="checkbox"/> IP-2	<input type="checkbox"/> IP-3	<input type="checkbox"/> PLP
<input checked="" type="checkbox"/> JAF	<input type="checkbox"/> PNPS	<input type="checkbox"/> RBS	<input type="checkbox"/> VY	<input type="checkbox"/> W3	
<input type="checkbox"/> NP-GGNS-3	<input type="checkbox"/> NP-RBS-3				
CALCULATION COVER PAGE	⁽¹⁾ EC # 36003			⁽²⁾ Page 1 of <u>56</u>	
⁽³⁾ Design Basis Calc. <input checked="" type="checkbox"/> YES <input type="checkbox"/> NO		⁽⁴⁾ <input checked="" type="checkbox"/> CALCULATION <input type="checkbox"/> EC Markup			
⁽⁵⁾ Calculation No: JAF-CALC-12-00015				⁽⁶⁾ Revision: 0	
⁽⁷⁾ Title: Core Plate Bolt Fracture Mechanics Evaluation (SIA File No. 1101291.303 Rev 0)				⁽⁸⁾ Editorial <input type="checkbox"/> YES <input checked="" type="checkbox"/> NO	
⁽⁹⁾ System(s): 02-1 Reactor Vessel		⁽¹⁰⁾ Review Org (Department): DE - Civil			
⁽¹¹⁾ Safety Class: <input checked="" type="checkbox"/> Safety / Quality Related <input type="checkbox"/> Augmented Quality Program <input type="checkbox"/> Non-Safety Related		⁽¹²⁾ Component/Equipment/Structure Type/Number: 02V-1			
⁽¹³⁾ Document Type: DCAL					
⁽¹⁴⁾ Keywords (Description/Topical Codes): Core Plate Bolt					
REVIEWS					
⁽¹⁵⁾ Name/Signature/Date <u>Structural Integrity Associates</u> Responsible Engineer		⁽¹⁶⁾ Name/Signature/Date <u>R. Casella / R. Casella 9/10/12</u> <input type="checkbox"/> Design Verifier <input checked="" type="checkbox"/> Reviewer <input type="checkbox"/> Comments Attached		⁽¹⁷⁾ Name/Signature/Date <u>G. Foster / See AS EC 36003</u> Supervisor/Approval <input type="checkbox"/> Comments Attached	

CALCULATION REFERENCE SHEET		CALCULATION NO: <u>JAF-CALC-12-00015</u>				
		REVISION: <u>0</u>				
I. EC Markups Incorporated (N/A to NP calculations) N/A						
1.						
2.						
3.						
4.						
5.						
II. Relationships:	Sht	Rev	Input Doc	Output Doc	Impact Y/N	Tracking No.
1. JAF-CALC-12-00013		0	<input checked="" type="checkbox"/>	<input type="checkbox"/>		
2. JAF-CALC-12-00014		0	<input checked="" type="checkbox"/>	<input type="checkbox"/>		
3.			<input type="checkbox"/>	<input type="checkbox"/>		
4.			<input type="checkbox"/>	<input type="checkbox"/>		
5.			<input type="checkbox"/>	<input type="checkbox"/>		
III. CROSS REFERENCES: See body of calculation.						
1.						
2.						
3.						
4.						
5.						
IV. SOFTWARE USED:						
Title: <u>None</u> Version/Release: _____ Disk/CD No. _____						
V. DISK/CDS INCLUDED:						
Title: <u>N/A</u> Version/Release _____ Disk/CD No. _____						
VI. OTHER CHANGES: None						

Revision	Record of Revision
0	Initial issue.



Structural Integrity Associates, Inc.®

CALCULATION PACKAGE

File No.: 1101291.303

Project No.: 1101291

Quality Program: Nuclear Commercial

PROJECT NAME:

JAF Core Plate Bolt Evaluation

CONTRACT NO.:

10340564

CLIENT:

Entergy Nuclear

PLANT:

James A. Fitzpatrick Nuclear Plant

CALCULATION TITLE:

Core Plate Bolt Fracture Mechanics Evaluation

NOTE: This document references vendor proprietary information. Such information is identified with -2xxP SI Project File numbers in the list of references. Any such references and the associated information in this document where those references are used are identified so that this information can be treated in accordance with applicable vendor proprietary agreements.


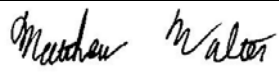



Document Revision	Affected Pages	Revision Description	Project Manager Approval Signature & Date	Preparer(s) & Checker(s) Signatures & Date
0	1 - 45 A-1 - A-8	Initial Issue	 D. V. Sommerville 31AUG12	<p><u>Responsible Engineers</u></p>  M. C. Walter 31AUG12  M. Qin 31AUG12 <p><u>Responsible Verifiers</u></p>  H. L. Gustin 31AUG12  D. V. Sommerville 31AUG12



Table of Contents

1.0 INTRODUCTION 5

2.0 OBJECTIVES 6

3.0 LITERATURE SEARCH 6

 3.1 Crack Morphology for Threaded Components 6

 3.2 Available Fracture Mechanics Solutions 7

 3.3 Existing JAF CP Bolt Fracture Mechanics Evaluations 8

4.0 METHODOLOGY 13

 4.1 Finite Element Model 13

 4.1.1 Loading 15

 4.1.2 Material Properties 16

 4.2 Crack Growth Calculation 16

 4.3 Crack Cases 18

 4.4 Benchmarking and Model Validation 19

5.0 DESIGN INPUT 19

 5.1 Geometry 19

 5.2 Loads and Temperatures 21

 5.3 Materials 21

 5.4 Water Chemistry 23

6.0 ASSUMPTIONS 24

7.0 FINITE ELEMENT MODELS AND CRACK CASES 25

 7.1 General Description and Boundary Conditions for Uncracked FEM 25

 7.2 Single Crack Case 30

 7.3 Adjacent Crack Case 30

 7.4 Far Crack Case 30

 7.5 Single-Max Crack Case 30

 7.6 Thumbnail Crack Case 30

 7.7 ANSYS and Zencrack Input Files 33

8.0 RESULTS 34

 8.1 Calculation of Minimum Acceptable Preload 34

 8.2 Calculation of C Values for Crack Growth Rate Equations 36

 8.3 Single Crack Case 37

 8.4 Adjacent, Far and Single-Max Crack Cases 39

 8.5 Thumbnail Crack Case 40

 8.6 FE LEFM benchmark against Available Hand Calculations 41

9.0 DISCUSSIONS AND CONCLUSIONS 43

10.0 REFERENCES 44

Appendix A ADDITIONAL FE LEFM RESULTS A-1

List of Tables

Table 4-1: Crack Cases	19
Table 5-1: Material Properties	21
Table 5-2: True Stress-Stain Data for Type 304 Stainless Steel at 550°F	22
Table 5-3: JAF Historical Water Chemistry	23
Table 7-1: ANSYS and Zencrack Input Files	33
Table 8-1: Calculated C Values for Each Year	36

List of Figures

Figure 1-1: Core Plate Bolt Assembly	5
Figure 3-1: Typical Crack Configurations for IGSCC and Fatigue Cracks.	9
Figure 3-2: Bolt Initial Crack Orientations	10
Figure 3-3: LEFM Solution and Applicable Coefficients for “Nut” Loaded Threaded Fastener Solution	11
Figure 3-4: Finite Element Model for “Nut” Loaded Threaded Fastener LEFM Solution.	11
Figure 3-5: Summary of Available K Solutions for Threaded Fasteners Provided by Oster and Mills	12
Figure 4-1: Methodology for Determining the Maximum Energy Release Rate by Zencrack	14
Figure 5-1: Bolt and Nut Thread Dimensions with Maximum Tolerance	20
Figure 5-2: Engineering Stress-Stain Data for Type 304 Stainless Steel at 550°F	22
Figure 7-1: Finite Element Model	26
Figure 7-2: Finite Element Model, Bolt and Nut Thread Detail View	27
Figure 7-3: Boundary Conditions Applied to Model	27
Figure 7-4: Pressure Applied for Preload Analysis	28
Figure 7-5: First Principal Stress for Preload Analysis	28
Figure 7-6: Axial Displacement for Preload Analysis, Side View	29
Figure 7-7: Axial Displacement for Preload Analysis, Oblique View	29
Figure 7-8: Axial Displacement as Modeled	29
Figure 7-9: Single Crack Model, Initial Crack Front	31
Figure 7-10: Adjacent Crack Model, Initial Crack Fronts	31
Figure 7-11: Far Crack Model, Initial Crack Fronts	31
Figure 7-12: First Principal Stress Intensity for Uncracked Model	32
Figure 7-13: Single-Max Crack Model, Initial Crack Front	32



Figure 7-14: Thumbnail Crack Model, Initial Crack Front32

Figure 8-1: Single Crack Case, K vs. da Curve37

Figure 8-2: Crack Growth Curves - Single Crack Case, Various Initiation Times38

Figure 8-3: Time Increment Sensitivity Analysis38

Figure 8-4: Comparison of Crack Growth for Each Case39

Figure 8-5: Comparison of K vs. Sum of da for Each Case39

Figure 8-6: Crack Front Propagation, Thumbnail Crack Case40

Figure 8-7: Comparison of K vs. Sum of da for single circumferential crack case –
Oster & Mills, FE LEFM42

Figure 8-8: Comparison of Non-dimensional K Solutions for single circumferential
crack case – Oster & Mills, FE LEFM42

Figure A-1: Crack Front Propagation, Top View, Single Crack Case A-2

Figure A-2: Crack Propagation, Side View, Single Crack Case A-2

Figure A-3: Crack Propagation, Front View, Single Crack Case A-2

Figure A-4: Crack Front Propagation, Top View, Adjacent Crack Case A-3

Figure A-5: Crack Propagation, Side View, Adjacent Crack Case A-3

Figure A-6: Crack Propagation, Front View, Adjacent Crack Case A-3

Figure A-7: Crack Front Propagation, Top View, Far Crack Case A-4

Figure A-8: Crack Propagation, Side View, Far Crack Case A-4

Figure A-9: Crack Propagation, Front View, Far Crack Case A-4

Figure A-10: Crack Front Propagation, Top View, Single-Max Crack Case A-5

Figure A-11: Crack Propagation, Side View, Single-Max Crack Case A-5

Figure A-12: Crack Propagation, Front View, Single-Max Crack Case A-5

Figure A-13: Adjacent Crack Case, K vs. sum of da Curve A-6

Figure A-14: Crack Growth Curves - Adjacent Crack Case, Various Initiation Times A-6

Figure A-15: Far Crack Case, K vs. sum of da Curve A-7

Figure A-16: Crack Growth Curves – Far Crack Case, Various Initiation Times A-7

Figure A-17: Single-Max Crack Case, K vs. sum of da Curve A-8

Figure A-18: Crack Growth Curves – Single-Max Crack Case, Various Initiation Times . A-8

1.0 INTRODUCTION

The James A. Fitzpatrick (JAF) nuclear power plant license renewal commitment number 23 [1, Attachment 1] states that JAF will either install core plate wedges prior to the period of extended operation or complete a plant specific analysis to develop and justify a core plate bolt inspection plan. The inspection plan must include acceptance criteria which meet the requirements of BWRVIP-25 [2]. Figure 1-1 illustrates the main components of the core plate bolt assembly.

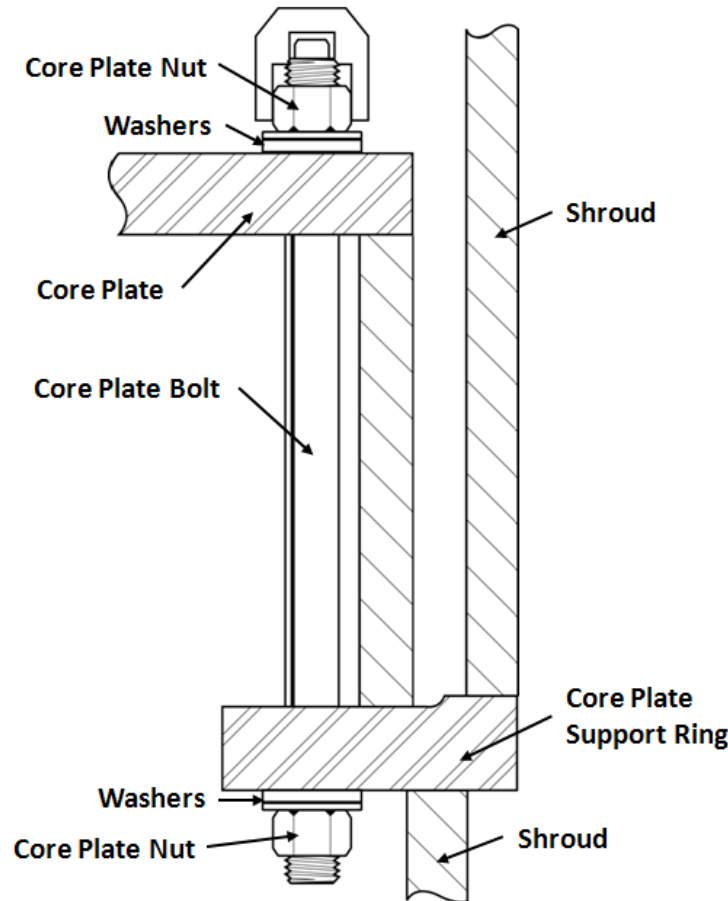


Figure 1-1: Core Plate Bolt Assembly

SI has been contracted by Entergy to perform engineering evaluations necessary to develop an inspection protocol for the JAF core plate bolting which satisfies the requirements of BWRVIP-25 [2]. These evaluations include fracture mechanics evaluations of the Core Plate (CP) bolting. This calculation package documents the fracture mechanics evaluations performed for the JAF core plate bolting in support of the broader effort to develop a CP bolt inspection protocol.

2.0 OBJECTIVES

The objective of this calculation is to evaluate the flaw tolerance of the JAF core plate bolt configuration. The results of this evaluation are used to support development of an appropriate inspection protocol for the JAF core plate bolts.

3.0 LITERATURE SEARCH

This section presents the results of a literature search regarding existing fracture mechanics solutions for threaded fasteners as well as characteristics of intergranular stress corrosion cracking (IGSCC) and fatigue cracking in threaded components. Further, previous JAF CP bolt fracture mechanics evaluations are summarized.

Three symposia focused on structural integrity of fasteners have been hosted by the American Society of Testing and Materials [3, 4, 5]. The proceedings published for these symposia contain an excellent summary of the work performed in the field of fracture mechanics of threaded fasteners. These symposia proceedings are not expected to be comprehensive reviews of all work available on the subject; however, they are considered to be a reasonable and representative review of the state of knowledge in this field. From this work as well as previous calculations performed by SI, the following items are discussed separately below:

1. Crack morphology appropriate for expected forms of degradation in JAF CP bolting,
2. Available fracture mechanics solutions and their limitations,
3. Existing JAF CP bolt fracture mechanics evaluations and their limitations.

3.1 Crack Morphology for Threaded Components

SI evaluated the JAF CP bolting against known forms of degradation in the Boiling Water Reactor (BWR) environment in order to identify the applicable forms of degradation which might affect integrity of this component during the period of original license and extended operation [6]. The results of this evaluation concluded that fatigue cracking and IASCC is not expected. Although the component was considered to possess little susceptibility to IGSCC, the possibility of IGSCC could not be conclusively eliminated. Consequently, the only form of degradation, which could affect integrity of the load carrying member, is IGSCC.

IGSCC initiates under the simultaneous presence of a sustained tensile stress, an oxidizing environment, and a susceptible material. Review of the CP bolt configuration [6] concluded that the likely place for IGSCC initiation, if it were to initiate, would be at the root of the threads. Since the peak stress at the root of a threaded fastener exhibits little variation along the length of the first engaged thread, it is likely that IGSCC could initiate anywhere along the highest stressed thread. Further, since load transfer across a threaded joint occurs across the first few engaged threads, it is possible that IGSCC could initiate at adjacent threads, either immediately adjacent or separated by a few threads. Recognizing that the presence of threads contributes a stress concentration in the threaded fastener and that this stress concentration will intensify the stress at the root of the thread along the entire threaded length, it is possible that IGSCC could initiate at the root of any thread; however, the probability of initiation is expected to be higher at the location of largest stress.

Existing studies have shown that IGSCC will initiate at multiple sites along the length of a thread root. These incipient cracks will then grow until they coalesce and form a quasi-circumferential crack [7]. In contrast to this, a fatigue crack typically initiates at a single site and grows until it achieves an “edge crack” configuration [8]. These two configurations are illustrated in Figure 3-1.

Renauld, Lien, and Wilkening [9] used two-dimensional, elastic plastic finite element modeling to explain observed stress corrosion cracking (SCC) initiation behavior of test fasteners in pressurized water. Figure 3-2 illustrates the crack orientations observed in the thread roots and a corresponding finite element fringe plot of maximum principal stress. The macroscopic angle of crack initiation and growth rotates from nearly perpendicular to the free surface of the fastener for the first unengaged thread to around 30° along the pressure flanks for the second and third engaged thread. The maximum principal stress predicted by the elastic plastic finite element model rotates in a similar fashion.

Consequently the expected flaw configuration for IGSCC flaws in the CP bolting is somewhere between a fully circumferential crack and a single edge crack with the crack initiating normal to the direction of the maximum principal stress. Presence of multiple cracks in adjacent threads can be addressed by considering fully circumferential cracks in multiple threads.

3.2 Available Fracture Mechanics Solutions

Oster and Mills [10] developed a linear elastic fracture mechanics (LEFM) solution for an opening (tensile) mode (mode I) loading of standard Unified National Coarse (UNC) thread forms for remote loading and nut loading cases. “Remote” loading refers to a situation where the load is applied remote from the crack location; whereas, “nut” loading refers to the situation where the load is applied to the threaded fastener through the thread faces, from a nut. Figure 3-3 is an excerpt from Oster and Mills [10] which shows the form of the LEFM solution and the appropriate coefficients for use with the “remote” and “nut” loaded solutions. Figure 3-4 illustrates the configuration of the “nut” loaded condition. This LEFM solution was developed based on two-dimensional finite element models with an initial horizontal continuous circumferential crack. The direction of the crack propagation is assumed to remain normal to the direction of the remote loading (horizontal in Figure 3-4). Figure 3-5, also excerpted from Oster and Mills [10], presented the normalized stress intensity factor for mode I loading (K_I) for many of the threaded component K_I solutions available at the time, for both edge crack and fully circumferential crack configurations, also for both “nut” and “remote” loading.

The results presented in Figure 3-5 illustrate the following:

1. The fully circumferential crack case produces larger K_I values than the edge crack configuration,
2. The “nut” loaded condition produces larger K_I values than the “remote” loaded condition when the crack depth is in the vicinity of the thread root; whereas, when the crack depth extends beyond the thread root the “nut” and “remote” loaded conditions produce essentially equal K_I values.

3.3 Existing JAF CP Bolt Fracture Mechanics Evaluations

SI has previously performed two fracture mechanics evaluation of the JAF CP bolting [11, 12]. One evaluation considered a postulated fully circumferential crack [11] and the other considered a postulated edge crack [12]. Both evaluations considered the water chemistry data available for operation up to the time of the calculation and applied assumed water chemistry values for future operation. One evaluation used a hand solution for a “remote” loaded rod in which the effective depth of the crack was taken as the depth of the thread plus the crack depth [11]. The second evaluation used finite element fracture mechanics to determine stress intensity factor distributions along the crack front for semi-elliptical edge cracks of varying depths. Thermal relaxation was considered; however, primary creep and radiation induced relaxation effects were conservatively omitted from these evaluations. Crack growth evaluations were performed in both calculations using the K_I versus crack depth relationships determined from these evaluations. The CP bolt exhibited little flaw tolerance when the fully circumferential crack condition was evaluated. Similarly, the CP bolt exhibited little flaw tolerance when the highest K_I values along the edge crack front were considered. When the K_I values at the deepest point of the edge crack were considered then the CP bolt exhibited substantially greater flow tolerance.

Although these earlier evaluations provide useful insight into the structure they do include some inherent limitations:

1. The “remote” loaded condition has been shown to produce lower K_I values when a crack is small (near the region in which the stress concentration caused by the thread root is dominant).
2. An edge crack configuration is inconsistent with the expected IGSCC morphology.
3. Actual water chemistry data exists for the period of operation between 2001 and 2012; therefore, these data should be considered rather than the assumed parameters used in the previous work.
4. The previous evaluations did not consider the possible presence of multiple cracks in adjacent threads.
5. The previous evaluations forced the crack to remain horizontal. Crack front turning and its possible beneficial effect on flaw tolerance of the structure was not evaluated.

Consequently, a refined evaluation is performed, as documented in this calculation, in order to address these items.



FIG. 3—Crack surface in a threaded bar. Courtesy of R. R. Cervay.

a) Typical fatigue crack configuration. [8]

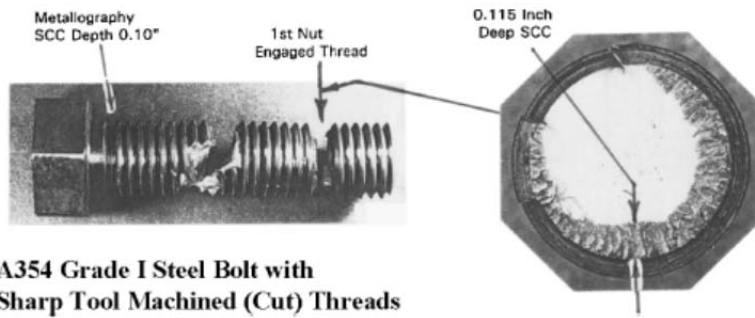


FIG. 3—IGSCC site shape and crack depth in cut threads of grade steel fasteners, tensioned for fractographic evaluation, after one day of SCC testing at 414 MPa.

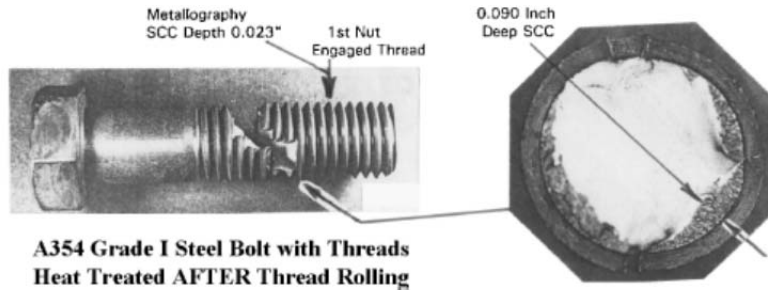


FIG. 4—IGSCC site shape and crack depth in grade 8 bolts heat treated AFTER thread rolling, after one day of SCC testing at 531 MPa.

b) Typical IGSCC configuration. [7]

Figure 3-1: Typical Crack Configurations for IGSCC and Fatigue Cracks [7, 8].

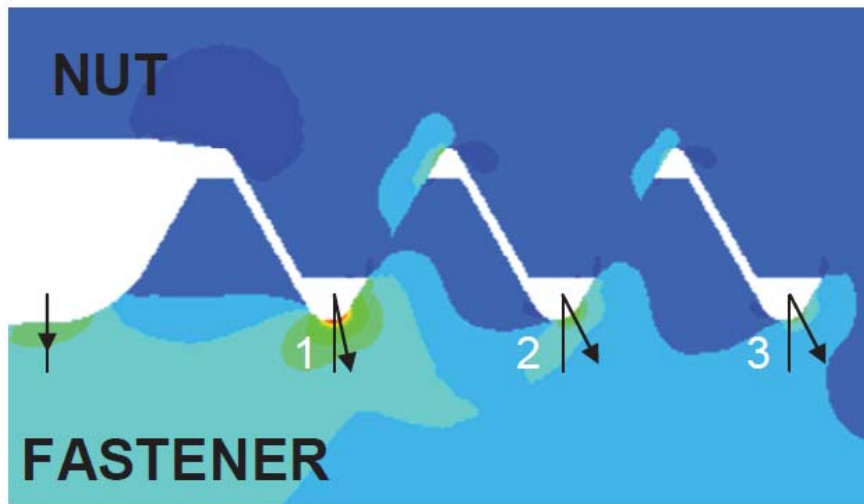
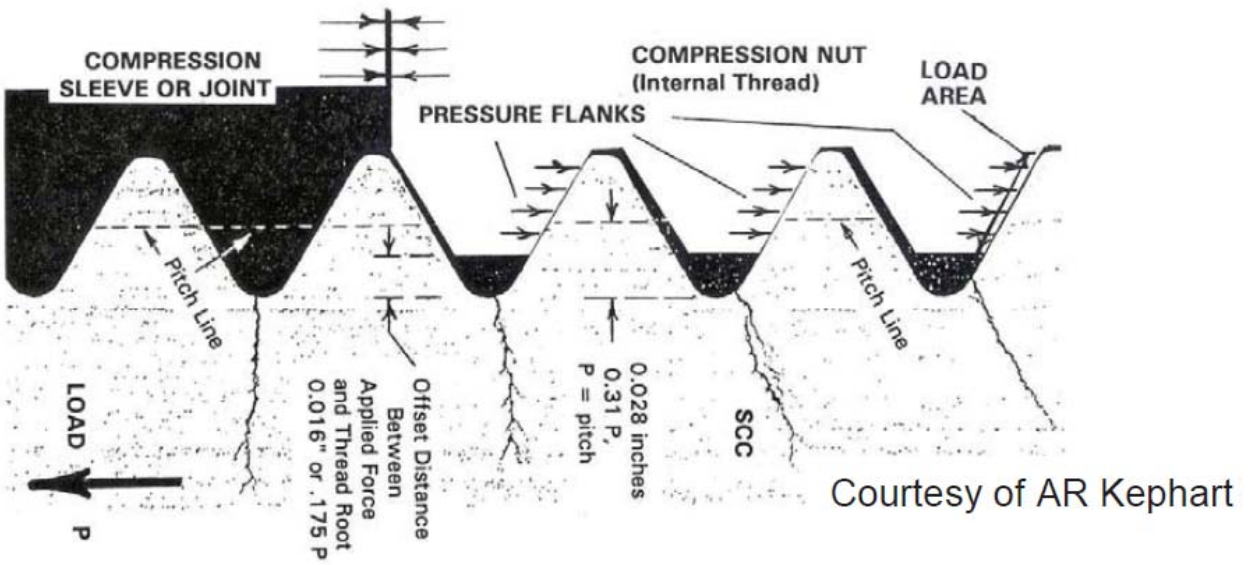


Figure 3-2: Bolt Initial Crack Orientations [9, Figure 10]

TABLE 2—Regression constants for nondimensional K solutions for continuous circumferential cracks in notched bars and UNC threaded fasteners.

Thread Form	q	r	s	t	u	v	w	x	y
NOTCH/Remote Loading (Validity Range: $0.005 \leq a/d \leq 0.4$)									
1/4-20	2.9724	2.3701	146.14	-49.168	663.24	-4756.3	19 040.4	-39 186.6	32 963.9
1/2-13 to 2-4.5	2.6878	2.3931	156.61	-43.165	598.38	-4372.3	17 803.4	-37 149.5	31 623.6
4-4	2.2356	2.6467	199.32	-32.956	483.94	-3651.2	15 267.7	-32 539.5	28 264.2
THREADED FASTENER/Remote Loading (Validity Range: $0.003 \leq a/d \leq 0.4$)									
1/4-20	2.1209	1.6351	181.09	-35.837	574.20	-4517.7	19137.2	-40763.3	34960.7
1/2-13 to 2-4.5	1.7303	1.4640	198.17	-24.232	435.79	-3682.2	16443.9	-36347.5	32073.7
4-4	1.4137	1.5347	299.43	-12.082	253.55	-2366.9	11529.0	-27203.4	25391.2
THREADED FASTENER/Nut Loading (Validity Range: $0.003 \leq a/d \leq 0.4$)									
1/4-20 to 2-4.5	3.0149	2.4902	166.26	-51.624	722.92	-5342.9	21757.0	-45123.3	37900.2

$$\frac{K}{\sigma\sqrt{\pi a}} = q + r e^{-s(a/d)} + t \frac{a}{d} + u \left(\frac{a}{d}\right)^2 + v \left(\frac{a}{d}\right)^3 + w \left(\frac{a}{d}\right)^4 + x \left(\frac{a}{d}\right)^5 + y \left(\frac{a}{d}\right)^6$$

where a = crack depth, measured from root of notch or thread, and d = minor diameter of notch or thread.

Figure 3-3: LEFM Solution and Applicable Coefficients for “Nut” Loaded Threaded Fastener Solution [10]

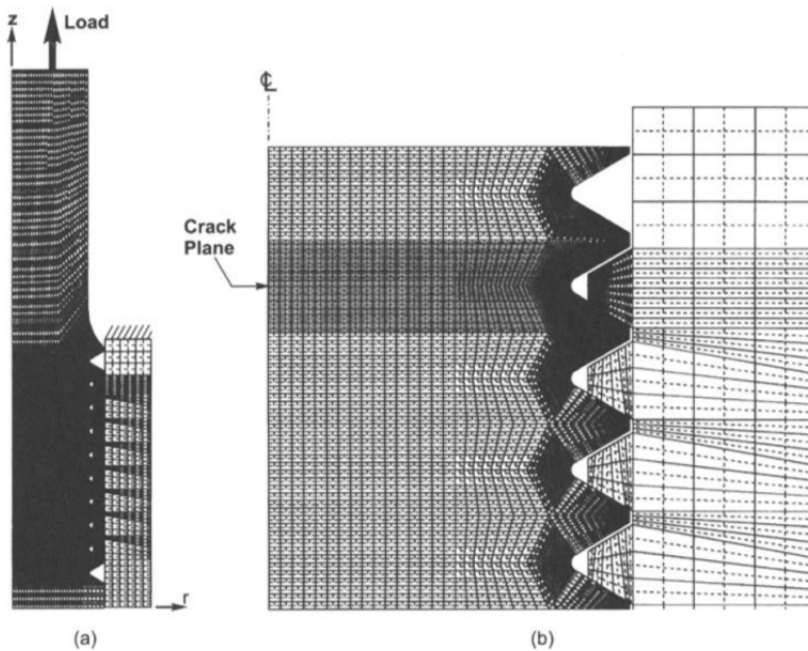


FIG. 2—Finite-element model of stud subjected to nut loading. (a) Axisymmetric model of stud and nut. (b) Enhanced detail of thread/nut engagement (all threads are not shown).

Figure 3-4: Finite Element Model for “Nut” Loaded Threaded Fastener LEFM Solution [10]

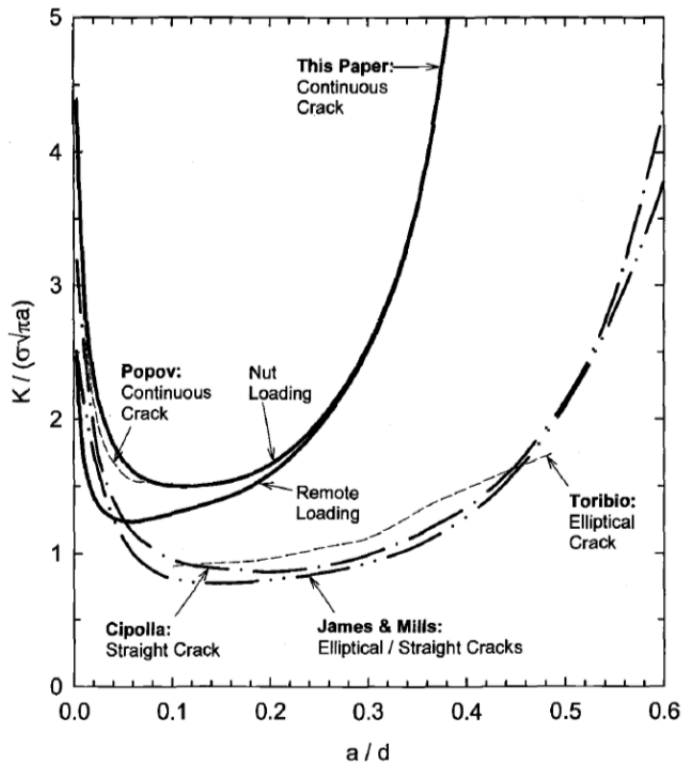


FIG. 11—Comparison of nondimensional K solutions developed by FEM analysis for fasteners subjected to nut loading and remote loading (solid curves) with literature solutions (broken curves) [1-3,6,7].

Figure 3-5: Summary of Available K Solutions for Threaded Fasteners Provided by Oster and Mills [10]

4.0 METHODOLOGY

The methodology selected for this evaluation is intended to address the limitation of the previous evaluations identified above and incorporate information presented in the open literature subsequent to the previous evaluations [11, 12]. The general methodology used for this evaluation is identified first followed by detailed discussion of each aspect of the methodology in separate subsections below:

1. Use 3-D finite element analysis (FEA) in order to simulate contact between the nut and bolt and to perform finite element (FE) linear elastic fracture mechanics (LEFM) evaluations of single and multiple crack cases of various crack configurations. This method enables consideration of crack front turning, and the effects of non-uniform crack front stress intensity factor distribution on crack growth.
2. Use elastic plastic FEA to quantify compliance induced relaxation as the crack grows deeper into the cross-section of the CP bolt.
3. Use BWRVIP-14-A [13] crack growth rate (CGR) correlations for K-dependent and environment dependent crack growth rates in the stainless steel CP bolting.
 - a. This CGR correlation provides crack growth rates representative of a 95% confidence interval “upper bound” on the data set used to develop the correlations.
 - b. Plant specific water chemistry data is used for periods of prior operation and expected plant values are used for future operation.
 - c. The FE LEFM results are used to provide the K versus crack depth relationships for each crack cases considered.
4. Determine the residual life of a CP bolt for various crack cases considering different assumed crack initiation times.
 - a. Data presented in the open literature are used to identify crack locations, number of cracks, and crack shapes considered in the evaluations
 - b. Crack growth simulations are terminated once the retained preload becomes less than the normal operation applied loading on each bolt. At this time it is assumed that leakage flow may develop since the core plate assembly can lift off the core support ring. Since this condition is inconsistent with the design basis of the assembly it is not considered acceptable. Further, if there is zero net normal force between the core plate assembly and core support ring then there is no friction force available to resist the lateral loading on the core plate assembly caused by a seismic event. This would enable lateral core plate assembly movement which could impede control rod insertion which is also unacceptable.

4.1 Finite Element Model

This section describes the finite element model (FEM) built for both the compliance induced relaxation and the LEFM calculations.

The core plate bolt assembly is modeled using the ANSYS 12.1 finite element software [16] using 3-dimensional structural solid elements (SOLID185 with enhanced strain formulation). Contact between the nut and bolt surfaces is simulated using contact elements (CONTA174 and TARGE170). A quarter-

symmetry model is used for all crack cases. Since the minimum bolt size and maximum nut size defined by the thread form tolerance will cause higher stresses at the thread root, these dimensions are used for the evaluation.

Generation of the cracked mesh, calculation of the fracture mechanics parameters, and incremental advance of the crack front is performed using the Zencrack program developed by Zentech [17]. Zencrack uses the magnitude and direction of maximum energy release rate for fracture mechanics calculations. Zencrack determines the energy release rate by using nodal displacements near the crack tip to calculate stress intensity factors, followed by conversion to energy release rate. In this method, the crack tip displacements and nodal displacements on the crack face near the crack front are used for calculating stress intensity factors. The crack growth direction is determined by the maximum energy release rate direction. This is calculated at an angle to the local crack face in a local opening (tensile) mode for Mode I and an in-plane sliding (shear) mode for Mode II plane at each crack front node. Figure 4-1 shows the methodology to determine the maximum energy release rate. First, 7 virtual crack extensions are assumed for each crack front node in the Mode I and II plane. Second, the energy release rate is calculated for each direction and an energy release rate vs. direction curve is generated. Finally, the maximum energy release rate (G_{\max}) and corresponded direction (θ_{\max}) are determined.

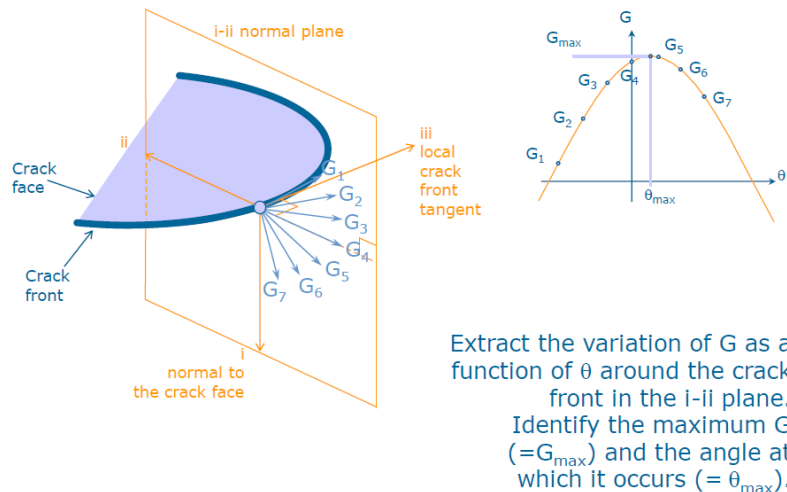


Figure 4-1: Methodology for Determining the Maximum Energy Release Rate by Zencrack [17]

First, Zencrack creates an initial “cracked” meshed starting from an uncracked ANSYS model and user-defined crack locations, sizes, and crack growth data. Next, the user defined load cases are evaluated in ANSYS using the “cracked” mesh and the ANSYS built-in fracture mechanics calculation functions are used to calculate the stress intensity factor and energy release rate at each node along the crack front. These results are then analyzed in Zencrack to determine the nodal crack growth direction and crack growth distance. Crack growth is determined using a user defined crack growth rate equation. Zencrack rebuilds the cracked model by advancing the nodal positions along the crack front. Finally, this process is repeated and the crack front is grown until Zencrack reaches a use defined termination criterion or a modeling error occurs which forces the process to terminate. If further crack growth simulation is desired then the mesh can be adjusted and a new crack run can be initiated starting with a crack of size and shape determined by the final available solution from the previous run.

The crack growth simulation in Zencrack is terminated when the retained preload is approximately equal to the value of the applied vertical loading per bolt contributed by the reactor internal pressure difference. This load is the applied loading acting on the core plate assembly during normal operation, except for the infrequently assumed Level A/B seismic event or the postulated Level C/D seismic event. This evaluation assumes that once the retained preload is less than the applied loading that some amount of separation between the core support ring and core plate assembly may occur and bypass leakage may occur. This condition could result in flow induced vibration damage or fretting; thus, it is not an acceptable design condition.

4.1.1 Loading

The bolt preload is the only relevant load for this evaluation. The bolted joint is designed such that the initial preload is sufficient to ensure the core plate assembly remains in position and such that the preload is larger than the applied vertical loading. Lateral loads acting on the core plate assembly are reacted by friction loading between the core support ring and the core plate assembly rim. The core plate bolt assembly includes cylindrical washers between the core plate and nut on the top and the core support ring and nut on the bottom; therefore, the applied loading remains purely axial.

The effects of thermal relaxation, primary creep and radiation relaxation on the applied preload is evaluated in Reference [14]. Thermal relaxation is calculated to be approximately 23.4% and primary creep results in an additional 6.8% reduction in preload. These two effects occur in a very short time period during initial heat-up and within a short period following operation at full temperature. Consequently, the cumulative relaxation from these two mechanisms is applied at time zero for this evaluation. The radiation induced relaxation is calculated to be approximately 8% after 60 years of plant operation. Radiation relaxation is conservatively ignored in this calculation since this effect is time-dependent and would require a time-dependent relaxation logic to be included in the FEA. Since a lower preload will reduce the driving force on the crack which in turn reduces the crack growth rate, omission of this effect is an inherent conservatism in this evaluation.

As the postulated crack grows deeper into the CP bolt the increased compliance will reduce the retained preload. This reduction in preload will reduce the driving force on the crack which in turn will reduce the crack growth rate. To simulate this effect the preload is applied to the FEM as a constant displacement at the nut. This displacement is calculated from the “uncracked” FEM by applying a pressure on the nut equivalent to the axial force applied to the CP bolt from the initial torque, determined using the following formula:

$$P = F / [(D_o^2 - D_i^2) \cdot \pi / 4]$$

Where,

P	=	Applied pressure, psi
F	=	Preload, lbf
D _o	=	Width across flat of nut, in
D _i	=	Minor diameter of nut, in

The average displacement at the bottom of the nut is then determined from ANSYS and applied to the subsequent analyses as the applied loading.

This analysis uses linear elastic fracture mechanics for the crack growth analysis. If elastic plastic properties were considered, the compliance of the cracked model would reduce the stresses in the crack region and therefore a slower crack growth rate would be calculated. Therefore, the linear elastic fracture mechanics analysis is conservative for the crack growth analysis. An elastic plastic analysis is only performed in order to ensure the remaining preload is greater than the minimum required preload. If the elastic plastic analysis calculates a remaining preload that is less than the minimum required preload, this constitutes a failure of the bolt.

Although compliance induced preload relaxation is determined using an elastic plastic material model, all LEFM evaluations are performed using a linear elastic material model.

4.1.2 Material Properties

Since the crack growth rate correlation used for this evaluation uses the Mode I stress intensity factor, K_I , which is a LEFM parameter, linear elastic material properties are used for the Zencrack crack growth analyses.

Compliance induced preload reduction is determined using an elastic plastic material model in order to more accurately simulate when large scale plasticity in the vicinity of the crack tip might result in loss of preload. The stress strain curve for Type 304 stainless steel contained in Reference [15] is used in this evaluation. A multilinear model is used for this process.

4.2 Crack Growth Calculation

BWRVIP-14-A [13] lists three methods which can be used for calculation of a CGR in stainless steel materials in the BWR environment:

1. K Independent Approach
2. K Dependent Approach
3. K and Environment Dependent Approach

The K independent approach is developed using a stress intensity factor of $25 \text{ ksi}\sqrt{\text{in}}$, an ECP = 200 mV[SHE], and an average conductivity = $0.15 \mu\text{S}/\text{cm}$. Since the present evaluation will consider variations in water chemistry indicative of actual operation of the JAF nuclear power plant and since it is already known [11, 12] that the expected K_I for the core plate bolt assembly will range both above and below $25 \text{ ksi}\sqrt{\text{in}}$ the K independent approach is not considered appropriate for the intent of this evaluation. Although the K and Environment dependent approach is ideal for the present evaluation since it inherently considers variations in water chemistry and stress intensity factor, its application is limited to water conductivity less than $0.3 \mu\text{S}/\text{cm}$. For this evaluation the K dependent method is used for the period of time for which the JAF water chemistry violates the conductivity limits of the K and environment dependent approach. Although there are also water chemistry limits applied to the K dependent approach it is readily apparent, when the results of this evaluation are observed, that the difference in flaw tolerance of the core plate bolt assembly, early in plant life, is negligible regardless of which CGR is used.

[Redacted Proprietary Information]

The conductivity and electrochemical corrosion potential are obtained from plant data for historical operation and assumed for future operation. Stress intensity factor input comes from the FE LEM evaluations performed using ANSYS and Zencrack.

In this calculation, flaws are assumed to initiate at 0, 15, 20, 25, and 30 years of operation. These times are used to investigate the relative flaw tolerance of the core plate bolt assembly considering the variation in water chemistry over plant life.

A Visual Basic algorithm is written to perform the numerical integration for crack growth. The FE LEFM K distribution and the plant specific water chemistry input are input into this algorithm along with a user defined initial flaw size, crack initiation time, and integration time interval. The integration is performed as a simple summation of incremental crack growth calculations. Since the K distribution obtained from the FE LEFM evaluation is a series of stress intensity factors for various crack depths, a polynomial curve fit is determined to facilitate calculation of a K for each crack growth iteration rather than use of a look-up table. Conversely the JAF plant specific water chemistry was not amenable to a smooth curve fit; therefore, a look-up table is used for the crack growth calculation. Crack growth calculations are performed using two different time increments in order to validate that the time increment selected was sufficient.

4.3 Crack Cases

Based on the results of the literature search [7], it is expected that actual IGSCC in the JAF core plate bolting would exhibit a shape somewhere between the fully circumferential and edge crack cases. It is expected that the fully circumferential case is a more appropriate representation of IGSCC since multiple initiation sites are possible and test data [7], as well as existing fracture mechanics studies [12] show that multiple thumbnail cracks would likely coalesce into one sickle shaped or circumferential crack. Consequently, the fully circumferential crack shape is considered in this evaluation. This shape is a worst case, bounding configuration since this shape will result in the highest stress intensity factor and the quickest reduction in net section. For additional information, a test run is performed using a thumbnail shaped crack to validate the crack growth behavior inferred from References [7, 12].

An initial crack depth of 0.01 inches is assumed for all crack cases. The initial flaw is located at the highest stressed thread in the bolt. The initial flaw orientations are assumed as horizontal at the root of the thread in the bolt or normal to the direction of maximum principal stress at the highest stressed location in the thread root. To investigate the effect of multiple flaws having initiated in separate threads, two different two-flaw cases are studied in this analysis. One case postulates that the second flaw is at the adjacent thread, and the other case postulates the second flaw is at furthest thread away. It is expected that cracks in multiple threads simultaneously will be bounded by or at least reasonably represented by the single crack case since multiple cracks will tend to be shielded by the first crack in the load path. Rather than make this assumption, the multiple crack cases were performed to show this behavior. Table 4-1 describes each crack case considered in this evaluation.

Table 4-1: Crack Cases

Name	Crack Locations	Initial Crack Orientation	Shape
Single	1 crack at high stressed thread	Horizontal at root of thread	Fully circumferential
Adj	2 cracks, one at highest stressed thread and the other at the adjacent thread		Fully circumferential
Far	2 cracks, one at highest stressed thread and the other at the thread furthest away		Fully circumferential
Single-Max	1 crack at high stressed thread	Normal to the direction of the maximum principal stress location	Fully circumferential
Thumbnail	1 crack at high stressed thread	Horizontal at root of thread	Semi-circular

Note: All crack cases assume a flaw depth of 0.01”.

4.4 Benchmarking and Model Validation

Adequacy of the FE implementation and calculation of the fracture mechanics parameters are assessed by comparing FE results to results obtained from an available hand solution for a similar configuration. Adequacy of the Zencrack software is documented in numerous benchmark cases described in the Zencrack QA manual [30].

Adequacy of the time step size used in the numerical crack growth integration is assessed by performing a temporal sensitivity study using a smaller time step and comparing crack growth results for a sample case.

5.0 DESIGN INPUT

The design inputs used in the core plate bolt fracture mechanics evaluation are discussed in this section.

5.1 Geometry

The core plate bolt and core plate geometry are listed below:

- Bolt nominal diameter: 1.125 inches [18, 19]
- Bolt thread form: 1 1/8-12UNF-2A [18, 19]
- Bolt length (between nuts): 21.813 inches (minimum) [19]
- Pitch, P 1/12” [page 1837, 20]
- Height of a sharp V-thread, H 0.8660P [page 1727, 20]
- Min. Major Dia. of bolt 1.1118” [page 1745, 20]
- Min. Pitch Dia. of bolt 1.0631” [page 1745, 20]
- Max. Minor Dia. of nut 1.053” [page 1745, 20]
- Max. Pitch Dia. of nut 1.0787” [page 1745, 20]

- Height of nut 1" [page 1520, 20]
- Width across flats of nut 1.688" [page 1520, 20]
- Inner diameter of core plate 166" [21]
- Diameter of fuel hole 10.875" [22]
- Number of fuel holes 137 [21]
- Inner diameter of peripheral bundle 3.5625" [21]
- No. of peripheral bundles 12 [21]
- Instrument hole diameter 1.863" [21]
- No. of instrument holes 43 [21]

Since the minimum bolt and maximum nut tolerance dimensions will cause higher stresses at the bolt thread root location, these tolerance dimensions are used for this evaluation. Figure 5-1 shows the bolt and nut thread dimensions.

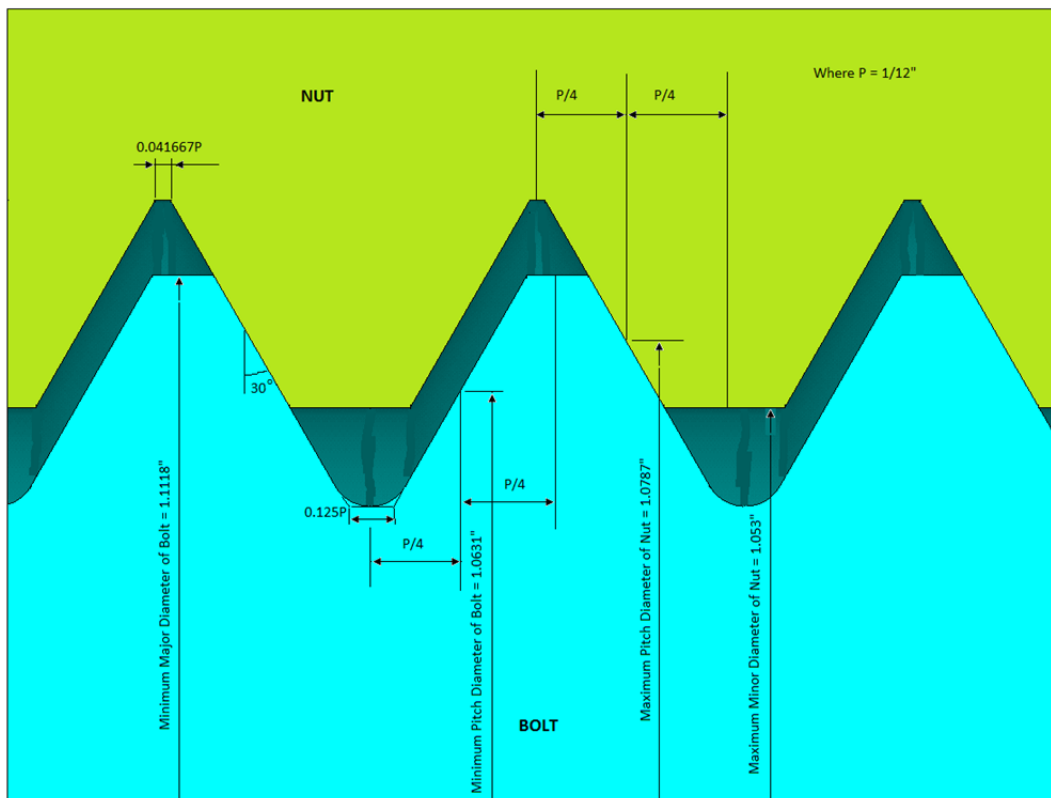


Figure 5-1: Bolt and Nut Thread Dimensions with Maximum Tolerance [20, p. 1774]

5.2 Loads and Temperatures

The core plate bolt preload, relaxation, and reactor vessel loads are listed below:

- Initial bolt preload 19,556 lbf [14]
- Preload reduction due to thermal relaxation 23.4% [14]
- Preload reduction due to stress relaxation 6.8% [14]
- Preload reduction due to Radiation relaxation 8.0% [14]
- Preload reduction after thermal and stress relaxation $19,566(1 - 0.234)(1 - 0.068) = 13,961$ lbf
- Reactor internal pressure differences (RIPD) at Level A/B 29.76 psi [18]

The temperatures and pressures in different regions of the JAF reactor pressure vessel (RPV) are taken from the RPV thermal cycle diagram (TCD) [23]. The core plate is located below the core, which corresponds to either the bottom of Region B or the top of Region C [23]. Both regions are considered and the bounding service conditions are summarized as follows:

- RPV normal operating pressure: 1040 psig [23]
- Regions B and C normal operating temperature: 527°F [23]
- Region B maximum temperature: 551°F [23]

5.3 Materials

The CP bolt material is Type 304 stainless steel in accordance with ASTM A-193, Grade B-8 [18, 24]. The elastic modulus for Type 304 SS is taken from the ASME Boiler & Pressure Vessel Code, Section III 1965 edition with Addenda through 1966 [25] and is listed in Table 5-1 below at 70 °F and 550 °F. The stress-strain curve for Type 304 stainless steel material at 550°F is taken from Reference [15] and summarized in Table 5-2 and Figure 5-2 below.

Table 5-1: Material Properties

Material Property	Temperature	
	70 °F	550 °F
Elastic Modulus, E (ksi)	27,400	25,700

Table 5-2: True Stress-Stain Data for Type 304 Stainless Steel at 550°F [15, Table 3-3]

Strain (in/in)	Stress (ksi)
1.55E-04	3.96E+00
3.17E-04	7.91E+00
5.09E-04	1.19E+01
7.81E-04	1.58E+01
1.21E-03	1.98E+01
1.93E-03	2.37E+01
3.07E-03	2.77E+01
4.85E-03	3.17E+01
7.52E-03	3.56E+01
1.14E-02	3.96E+01
1.68E-02	4.35E+01
2.41E-02	4.75E+01
3.39E-02	5.14E+01
4.66E-02	5.54E+01
6.28E-02	5.94E+01
8.32E-02	6.33E+01
1.09E-01	6.73E+01
1.40E-01	7.12E+01
1.77E-01	7.52E+01
2.23E-01	7.91E+01
2.76E-01	8.31E+01
3.40E-01	8.71E+01

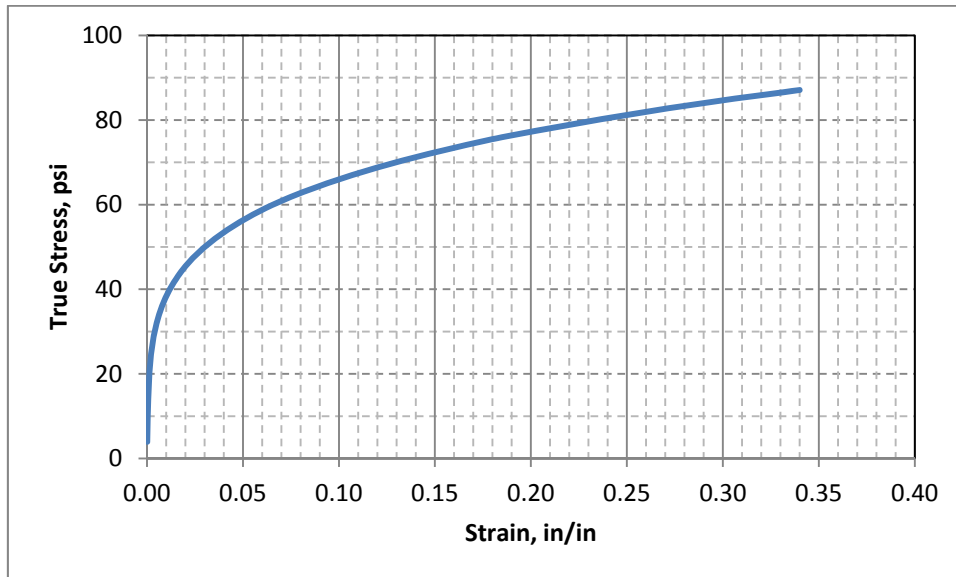


Figure 5-2: Engineering Stress-Stain Data for Type 304 Stainless Steel at 550°F [15, Table 3-3]

5.4 Water Chemistry

Water chemistry inputs are taken from References [18, 26, and 27], and are summarized in Table 5-3 below. The C value for use with Equation 4 can be calculated using the conductivity and ECP values from Table 5-3 and using a water temperature of 550°F.

Table 5-3: JAF Historical Water Chemistry

Year	Rx Water Conductivity, ($\mu\text{S}/\text{cm}$)	ECP, (mV SHE)
1975	1.315	+200
1976	0.485	+200
1977	0.998	+200
1978	0.793	+200
1979	1.103	+200
1980	2.053	+200
1981	0.796	+200
1982	0.507	+200
1983	0.540	+200
1984	0.230	+200
1985	0.389	+200
1986	0.115	+200
1987	0.342	+200
1988	0.427	+200
1989	0.125	+200
1990	0.255	+200
1991	0.171	+200
1992	0.001 ⁽¹⁾	-1000 ⁽¹⁾
1993	0.100	+200
1994	0.095	+200
1995	0.074	-50 ⁽²⁾
1996	0.071	-50 ⁽²⁾
1997	0.066	-50 ⁽²⁾
1998	0.067	-50 ⁽²⁾
1999	0.085	Jan. - Nov. +200 Dec. -230
2000	0.095	-230
2001	0.069	-230
2002	0.09	-400
2003	0.09	-400
2004	0.10	-400
2005	0.10	-400
2006	0.11	-400
2007	0.11	-400
2008	0.14	-400
2009	0.17	-400
2010	0.15	-400
2011	0.11	-400
2012 - 2035 ⁽³⁾	0.1	-400

- Notes: 1. Conductivity and ECP are assumed to be 0.001 $\mu\text{S}/\text{cm}$ and -1,000 mv SHE, respectively while the plant was shut down in 1992. In general, there is no crack growth during the shutdown period.
 2. The higher of the two ECP values provided in Reference [26] is used for conservatism.
 3. The water chemistry values for 2012 – 2035 are assumed as described in Section 6.0, Assumption 3.



6.0 ASSUMPTIONS

The following assumptions are used in this evaluation:

1. The elastic modulus that is listed in Table 5-1 is based on 1965 ASME code with 1966 addenda [25], however, material properties used in the FEA are taken from the 2001 Edition of the ASME Code [28]. The difference between the values contained in these two Code years is insignificant; the value of elastic modulus contained in the 2001 Edition of the ASME Code is 25,550 ksi which is only 0.6% different than the value in Table 5-1.
2. Poisson's ratio for stainless steels is assumed as 0.3 [29, Section 46-4]. This is consistent with standard engineering practice and is representative for the materials considered in this calculation package.
3. The water chemistry values for 2012 through 2035 (end of period of extended operation) are assumed based on input provided by Entergy in Reference [27]. These assumed values are considered reasonable based on the water chemistry history from 2002 through 2011.
4. All material properties are based on a maximum Region B temperature of 550°F, which is considered sufficiently representative of the temperature of the core plate bolt.
5. Reference [15] used the ultimate tensile stress at 550°F to create the stress-strain curve and this data is unavailable in the 1965 ASME code with 1966 addenda [25]. Since the elastic modulus from both 1965 code and 2001 code are very close (see Assumption 1), the material properties contained in the 2001 Edition of the ASME Code [28] are used in this calculation.
6. A fully circumferential crack case is assumed in this analysis. This flaw shape is a worst case shape since it represents the condition which would result in the largest driving force. Multiple thumbnail flaws would each exhibit lower stress intensity factors and consequently slower growth through the depth direction; however, they would be expected to grow rapidly around the circumference of the thread and eventually coalesce into a larger fully circumferential crack. The circumferential crack shape assumed in this evaluation bounds the possibility of multiple initiation sites.
7. The initial crack is assumed to be located at the first engaged thread, since the first engaged thread has the highest stresses in the entire core plate bolt. Since IGSCC initiation is a function of sustained stress, susceptible material, and an oxidizing environment, it is considered more likely that IGSCC will initiate at the highest stress location since the material condition and environment are considered identical from thread to thread.
8. The initial flaw orientations are assumed to be horizontal at the root of thread or normal to maximum stress location at root of thread. The horizontal orientation is analytically expedient; whereas, the orientation normal to the direction of the maximum principal stress is considered more physically appropriate. This analysis includes both orientations; thus, conclusions can be drawn regarding adequacy of the horizontal assumption.
9. An initial crack depth of 0.01 inches is assumed. Flaw tolerance for larger assumed flaw depths can be determined from the results obtained from the 0.01 inch initial flaw size; thus, consideration of a 0.01 inch initial flaw size does not represent a limitation of the analysis. A

smaller flaw size was not considered in this evaluation since insufficient data exists from which to justify a true initiation size.

10. The models used in this analysis assume that threaded fasteners consist of a series of parallel notches, rather than a continuous helix. The effect of ignoring the helix shape on the Mode I stress intensity factor is judged to be small, particularly since the helix angles are small.
11. The worst tolerance for the bolt/nut geometry is assumed for this analysis, since it will cause the highest stress at the thread root which will result in a larger driving force and faster crack growth.
12. Radiation relaxation is omitted in this analysis since this effect is time-dependent and would result in a more complex crack growth calculation. Omission of this effect is conservative since additional relaxation of the applied loading would reduce the driving force and reduce crack growth rates.

7.0 FINITE ELEMENT MODELS AND CRACK CASES

This section describes the details of the “uncracked” and “cracked” FEMs built for this evaluation.

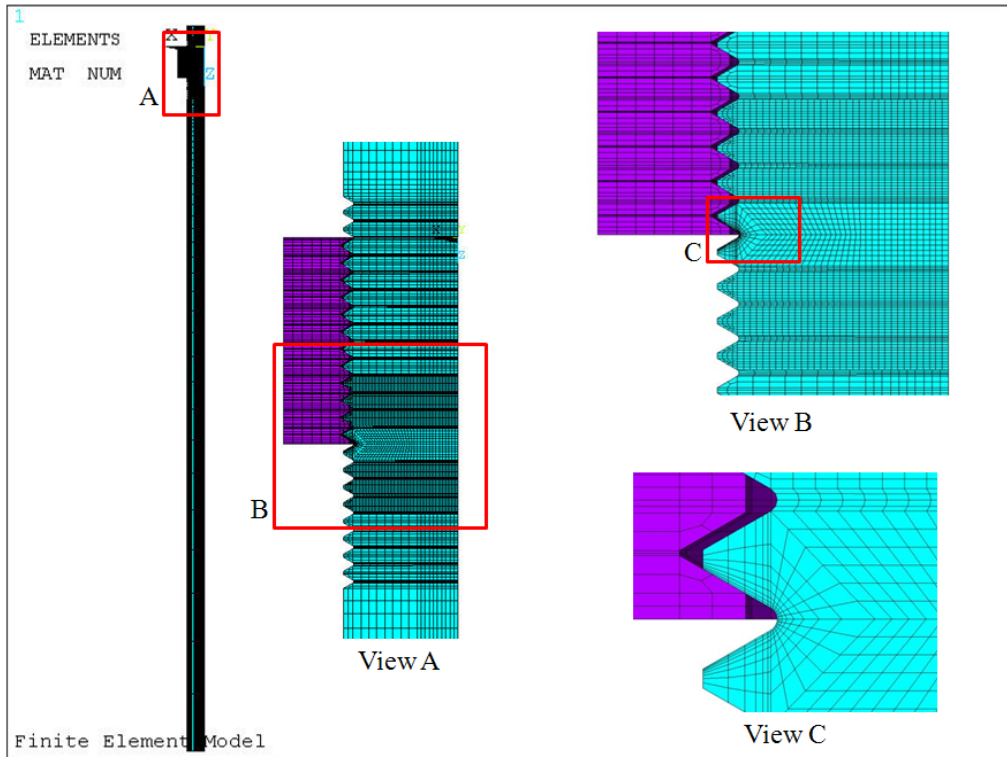
7.1 General Description and Boundary Conditions for Uncracked FEM

The core plate bolt and nut are modeled in ANSYS [16] using 3-dimensional structural solid elements (SOLID185) and contact between the nut and bolt surfaces is simulated with contact elements (CONTA174 and TARGE170). A quarter-symmetry model is used for all crack cases to reduce model size. Symmetric boundary conditions are applied to the two cut planes. The top nut (i.e. the nut in contact with the top of the core plate) is explicitly modeled. The length of bolt is modeled to the interface of the bottom of the core plate support ring and the bottom nut. The bottom nut is simulated by fixing the bottom of the model in the axial direction. This treatment ensures that the proper axial displacement will be considered in the FEA. Figure 7-1 and Figure 7-2 show the FEM. Figure 7-3 identifies the boundary conditions applied to the model.

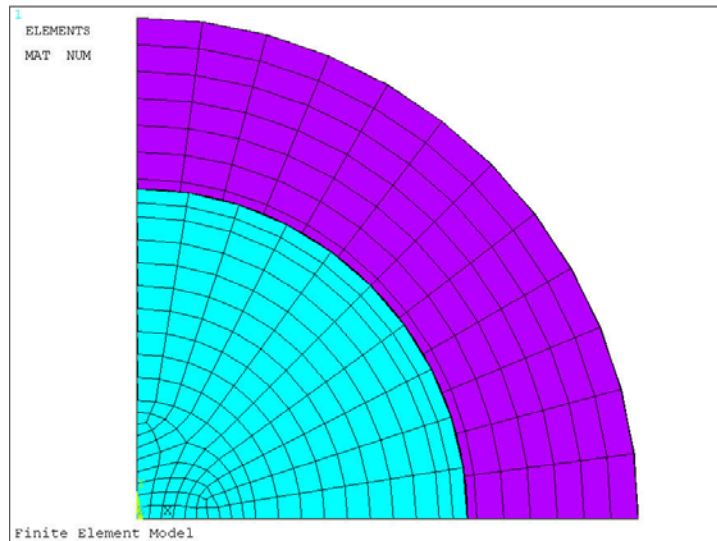
To determine the applied displacement on the bottom surface of the core plate nut, a preload force of 14,186 lbf is applied to the model. This is slightly higher than the preload force of 13,961 lbf calculated in Reference [14, Table 6-1]; however, a slightly higher number is conservative since it will result in a larger stress in the bolt section. Radiation relaxation is conservatively omitted. This force is converted to a pressure and applied to the bottom surface of the nut. The equivalent pressure is 10,387 psi. Figure 7-4 shows the FEM with the applied pressure of 10,387 psi. Figure 7-5 shows a stress contour plot of the first principal stress at the threads. Notice that the root of the first engaged thread has the highest principal stress. Figure 7-6 shows a side view of the axial displacement along the bolt threads. Figure 7-7 shows the axial displacement at the bottom surface of the nut.

The average axial displacement, as shown in Figure 7-7, at the nut bottom surface is 0.0128376 in. Therefore, a uniform displacement of 0.012837 is applied to the uncracked models in order to account for the bolt preload. Figure 7-8 shows the axial displacement for the as modeled condition using an axial displacement of 0.0128376 in on the nut surface. Notice that the displacement contours in Figure 7-7 and Figure 7-8 are nearly identical. The contours do not perfectly lineup since the displacements are slightly different and the contour bands are very thin. Since the contour bands represent <2% difference

in displacement, this is within the error of the design input and is reasonable. The ANSYS input file for the pressure preload is *Pressure_Displ.inp* and is in the supporting files.

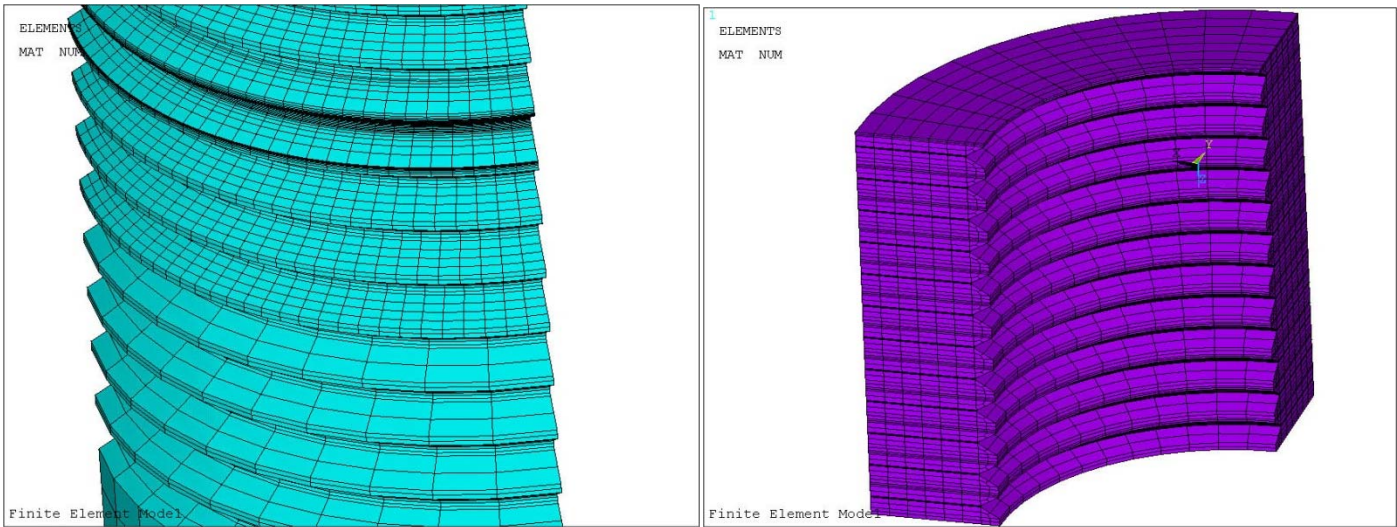


(Side View)



(Top View)

Figure 7-1: Finite Element Model



(Bolt)

(Nut)

Figure 7-2: Finite Element Model, Bolt and Nut Thread Detail View

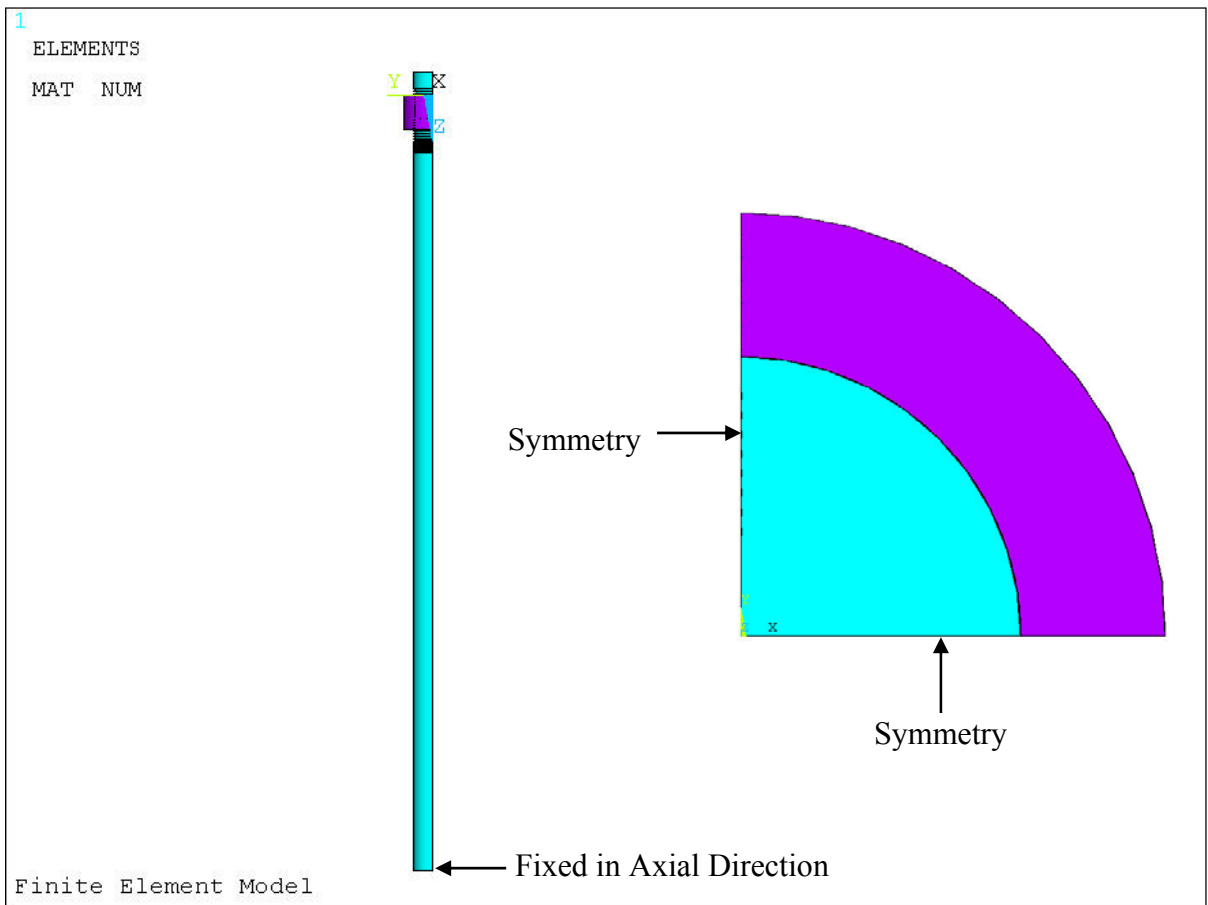


Figure 7-3: Boundary Conditions Applied to Model

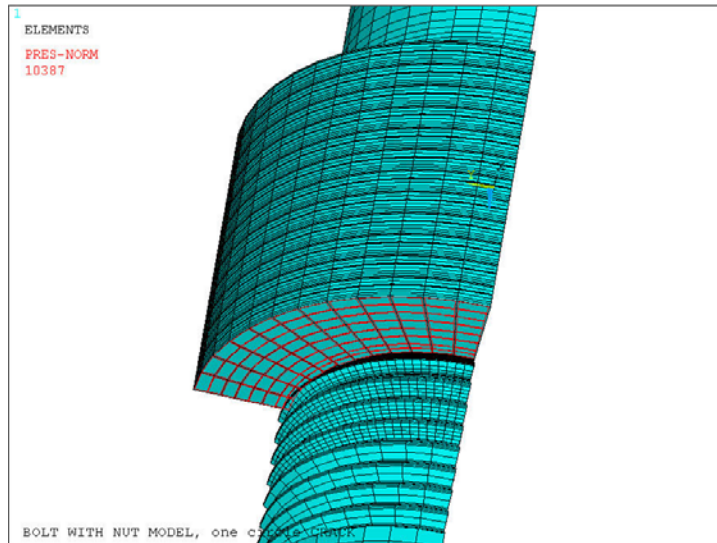


Figure 7-4: Pressure Applied for Preload Analysis

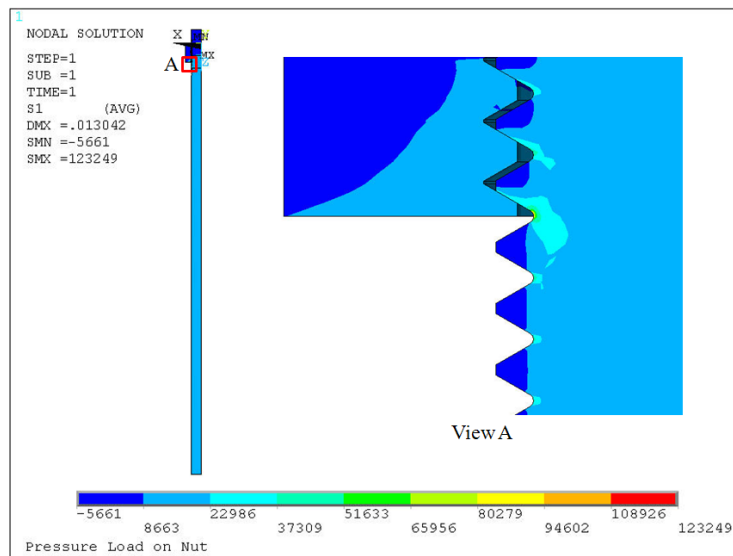


Figure 7-5: First Principal Stress for Preload Analysis

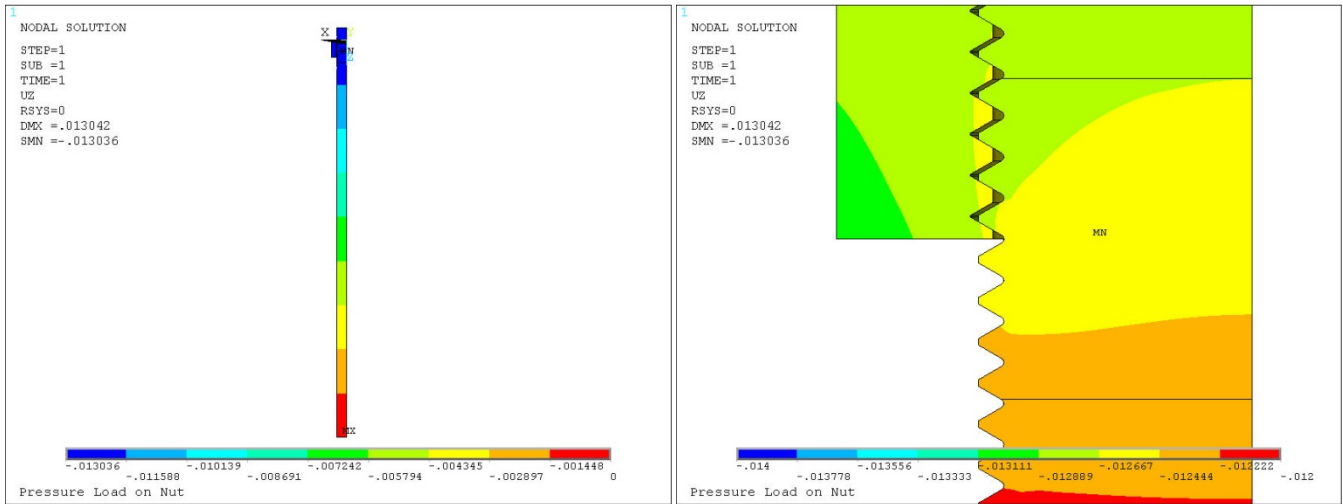


Figure 7-6: Axial Displacement for Preload Analysis, Side View

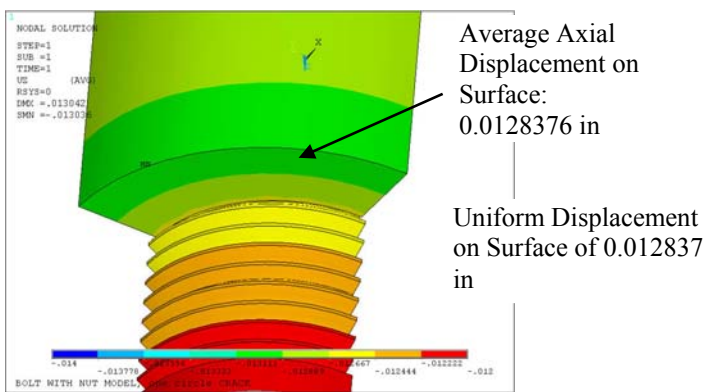


Figure 7-7: Axial Displacement for Preload Analysis, Oblique View

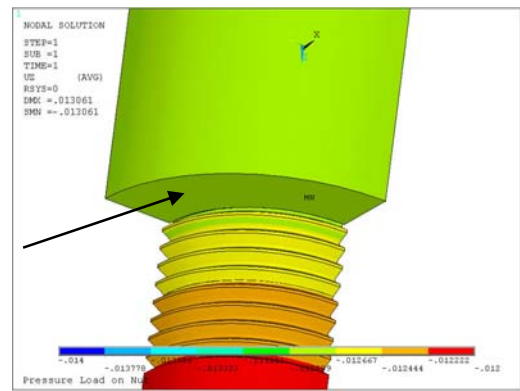


Figure 7-8: Axial Displacement as Modeled

7.2 Single Crack Case

A FEM is developed to analyze a single circumferential crack located at the root of the first engaged thread. This location corresponds to the highest stressed location in the CP bolt. The crack is oriented horizontally (normal to the applied load). The initial crack size is 0.010 inches. Figure 7-9 shows the location and orientation of the single crack case. ANSYS and Zencrack input and output files are summarized in Table 7-1.

7.3 Adjacent Crack Case

A FEM is developed to analyze two circumferential cracks, one located at the root of the first engaged thread and the second at the root of the adjacent thread directly below the first location. Both cracks are oriented horizontally (normal to the applied load). The initial crack size is 0.010 inches. Figure 7-10 shows the locations and orientations of the adjacent crack case. ANSYS and Zencrack input and output files are summarized in Table 7-1.

7.4 Far Crack Case

A FEM is developed to analyze two circumferential cracks, one located at the root of the first engaged thread and the second sufficiently far away to investigate if the shielding effect anticipated to occur for multiple cracks appears to diminish. For this case the second crack is located at the thread root six threads away from the highest stresses thread. Both cracks are oriented horizontally (normal to the applied load). The initial crack size is 0.010 inches. Figure 7-11 shows the locations and orientations of the far crack case. ANSYS and Zencrack input and output files are summarized in Table 7-1.

7.5 Single-Max Crack Case

A FEM is developed to analyze a single circumferential crack located at the highest stressed location on the root of the first engaged thread. Figure 7-12 shows a plot of the maximum principal stress from the “uncracked” model in the vicinity of the highest stress thread root. These results are obtained from the ANSYS input file *BOLT1-circle-max-stress-1-550-final.INP*. The maximum principal stress location is 3 nodes away from the deepest point in the root of the thread. The postulated crack is oriented normal to the thread face at this node; this is approximately normal to the direction of the maximum principal stress. This is consistent with experimentally observed cracking shown in Figure 3-2. The initial crack size is 0.010 inches. Figure 7-13 shows the location and orientation of the single-max crack case. ANSYS and Zencrack input and output files are summarized in Table 7-1.

7.6 Thumbnail Crack Case

A FEM is developed to analyze a thumbnail crack located at the root of the highest stressed thread. The crack is oriented horizontally (normal to the applied load). This case is performed to validate the observation that thumbnail shaped flaws will grow rapidly in the length direction such that they will coalesce into a sickle shaped or circumferential shaped flaw such as evaluated in this calculation. The initial crack shape is semi-circular with a radius of 0.010 inches. Figure 7-14 shows the location and orientation of the thumbnail crack case. ANSYS and Zencrack input and output files are summarized in Table 7-1.

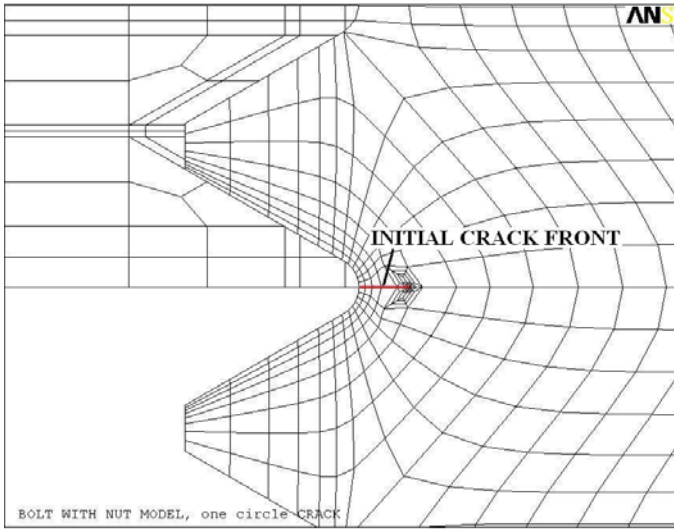


Figure 7-9: Single Crack Model, Initial Crack Front

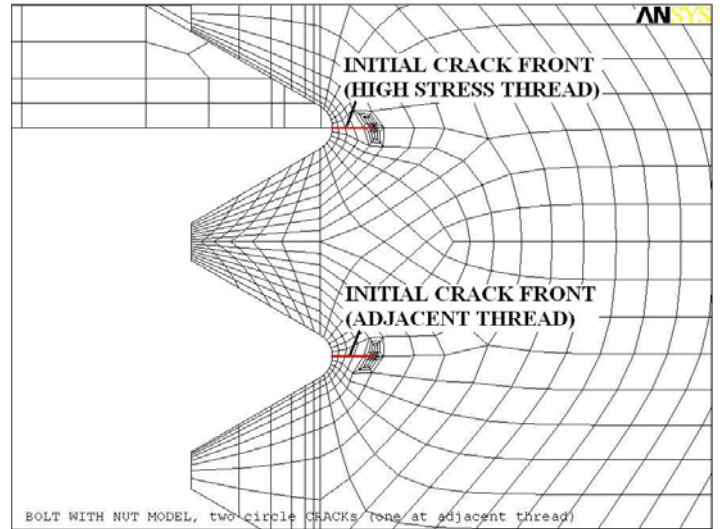


Figure 7-10: Adjacent Crack Model, Initial Crack Fronts

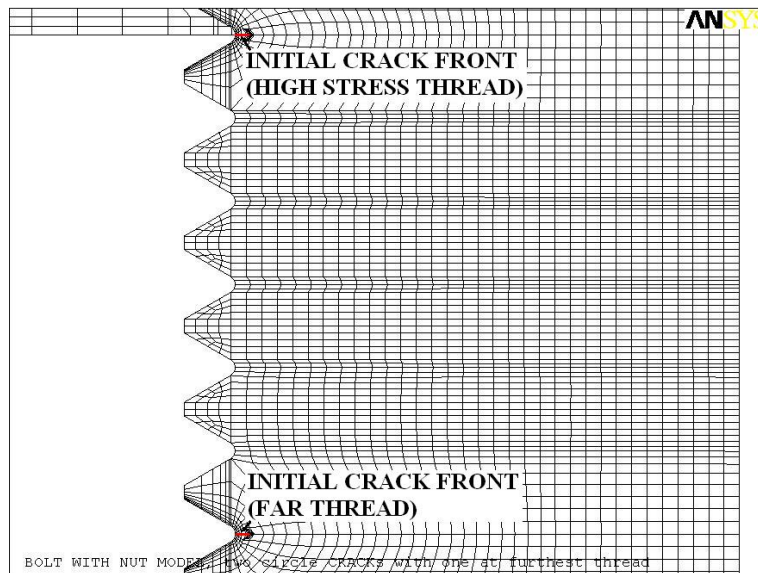


Figure 7-11: Far Crack Model, Initial Crack Fronts

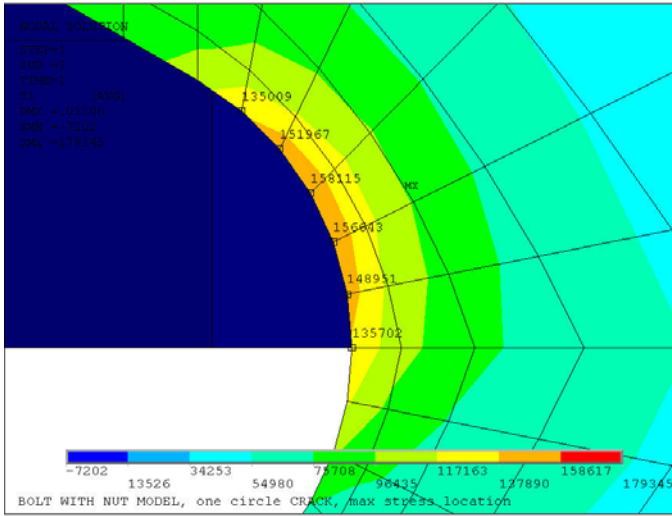


Figure 7-12: First Principal Stress Intensity for Uncracked Model

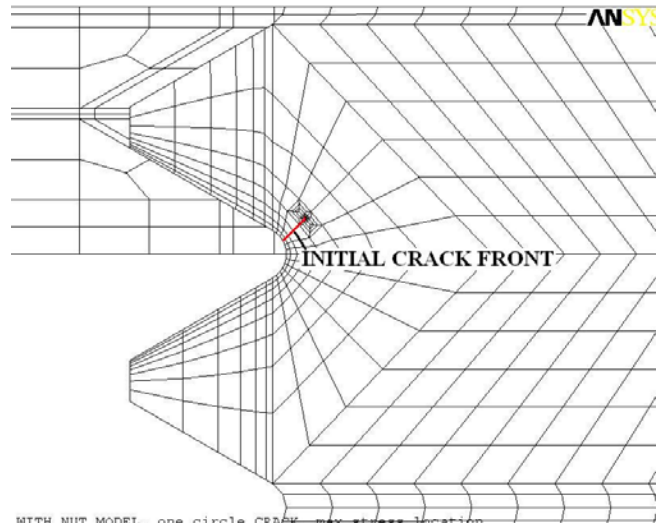


Figure 7-13: Single-Max Crack Model, Initial Crack Front

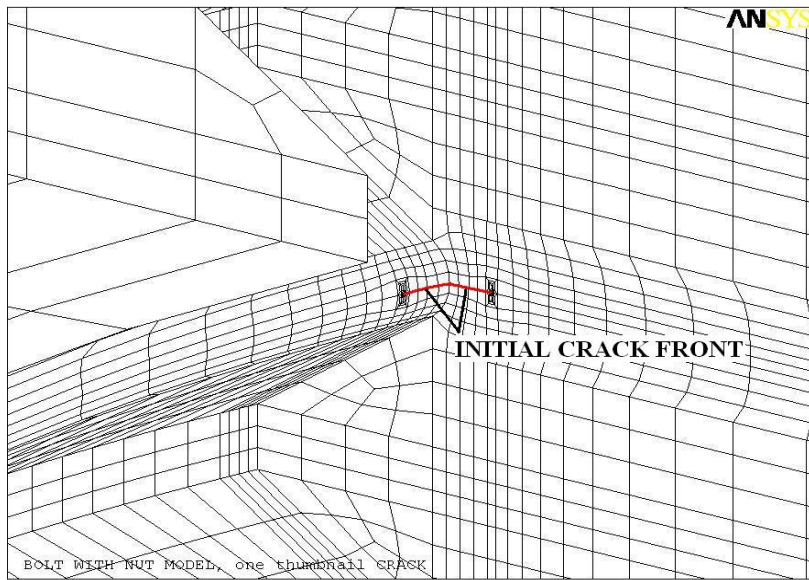


Figure 7-14: Thumbnail Crack Model, Initial Crack Front

7.7 ANSYS and Zencrack Input Files

Multiple Zencrack runs are required for each crack case. All ANSYS and Zencrack input and output files for this calculation are outlined in Table 7-1.

Table 7-1: ANSYS and Zencrack Input Files

Input Files			
File	Description		
time.dat	Zencrack header file, Calls time_subfile.dat		
time_subfile.dat	Zencrack routine to define crack growth rate da/dt		
user_dadt.f	Zencrack user subroutine to calculate time-dependent crack growth rates using Paris law for SCC per Section 4.0		
Crack Case	Run (#)	File Type	File Name
Single	1	ANSYS Uncracked FEM Zencrack	<i>BOLT1-circle-550-final.INP</i> <i>1-circle-crack.zcr</i>
	2, 3, 4, 5	ANSYS Uncracked FEM Zencrack	<i>BOLT1-circle-550-final-#.INP</i> <i>1-circle-crack-#.zcr</i>
	5	ANSYS Preload E-P	<i>reaction-force-5th-run-6.INP</i>
Adjacent ("Adj")	1	ANSYS Uncracked FEM Zencrack	<i>BOLT2-circle-adj-below-550-final.INP</i> <i>2-circle-crack-adj-below.zcr</i>
	2, 3, 4	ANSYS Uncracked FEM Zencrack	<i>BOLT2-circle-adj-below-550-final-#.INP</i> <i>2-circle-crack-adj-below_#.zcr</i>
	4	ANSYS Preload E-P	<i>reaction-force-4th-run-09.INP</i>
Far	1	ANSYS Uncracked FEM Zencrack	<i>BOLT2-circle-far-550-final.INP</i> <i>2-circle-far-crack.zcr</i>
	2, 3, 4	ANSYS Uncracked FEM Zencrack	<i>BOLT2-circle-far-550-final-#.INP</i> <i>2-circle-far-crack-#.zcr</i>
	4	ANSYS Preload E-P	<i>reaction-force-4th-run-15.INP</i>
Single-Max	1, 2, 3, 4	ANSYS Uncracked FEM Zencrack	<i>BOLT1-circle-max-stress-#-550-final.INP</i> <i>1-circle-crack-max-stress-#.zcr</i>
	4	ANSYS Preload E-P	<i>reaction-force-4th-run-26.INP</i>
Thumbnail	1	ANSYS Uncracked FEM Zencrack	<i>BOLT1-circle-thumbnail-#-550-final.INP</i> <i>1-thumbnail-crack.zcr</i>

Output Files

File Name	Description
%case%-#.rep	Zencrack output file, fracture mechanics parameters
%case%-#.shp	Zencrack output file, time-history crack front location
crack-growth-%case%.xls	Crack growth spreadsheet, combination of all runs

%case% = "single", "adj", "far" or "single-max"

= run number (1, 2, 3, 4 or 5)

8.0 RESULTS

This section presents the results of the following calculations:

1. Calculation of the minimum acceptable retained preload (failure criterion in FE LEFM evaluation),
2. Calculation of the CGR constant for use in Equations 3 and 4,
3. FE LEFM results,
4. Flaw tolerance results,
5. FE LEFM benchmark against available hand calculation solutions.

Each item is presented separately below.

8.1 Calculation of Minimum Acceptable Preload

The minimum bolt preload below which the normal operation applied loading results in zero friction force between the core plate assembly and core support ring can be calculated as follows:

$$\text{Min. Preload}_{\text{per bolt}} = F_{\text{pressure, per bolt}} - \text{Deadweight}_{\text{per bolt}}$$

The pressure force per bolt is calculated as follows:

$$F_{\text{pressure, per bolt}} = \text{RIPD} \cdot A_{\text{CP}} / 72$$

$$\begin{aligned} \text{Where, RIPD} &= \text{Reactor Internal Pressure Difference, psi} \\ &= 29.76 \text{ psi [18]} \end{aligned}$$

The core plate area, A_{CP} , is calculated by subtracting the area of the holes in the core plate from the total core plate area from Section 5.1:

Therefore, A_{CP} can be calculated as:

$$A_{\text{CP}} = \pi / 4 \cdot (166^2 - 137 \cdot 10.875^2 - 12 \cdot 3.5625^2 - 43 \cdot 1.863^2) = 8,680 \text{ in}^2$$

The $F_{\text{pressure, per bolt}}$ is then calculated as:

$$F_{\text{pressure, per bolt}} = 29.76 \cdot 8680 / 72 = 3,588 \text{ lbf}$$

The deadweight force per bolt is calculated as:

$$\text{Deadweight}_{\text{per bolt}} = (W_{\text{CP}} \cdot B + W_{\text{FB}} \cdot N_{\text{FB}}) / 72$$

$$\begin{aligned} \text{Where: } W_{\text{CP}} &= \text{Weight of the core plate, lbf} = 10,500 \text{ lbf [21]} \\ B &= \text{Buoyancy factor} \\ W_{\text{FB}} &= \text{Weight (wet) of peripheral fuel bundles, lbf} = 580 \text{ lbf [18]} \end{aligned}$$

$$N_{FB} = \text{Number of peripheral fuel bundles} = 12 \quad [21]$$

The buoyancy factor is calculated as:

$$B = 1 - \rho_{\text{water}} / \rho_{\text{steel}}$$

Where: $\rho_{\text{water}} = \text{Density of water, lbm/ft}^3 = 45.9 \text{ lbm/ft}^3$ [29, Appendix 35.A]
 $\rho_{\text{steel}} = \text{Density of stainless steel, lbm/ft}^3 = 488 \text{ lbm/ft}^3$ [29, Appendix 34.B]

Therefore, deadweight can be calculated as:

$$\begin{aligned} \text{Deadweight}_{\text{per bolt}} &= W_{CP} \cdot B + W_{FB} \cdot N_{FB} \\ &= (10,500 (1 - 45.9/488) + 580 \cdot 12)/72 \\ &= 229 \text{ lbf} \end{aligned}$$

The minimum preload per bolt is then:

$$\begin{aligned} \text{Min. Preload}_{\text{per bolt}} &= F_{\text{pressure, per bolt}} - \text{Deadweight}_{\text{per bolt}} \\ &= 3,588 - 229 \\ &= 3,359 \text{ lbf} \end{aligned}$$

If the preload is below this value, the bolt is considered failed for this analysis. If the vertical seismic force is considered then the minimum preload would be larger; however, for the purposes of this evaluation the above number is sufficient to determine the flaw tolerance of the core plate bolt assembly under various crack size, location, and water chemistry conditions. It is important to note that the “minimum” preload determined above is used only to identify the point at which the iterative FEA is terminated; this is a measure taken to reduce total solution time for each crack configuration. If a precise minimum preload value were of interest then it would be calculated using the seismic loading as well as consideration of the number of intact CP bolts assumed. In all cases this “minimum” preload would be larger than the value determined above and the results presented in this calculation would remain applicable.

8.2 Calculation of C Values for Crack Growth Rate Equations

The C values to be used in Equations 3 and 4, for each year, are calculated based on water chemistry data in Table 5-3 and considering a temperature of 550°F. The values are listed in Table 8-1.

Table 8-1: Calculated C Values for Each Year

Year	Total Month at End of Year	Rx Water Conductivity, (μS/cm)	ECP (mV SHE)	C	Note
Jul 1975	6	1.315	+200	4.1134E-12	Based on Equation 3
1976	18	0.485	+200	4.1134E-12	
1977	30	0.998	+200	4.1134E-12	
1978	42	0.793	+200	4.1134E-12	
1979	54	1.103	+200	4.1134E-12	
1980	66	2.053	+200	4.1134E-12	
1981	78	0.796	+200	4.1134E-12	
1982	90	0.507	+200	4.1134E-12	
1983	102	0.540	+200	4.1134E-12	
1984	114	0.230	+200	4.1134E-12	
1985	126	0.389	+200	4.1134E-12	
1986	138	0.115	+200	4.1134E-12	
1987	150	0.342	+200	4.1134E-12	
1988	162	0.427	+200	4.1134E-12	
1989	174	0.125	+200	3.1557E-12	Based on Equation 4
1990	186	0.255	+200	6.8541E-12	
1991	198	0.171	+200	4.9320E-12	
1992	210	0.001	-1000	1.5523E-32	
1993	222	0.100	+200	2.1757E-12	
1994	234	0.095	+200	1.9834E-12	
1995	246	0.074	-50	4.9014E-13	
1996	258	0.071	-50	4.4848E-13	
1997	270	0.066	-50	3.8136E-13	
1998	282	0.067	-50	3.9453E-13	
Jan. to Nov. 1999	293	0.085	+200	1.6068E-12	
Dec. 1999	294	0.085	-230	3.3879E-13	
2000	306	0.095	-230	4.1819E-13	
2001	318	0.069	-230	2.1956E-13	
2002	330	0.09	-400	2.0437E-13	
2003	342	0.09	-400	2.0437E-13	
2004	354	0.1	-400	2.4792E-13	
2005	366	0.10	-400	2.4792E-13	
2006	378	0.11	-400	2.9234E-13	
2007	390	0.11	-400	2.9234E-13	
2008	402	0.14	-400	4.2667E-13	
2009	414	0.17	-400	5.5773E-13	
2010	426	0.15	-400	4.7093E-13	
2011	438	0.11	-400	2.9234E-13	
2012 - 2035	726	0.1	-400	2.4792E-13	

8.3 Single Crack Case

Figure 8-1 shows a K vs. da plot of the single crack case using the excel file *crack-growth-single.xls*. Both K_I and K_{II} values are shown using different axes; K_I is plotted against the left vertical axis, K_{II} is plotted against the right vertical axis. A sixth degree polynomial curve fit is shown for K_I which is used to calculate time-dependent crack growth rates based on time-specific C values from Table 8-1. The general K_I curve is consistent with typical stress intensity factor versus crack depth solutions; thus, the results appear reasonable. Figure 8-2 shows the residual life for the single crack case for several different assumed crack initiation times. All cases consider a 0.010 inch initial crack size. Residual life for larger initial crack sizes can be determined by entering the curve at a point corresponding to any initial depth desired. The crack growth calculations are performed in the excel file *CP-Bolt-SCC-Growth-Spreadsheet.xls* using the stress intensity factor determine using the polynomial curve fit shown in Figure 8-1 and the crack growth rate constant, C, given in Table 8-1.

Equations 3 and 4, as appropriate based on the assumed crack initiation time, are used to calculate da/dt for each of the crack cases in Figure 8-2. A 100 hour time increment is used in these calculations. A time-sensitivity study is performed to demonstrate that 100 hours is an acceptable time increment. A 50 hour time increment is also tested for the Year 0 and Year 20 cases. The results of the 100 hour and 50 hour increment tests are shown in Figure 8-3. Since the maximum percent difference between 100 hours and 50 hours in total time to failure is less than 5%, the time increment of 100 hours is adequate.

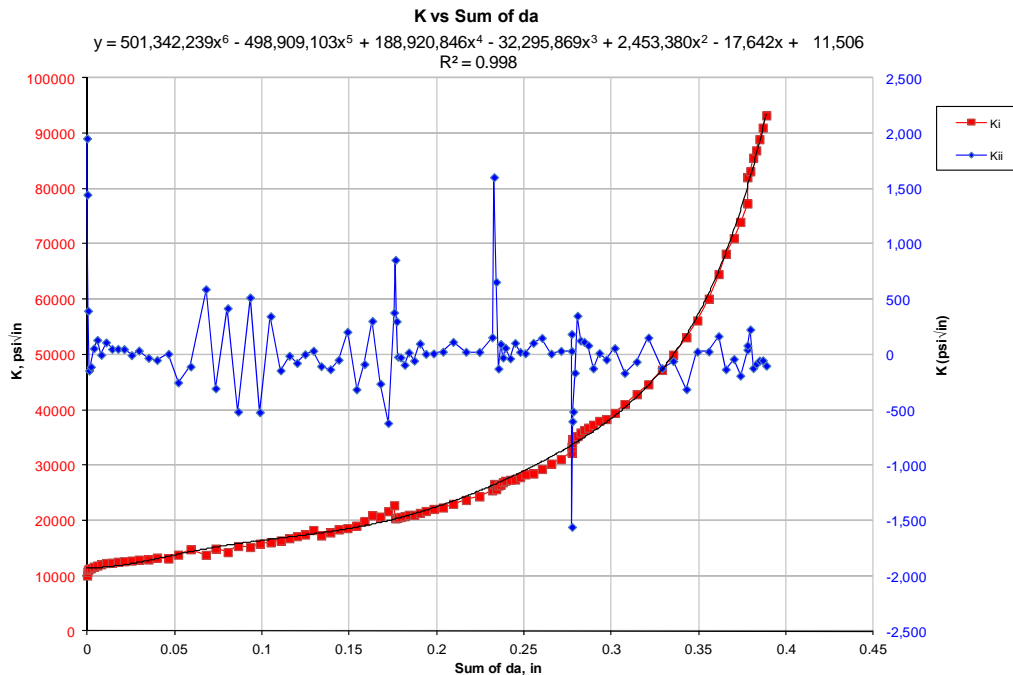


Figure 8-1: Single Crack Case, K vs. da Curve

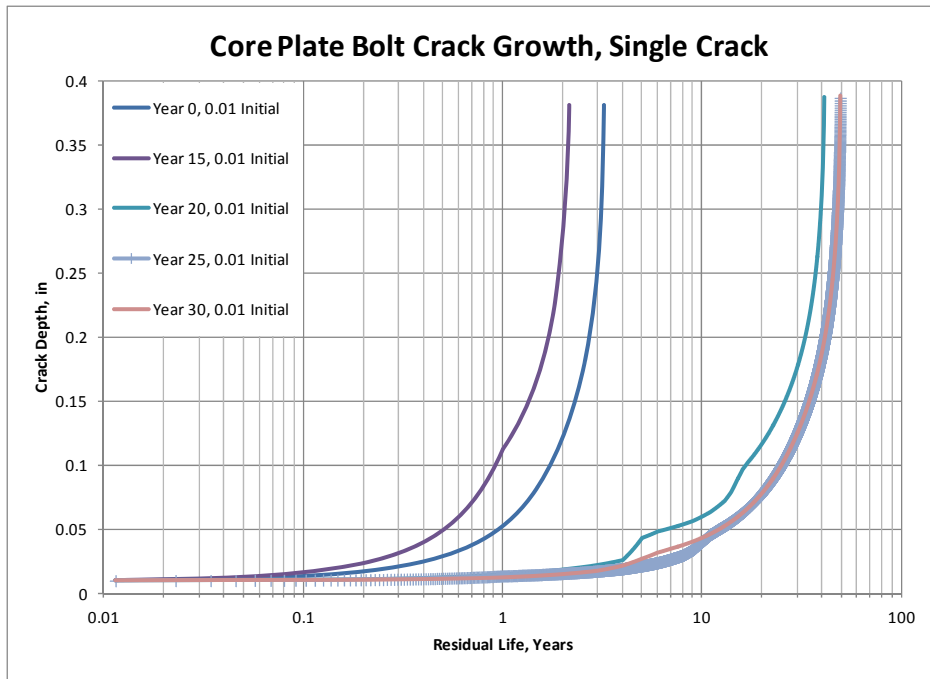


Figure 8-2: Crack Growth Curves - Single Crack Case, Various Initiation Times

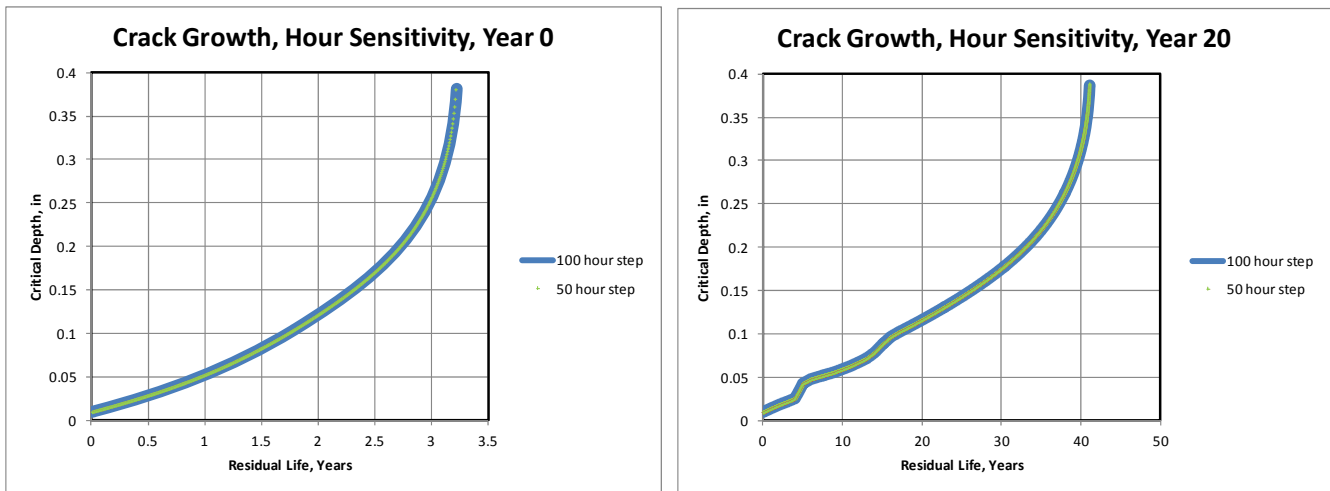
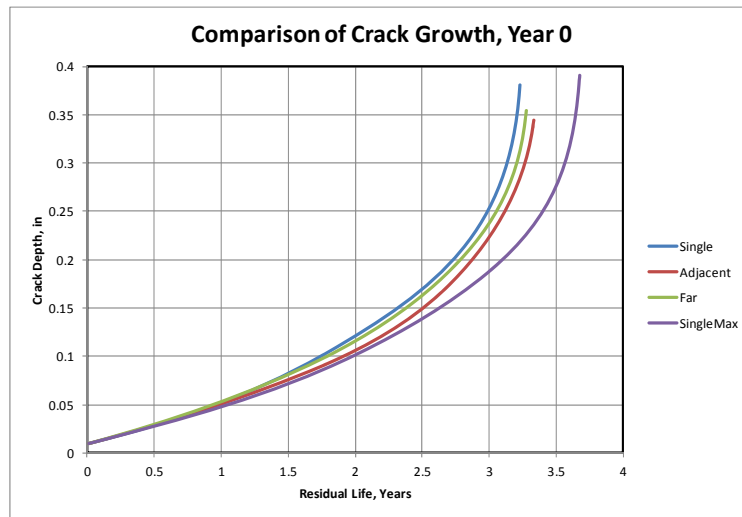


Figure 8-3: Time Increment Sensitivity Analysis

8.4 Adjacent, Far and Single-Max Crack Cases

Figure 8-4 shows a comparison of crack growth for the adjacent, far, and single-max crack cases. Figure 8-5 shows a comparison of K vs. sum of da for each case. Based on these plots, it can be seen that the single crack case is the most conservative case. Allowing the crack to initiate at the actual location of highest stress in the thread root and allowing the crack front to turn as driven by the local stress and strain field results in some amount of increased residual life; however, the difference between all cases is only on the order of 15-20%. Residual life curves for the adjacent, far, and single-max cases are given in Appendix A.



Note: Crack depth in this plot actually corresponds to total length of crack path; since the crack growth trajectory can curve the dimension reported is the sum of the initial flaw size and the summation of incremental crack front advance.

Figure 8-4: Comparison of Crack Growth for Each Case

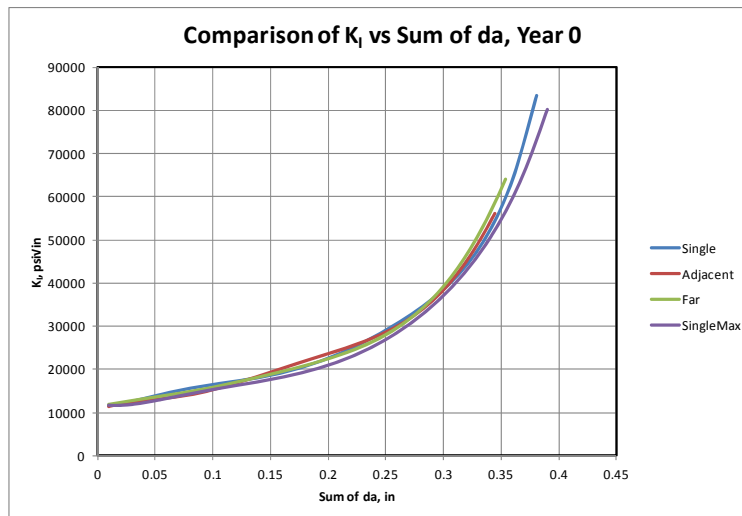


Figure 8-5: Comparison of K vs. Sum of da for Each Case

8.5 Thumbnail Crack Case

Figure 8-6 shows the crack front propagation for the thumbnail crack case. These results confirm the expectation that the crack front grows much more rapidly in the circumferential direction than in the radial direction for a thumbnail shaped flaw. This behavior is expected based on the observation that the peak stress occurs in the root of the thread form, which is the region in which the stress concentration exists, and attenuates quickly in the radial direction as the crack front grows out of the local region affected by the stress concentration contributed by the thread. Over time, this would have the effect of causing an initial thumbnail shaped crack to transition to a circumferential crack before the bolt is cracked through-wall. Further, if multiple thumbnail cracks existed in the same thread then these cracks would combine to produce a fully circumferential crack similar to the cases analyzed above. Also shown in Figure 8-6 is the trend for the deepest part of the crack to turn upward at an angle, similar to what was observed in the fully circumferential case. No attempt is made in this calculation to quantify the possible increase in residual life for cases with various numbers of assumed thumbnail flaws. Since it is not possible to know how many initiation sites would exist in a threaded fastener susceptible to SCC it is impractical to perform this type of study. Use of the fully circumferential initial crack size assumption is appropriate and bounding.

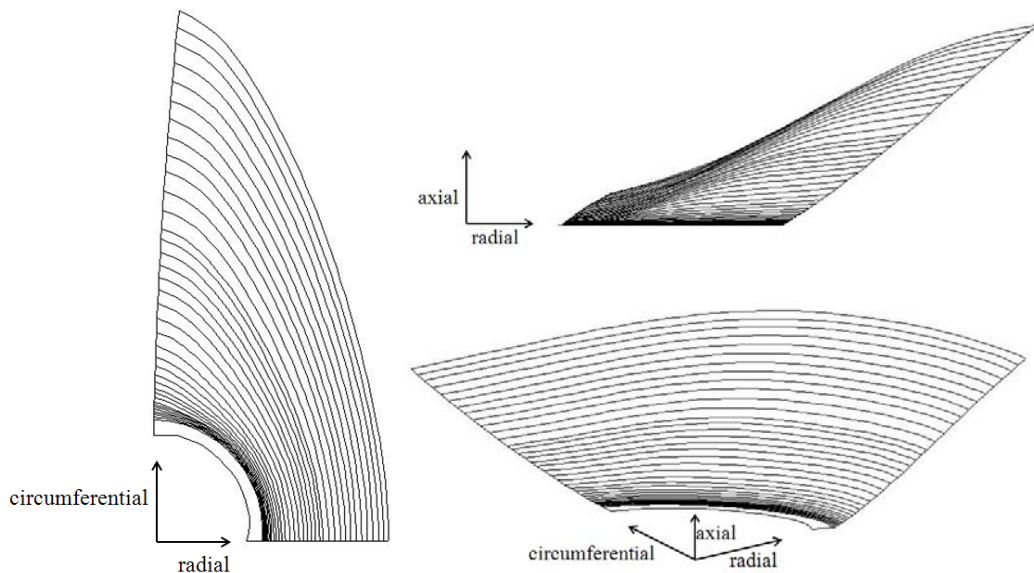


Figure 8-6: Crack Front Propagation, Thumbnail Crack Case

8.6 FE LEFM benchmark against Available Hand Calculations

Stress intensity factors for circumferential cracks in threaded fasteners were studied by Oster and Mills [10]. Their work also used finite element analysis, but forced a horizontal crack trajectory with the initiation site located at the root of the thread. Oster and Mills also considered only the UNC thread form; whereas, the JAF CP bolt is designed with a unified national fine (UNF) thread form. Despite the minor differences in thread form dimensions, the Oster and Mills solution [10] is well suited as a benchmark for the results obtained from the present study for the single crack case (Section 7.2, Section 8.3). A non-dimensional K_I value is presented in Reference [10] as (also shown on Figure 3-3):

$$\frac{K}{\sigma\sqrt{\pi a}} = q + r e^{-s(a/d)} + t \frac{a}{d} + u \left(\frac{a}{d}\right)^2 + v \left(\frac{a}{d}\right)^3 + w \left(\frac{a}{d}\right)^4 + x \left(\frac{a}{d}\right)^5 + y \left(\frac{a}{d}\right)^6 \quad (5)$$

For a threaded fastener with nut loading, Reference [10] gives the following parameters to be used in the equation above:

$$\begin{aligned} q &= 3.0149 \\ r &= 2.4902 \\ s &= 166.26 \\ t &= -51.624 \\ u &= 722.92 \\ v &= -5342.9 \\ w &= 21757 \\ x &= -45123.3 \\ y &= 37900.2 \end{aligned}$$

These values are applicable for $0.003 \leq a/d \leq 0.4$.

Other variables needed for the analysis are as follows:

d = minor thread diameter = 1.008973 in (based on geometry from Section 5.1)

P = retained preload on fastener = 14,186 lbf (Section 5.2)

σ = membrane stress on uncracked minor diameter = $P/(\pi \cdot d^2/4) = 17,742$ psi

Figure 8-7 shows the comparison of K_I vs. sum of da for the Oster and Mills solution [10] and the present FE LEFM analysis. Figure 8-8 shows the comparison of non-dimensional K_I values obtained from the Oster and Mills solution [10] and the present FE LEFM analysis. The results show good agreement and are within 5-10% of each other. All calculations are performed in the excel file *CP-Bolt-SCC-Growth-Spreadsheet.xls*. The results of this benchmark support the conclusion that the FE LEFM evaluations performed using ANSYS and Zencrack provide reasonable results. By extension, the ANSYS and Zencrack results for the more complicated cases, for which existing LEFM solutions are not available, are considered to be validated.

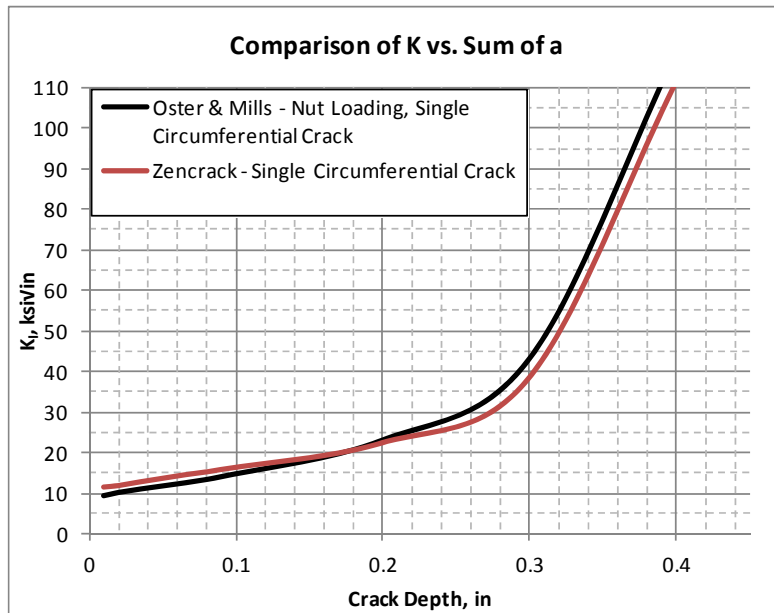


Figure 8-7: Comparison of K vs. Sum of da for single circumferential crack case – Oster & Mills [10], FE LEFM

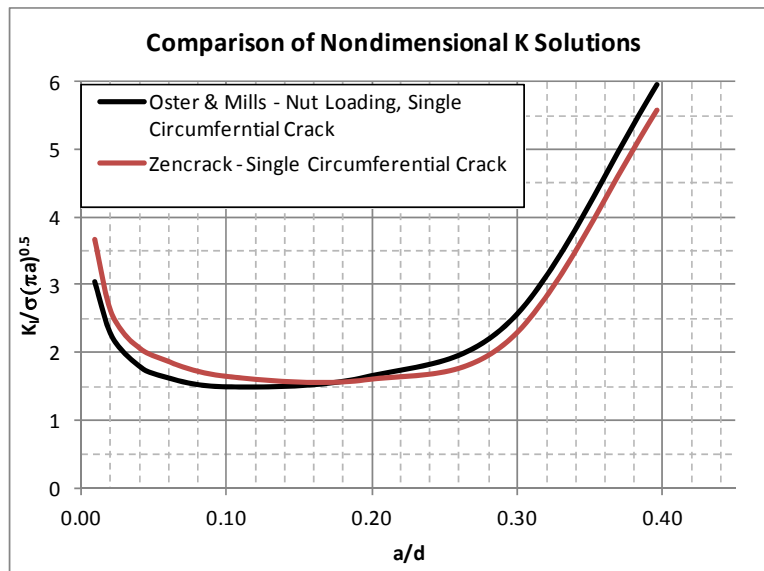


Figure 8-8: Comparison of Non-dimensional K Solutions for single circumferential crack case – Oster & Mills [10], FE LEFM

9.0 DISCUSSIONS AND CONCLUSIONS

Several different crack orientations and initiation scenarios have been analyzed. The crack shape and location are defined to be consistent with published data for IGSCC in threaded fasteners. Further, the results of this study have been benchmarked against existing LEFM solutions for simpler configurations. The results of this evaluation are consistent with related information in the literature and provide additional insight for complex crack orientations and multiple crack cases. Both single and multiple circumferential flaws have been analyzed with initiation times ranging from plant startup to 30 years after startup. Time-dependent water chemistry data for reactor conductivity and ECP were considered. The most important factor affecting the flaw tolerance of the JAF CP bolting is the assumption used for crack initiation time. If crack initiation is assumed to occur in the first 20 years of plant operation (prior to 1995) then the CP bolt exhibits little flaw tolerance. Conversely, if crack initiation is assumed to occur after the first 20 years of plant operation (subsequent to 1995) then the CP bolt exhibits substantial flaw tolerance. If single or multiple IGSCC occurred in the JAF CP bolting subsequent to 1995 then the residual life of the CP bolting is on the order of 40-50 years. Considering desired operation through 60 years, these results show adequate flaw tolerance of the CP bolting through 60-70 years of plant operation if IGSCC is assumed to occur after the first 20 years of operation. These results are considered to be a bounding assessment of the flaw tolerance of the CP bolting because of the inherent conservatism in this evaluation including:

1. Omission of radiation induced relaxation (i.e., postulated crack growth rates are higher),
2. Use of 95% percentile crack growth rates rather than “best estimate” crack growth rates,
3. Consideration of a fully circumferential initial flaw rather than one or more discrete thumbnail shaped flaws,
4. Consideration of the worst case thread form tolerance resulting in the maximum possible stress state rather than use of nominal dimensions,
5. Consideration of worst case flaw orientation (single case) rather than use of results from realistic flaw orientation (single max case).

The results of this evaluation are used, in concert with the results from other calculations performed for this project, to develop an inspection protocol for the JAF CP bolting in the period of extended operation.

10.0 REFERENCES

1. ADAMS Accession No. ML071060390, “James A. Fitzpatrick, License Renewal Application, Amendment 9.”
2. EPRI TR-107284, BWR Vessel and Internals Project, BWR Core Plate Inspection and Flaw Evaluation Guidelines (BWRVIP-25), December 1996, SI File No. BWRVIP-01-225P (**EPRI Proprietary Information**).
3. Toor, Pir M., Structural Integrity of Fasteners, STP 1236, 1995, American Society of Testing and Materials.
4. Toor, Pir M., Structural Integrity of Fasteners: Second Volume, STP 1391, 2000, American Society of Testing and Materials.
5. Toor, Pir M., Barron, Joseph, Structural Integrity of Fasteners Including the Effects of Environment and Stress Corrosion Cracking: 3rd Volume, STP 1487, 2007, American Society of Testing and Materials.
6. SI Calculation No. 1101291.301, Revision 0, “Core Plate Bolt Degradation Susceptibility Evaluation.”
7. Kephart, Alan R., “Optimum Thread Rolling Process that Improves SCC Resistance,” Structural Integrity of Fasteners Including the Effects of Environment and Stress Corrosion Cracking: 3rd Volume, ASTM STP 1487, P. M. Toor and J. Barron, Ed., American Society for Testing and Materials, West Conshohocken, PA, 2007, pp. 53-58.
8. Liu, A. F., “Behavior of Fatigue Cracks in a Tension Bolt,” Structural Integrity of Fasteners, ASTM STP 1236, P. M. Toor, Ed., American Society for Testing and Materials, Philadelphia, 1995, pp. 126-140.
9. Renauld, M.L., Lien, H., Wilkening, W.W., “Probing the Elastic-Plastic, Time-Dependent Response of Test Fasteners using Finite Element Analysis (FEA),” Structural Integrity of Fasteners Including the Effects of Environment and Stress Corrosion Cracking: 3rd Volume, ASTM STP 1487, P. M. Toor and J. Barron, Ed., American Society for Testing and Materials, West Conshohocken, PA, 2007, pp. 61-70.
10. Oster, D. M. and Mills, W. J., “Stress Intensity Factor Solutions for Cracks in Threaded Fasteners,” Structural Integrity of Fasteners: Second Volume, ASTM STP 1391, P. M. Toor, Ed., American Society for Testing and Materials, West Conshohocken, PA, 2000, pp. 85-101.
11. SI Calculation No. EPRI-179-331, “Core Plate Rim Hold-down Bolt Crack Growth Behavior for FitzPatrick.”
12. SI Calculation No. EPRI-179-346, “Updated Core Plate Rim Hold-down Bolt Crack Growth Behavior for FitzPatrick.”
13. BWRVIP-14-A: BWR Vessel and Internals Project, Evaluation of Crack Growth in BWR Stainless Steel RPV Internals. EPRI, Palo Alto, CA: 2008. 1016569, (**EPRI Proprietary Information**).
14. SI Calculation No. 1101291.302, Revision 0, “Core Plate Bolt Preload Relaxation.”

15. SI Calculation No. EPRI-179-330, “Derivation of Stress-Strain Curve for type 304 Stainless Steel Material.”
16. ANSYS Mechanical APDL and PrePost Release 12.1x64, ANSYS, Inc., November 2009.
17. Zencrack Software, Release 7.7, Zentech International Limited, www.zentech.co.uk/zencrack.htm.
18. SI Project No. 1101291, Design Input Request, Revision 4, SI File No. 1101291.200.
19. GE Drawing No. 158B7234, “Stud,” SI File No. 1101291.201.
20. E. Oberg, F. Jones, H. L. Horton, and H. H. Ryffel, Machinery’s Handbook, 27th Edition, Industrial Press Inc. 2004.
21. FITZ Drawing ID No. 11825-5.10-43A, Rev. 7, “Core Support for Core Structure,” SI File No. NYPA-58Q-201.
22. FITZ Drawing No. 5.10-22A, Rev. 2, “As Built Dimensions for Core Plate (MPL-B-11D003),” SI File No. NYPA-58Q-201.
23. General Electric Drawing No. 729E762, Revision 2, “Reactor Thermal Cycles,” SI File No. 0800846.202.
24. GE Document No. 21A1056, “Standard Requirements for Miscellaneous Piping and Hardware (Reactor Internals),” SI File No. 1101291.210.
25. ASME Boiler and Pressure Vessel Code, Section III 1965 edition with Addenda through 1966.
26. Email from Bob Carter (EPRI) to Dick Mattson (SI), Aug. 08 2002, 2:49 PM, “FW: Requested info for JAF-Core plate bolts,” SI File No. EPRI-179-207.
27. Email from M. Rose (JAF) to D. Sommerville (SI), March 19, 2012, 7:18 AM, “FW: Emailing: Item 4-1 EPRI-179-207-2 water chem,” SI File No. 1101291.202.
28. ASME Boiler and Pressure Vessel Code, Section II, Materials, Part D, Properties, 2001 Edition.
29. M. R. Lindeburg, Mechanical Engineering Reference Manual, 10th Ed., Professional Publications, Inc., 1998.
30. Zencrack Verification Manual, Revision 7.7, Zentech International Limited.

Appendix A

ADDITIONAL FE LEFM RESULTS

Single Crack Case

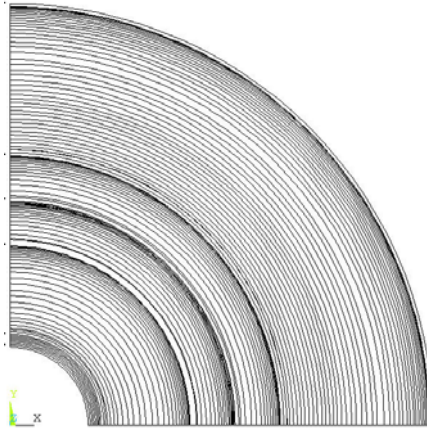


Figure A-1: Crack Front Propagation, Top View, Single Crack Case

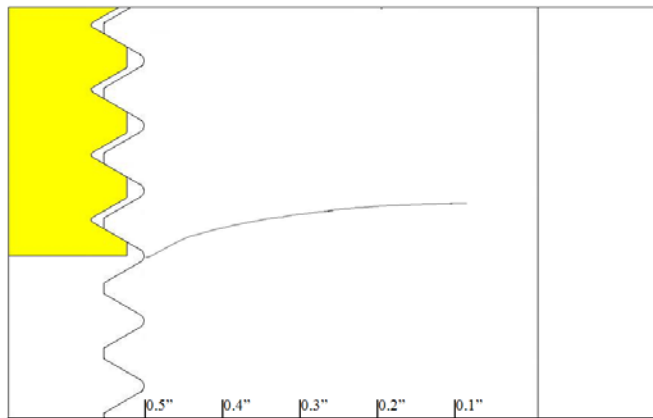


Figure A-2: Crack Propagation, Side View, Single Crack Case

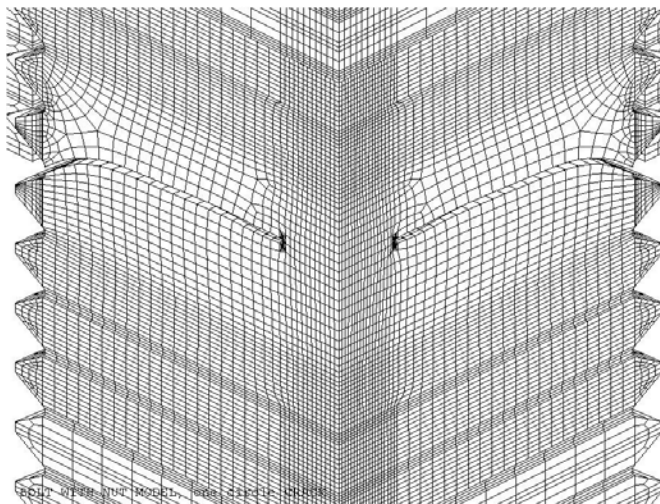


Figure A-3: Crack Propagation, Front View, Single Crack Case

Far Crack Case



Figure A-7: Crack Front Propagation, Top View, Far Crack Case

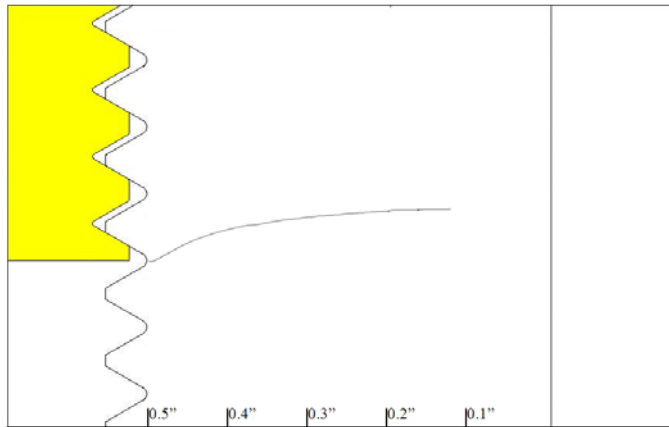


Figure A-8: Crack Propagation, Side View, Far Crack Case

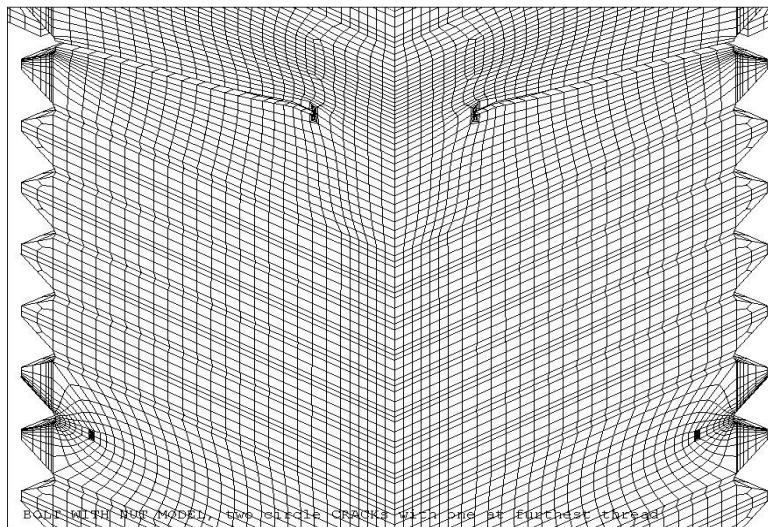


Figure A-9: Crack Propagation, Front View, Far Crack Case

Single-Max Crack Case

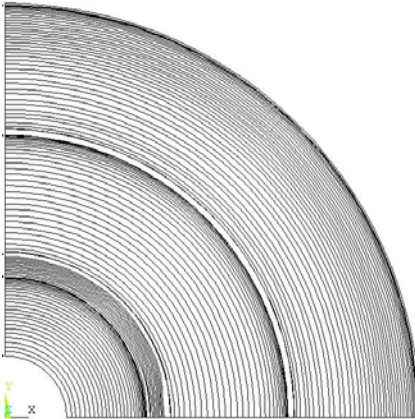


Figure A-10: Crack Front Propagation, Top View, Single-Max Crack Case

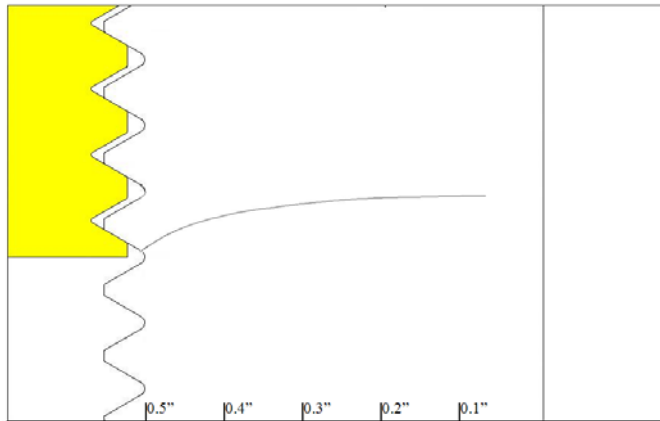


Figure A-11: Crack Propagation, Side View, Single-Max Crack Case

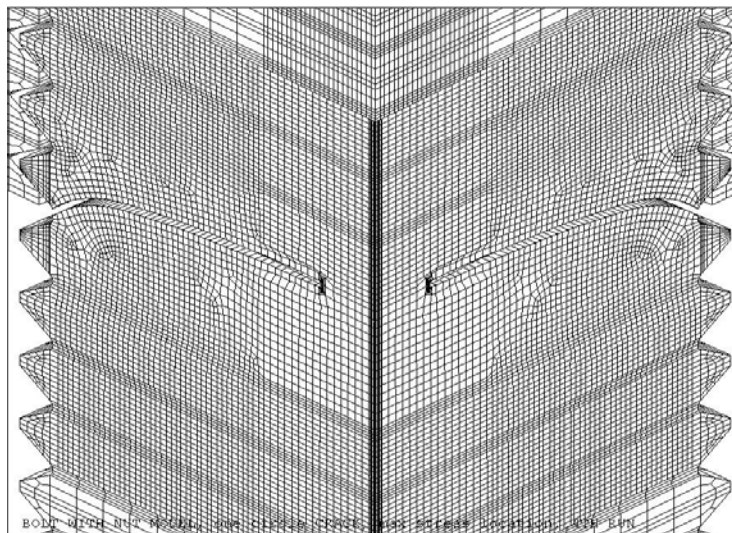


Figure A-12: Crack Propagation, Front View, Single-Max Crack Case

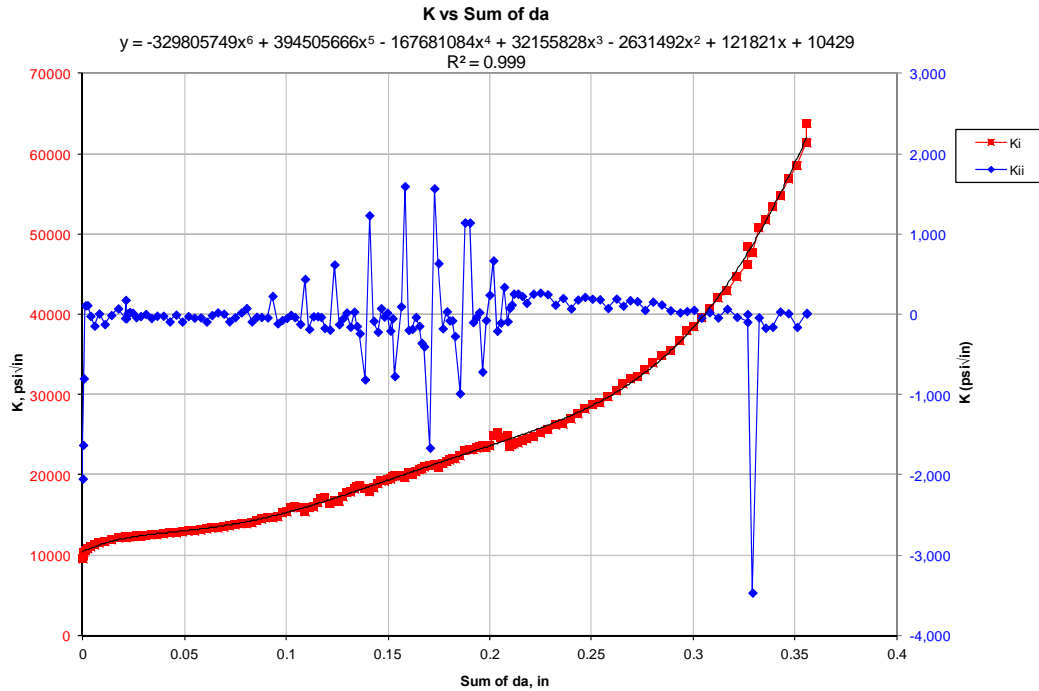


Figure A-13: Adjacent Crack Case, K vs. sum of da Curve

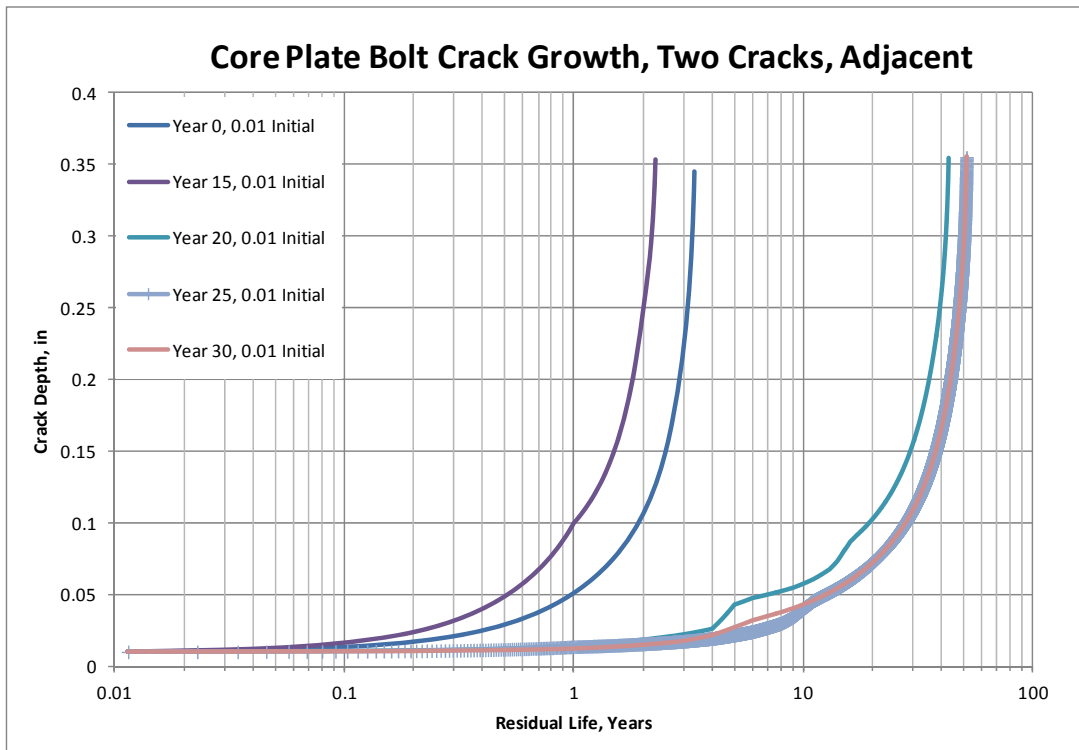


Figure A-14: Crack Growth Curves - Adjacent Crack Case, Various Initiation Times

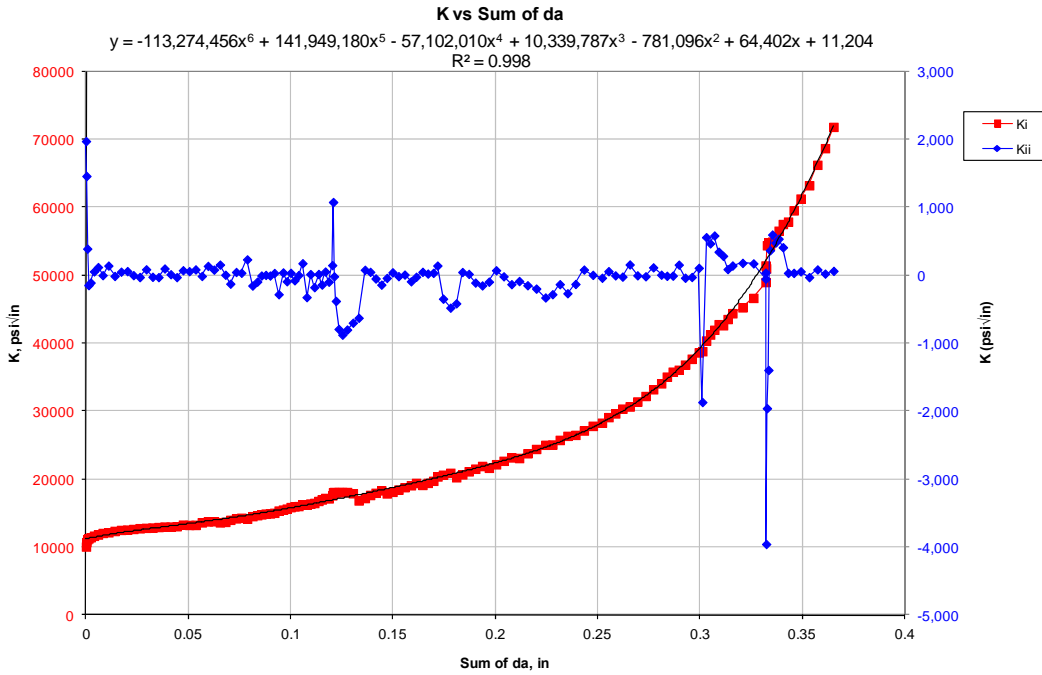


Figure A-15: Far Crack Case, K vs. sum of da Curve

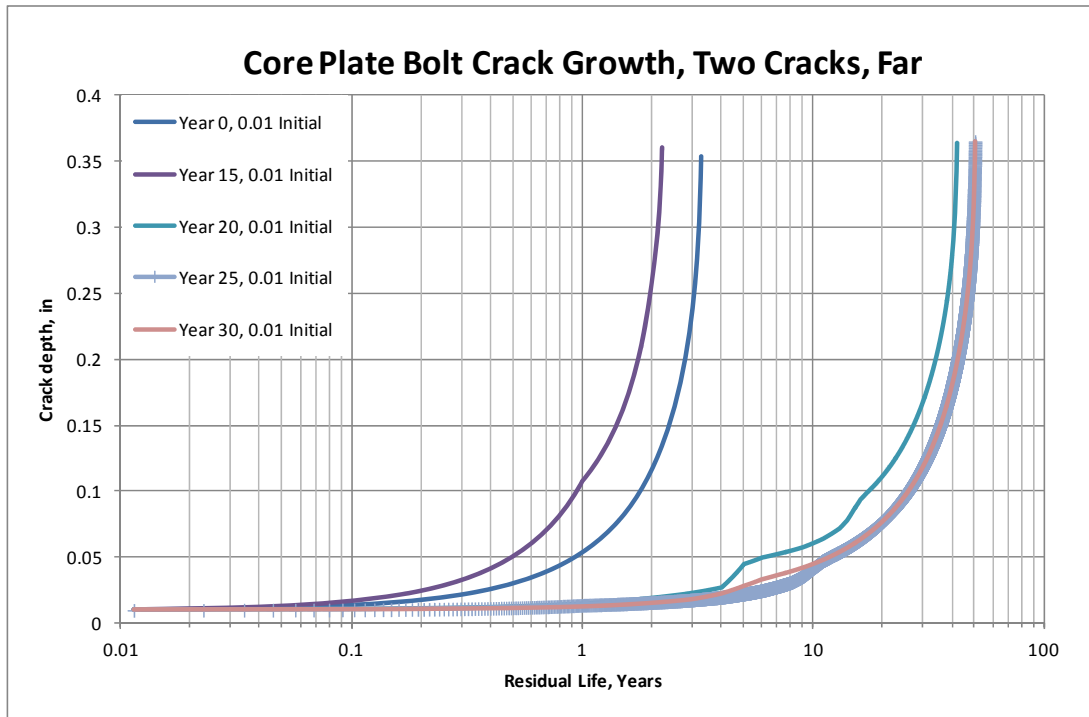


Figure A-16: Crack Growth Curves – Far Crack Case, Various Initiation Times

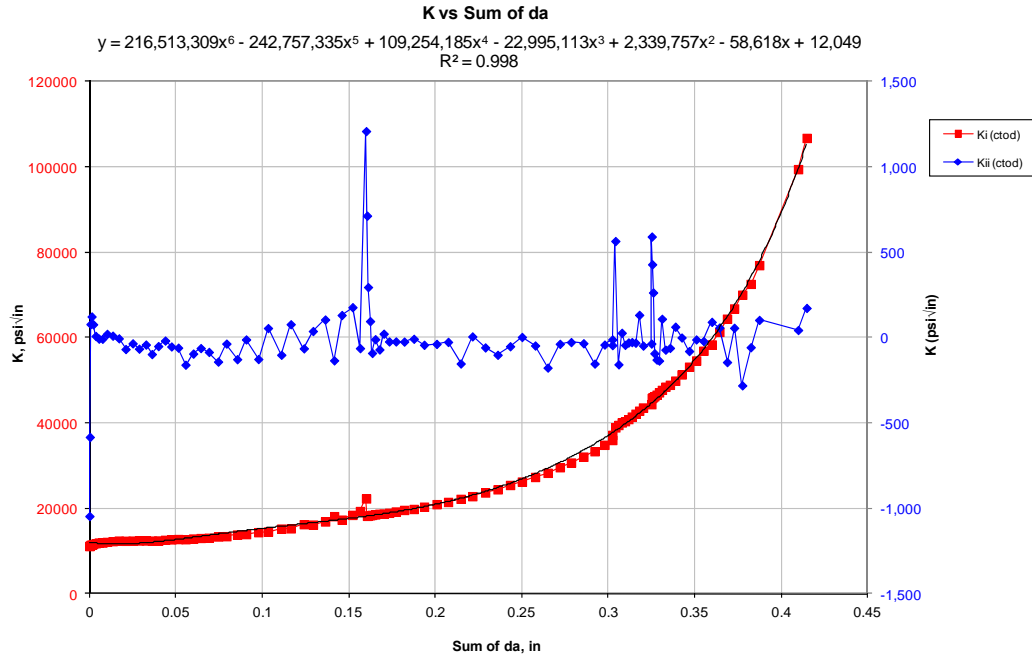


Figure A-17: Single-Max Crack Case, K vs. sum of da Curve

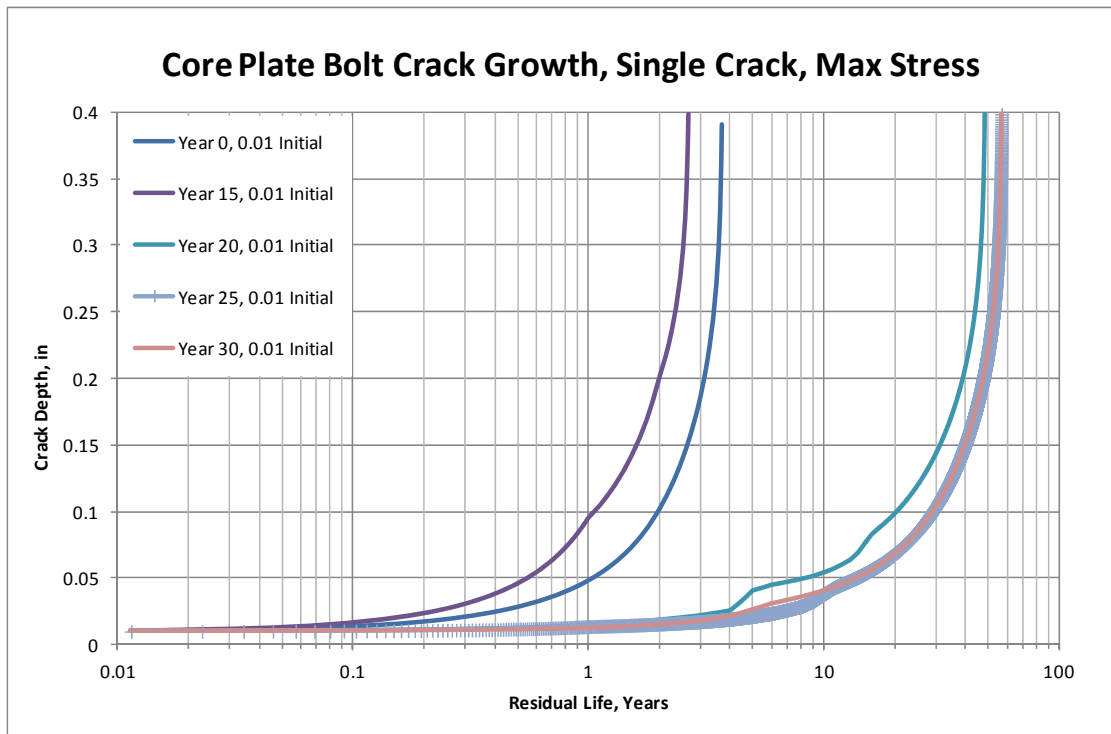


Figure A-18: Crack Growth Curves – Single-Max Crack Case, Various Initiation Times

<input type="checkbox"/> ANO-1	<input type="checkbox"/> ANO-2	<input type="checkbox"/> GGNS	<input type="checkbox"/> IP-2	<input type="checkbox"/> IP-3	<input type="checkbox"/> PLP
<input checked="" type="checkbox"/> JAF	<input type="checkbox"/> PNPS	<input type="checkbox"/> RBS	<input type="checkbox"/> VY	<input type="checkbox"/> W3	
<input type="checkbox"/> NP-GGNS-3	<input type="checkbox"/> NP-RBS-3				
CALCULATION COVER PAGE	(1) EC # 36003		(2) Page 1 of <u>14</u>		
(3) Design Basis Calc. <input checked="" type="checkbox"/> YES <input type="checkbox"/> NO		(4) <input checked="" type="checkbox"/> CALCULATION		<input type="checkbox"/> EC Markup	
(5) Calculation No: JAF-CALC-12-00016				(6) Revision: 0	
(7) Title: Minimum Required Number of Core Plate Bolts (SIA File No. 1101291.304 Rev 0)				(8) Editorial <input type="checkbox"/> YES <input checked="" type="checkbox"/> NO	
(9) System(s): 02-1 Reactor Vessel		(10) Review Org (Department): DE - Civil			
(11) Safety Class: <input checked="" type="checkbox"/> Safety / Quality Related <input type="checkbox"/> Augmented Quality Program <input type="checkbox"/> Non-Safety Related		(12) Component/Equipment/Structure Type/Number:			
		02V-1			
(13) Document Type: DCAL					
(14) Keywords (Description/Topical Codes): Core Plate Bolt					
REVIEWS					
(15) Name/Signature/Date <u>Structural Integrity Associates</u> Responsible Engineer		(16) Name/Signature/Date <u>R. Casella / R. Casella 9/10/12</u> <input type="checkbox"/> Design Verifier <input checked="" type="checkbox"/> Reviewer <input type="checkbox"/> Comments Attached		(17) Name/Signature/Date <u>G. Foster / See AS EC 36003</u> Supervisor/Approval <input type="checkbox"/> Comments Attached	

<p>CALCULATION REFERENCE SHEET</p>	<p>CALCULATION NO: <u> JAF-CALC-12-00016 </u></p> <p>REVISION: <u> 0 </u></p>																																				
<p>I. EC Markups Incorporated (N/A to NP calculations) N/A</p> <p>1.</p> <p>2.</p> <p>3.</p> <p>4.</p> <p>5.</p>																																					
<p>II. Relationships:</p>	<table border="1" style="width: 100%; border-collapse: collapse; text-align: center;"> <thead> <tr> <th style="width: 35%;">Sht</th> <th style="width: 10%;">Rev</th> <th style="width: 15%;">Input Doc</th> <th style="width: 15%;">Output Doc</th> <th style="width: 10%;">Impact Y/N</th> <th style="width: 15%;">Tracking No.</th> </tr> </thead> <tbody> <tr> <td>1. JAF-CALC-12-00013</td> <td>0</td> <td><input checked="" type="checkbox"/></td> <td><input type="checkbox"/></td> <td></td> <td></td> </tr> <tr> <td>2. JAF-CALC-12-00014</td> <td>0</td> <td><input checked="" type="checkbox"/></td> <td><input type="checkbox"/></td> <td></td> <td></td> </tr> <tr> <td>3. JAF-CALC-12-00015</td> <td>0</td> <td><input checked="" type="checkbox"/></td> <td><input type="checkbox"/></td> <td></td> <td></td> </tr> <tr> <td>4.</td> <td></td> <td><input type="checkbox"/></td> <td><input type="checkbox"/></td> <td></td> <td></td> </tr> <tr> <td>5.</td> <td></td> <td><input type="checkbox"/></td> <td><input type="checkbox"/></td> <td></td> <td></td> </tr> </tbody> </table>	Sht	Rev	Input Doc	Output Doc	Impact Y/N	Tracking No.	1. JAF-CALC-12-00013	0	<input checked="" type="checkbox"/>	<input type="checkbox"/>			2. JAF-CALC-12-00014	0	<input checked="" type="checkbox"/>	<input type="checkbox"/>			3. JAF-CALC-12-00015	0	<input checked="" type="checkbox"/>	<input type="checkbox"/>			4.		<input type="checkbox"/>	<input type="checkbox"/>			5.		<input type="checkbox"/>	<input type="checkbox"/>		
Sht	Rev	Input Doc	Output Doc	Impact Y/N	Tracking No.																																
1. JAF-CALC-12-00013	0	<input checked="" type="checkbox"/>	<input type="checkbox"/>																																		
2. JAF-CALC-12-00014	0	<input checked="" type="checkbox"/>	<input type="checkbox"/>																																		
3. JAF-CALC-12-00015	0	<input checked="" type="checkbox"/>	<input type="checkbox"/>																																		
4.		<input type="checkbox"/>	<input type="checkbox"/>																																		
5.		<input type="checkbox"/>	<input type="checkbox"/>																																		
<p>III. CROSS REFERENCES: See body of calculation.</p> <p>1.</p> <p>2.</p> <p>3.</p> <p>4.</p> <p>5.</p>																																					
<p>IV. SOFTWARE USED:</p> <p>Title: <u> None </u> Version/Release: <u> </u> Disk/CD No. <u> </u></p>																																					
<p>V. DISK/CDS INCLUDED:</p> <p>Title: <u> N/A </u> Version/Release <u> </u> Disk/CD No. <u> </u></p>																																					
<p>VI. OTHER CHANGES: None</p>																																					

Revision	Record of Revision
0	Initial issue.



Structural Integrity Associates, Inc.®

CALCULATION PACKAGE

File No.: 1101291.304

Project No.: 1101291

Quality Program: Nuclear Commercial

PROJECT NAME:

JAF Core Plate Bolt Evaluation

CONTRACT NO.:

10340564

CLIENT:

Entergy Nuclear

PLANT:

James A. Fitzpatrick Nuclear Plant

CALCULATION TITLE:

Minimum Required Number of Core Plate Bolts

NOTE: This document references vendor proprietary information. Such information is identified with -2xxP SI Project File numbers in the list of references. Any such references and the associated information in this document where those references are used are identified so that this information can be treated in accordance with applicable vendor proprietary agreements.




Document Revision	Affected Pages	Revision Description	Project Manager Approval Signature & Date	Preparer(s) & Checker(s) Signatures & Date
0	1 - 9 A-1 - A-2	Initial Issue	 D. V. Sommerville 31AUG12	<p><u>Responsible Engineer</u></p>  C. J. Oberembt 31AUG12
				<p><u>Responsible Verifier</u></p>  H. L. Gustin 31AUG12

Table of Contents

1.0	INTRODUCTION	3
2.0	TECHNICAL APPROACH	4
3.0	DESIGN INPUTS.....	6
4.0	ASSUMPTIONS.....	7
5.0	CALCULATIONS.....	8
6.0	RESULTS OF ANALYSIS	8
7.0	CONCLUSIONS	9
8.0	REFERENCES	9
	APPENDIX A CALCULATIONS	A-1

List of Tables

Table 3-1:	Design Inputs	6
Table 6-1:	Results Summary	9

List of Figures

Figure 1-1:	Core Plate Bolt Assembly.....	3
Figure 2-1:	Core Plate Bolt Free-body Diagram	6

1.0 INTRODUCTION

The James A. Fitzpatrick (JAF) nuclear power plant license renewal commitment number 23 [1, Attachment 1] states that JAF will either install core plate wedges prior to the period of extended operation or complete a plant specific analysis to develop and justify a core plate bolt inspection plan. The inspection plan must include acceptance criteria which meet the requirements of BWRVIP-25 [2].

If sufficient horizontal displacement of the core plate were to occur, the resulting misalignment could potentially prevent the control rods from inserting properly. An evaluation of the minimum number of core plate bolts required to prevent horizontal displacement of the core plate is useful for the development of an inspection protocol. Figure 1-1 illustrates the core plate bolt assembly. Applied loads including bolt preload, dead weight, core plate differential pressure (ΔP) and seismic loads are considered. This document contains the methodology and calculations utilized to determine the minimum number of required bolts.

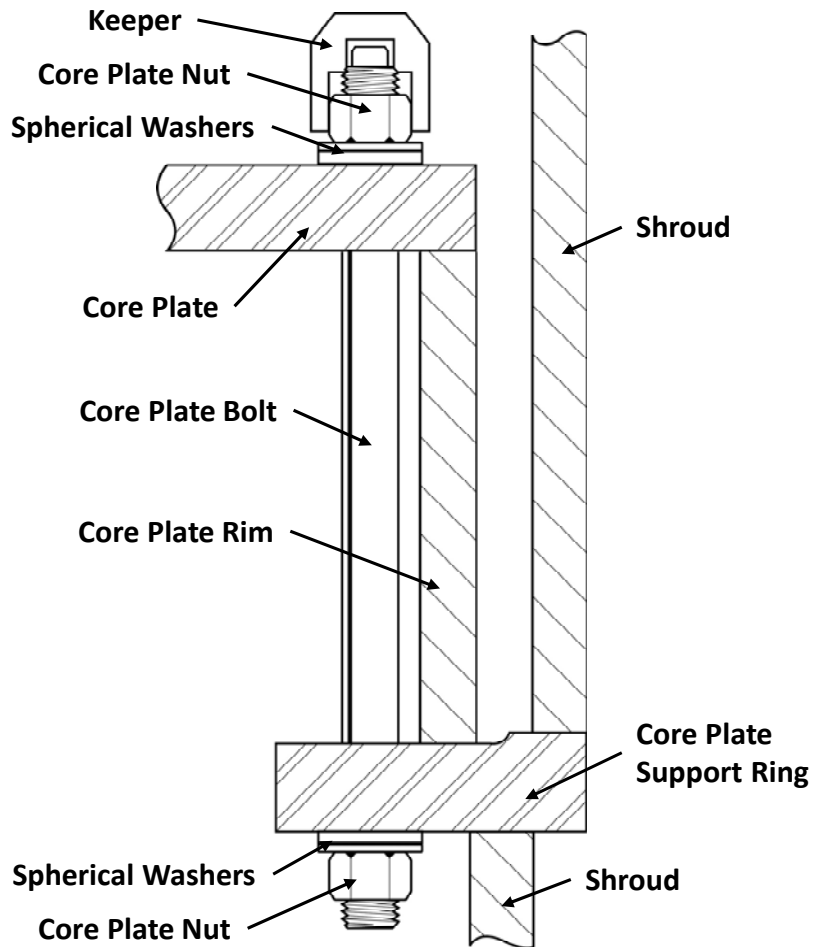


Figure 1-1: Core Plate Bolt Assembly

2.0 TECHNICAL APPROACH

This section contains a description of the technical approach used for the minimum number of required bolts calculations. The core plate to core plate support ring bolted joint is evaluated as a friction-type joint when considering horizontal displacement. As described in Reference [3, pg. 506], the amount of friction at the joint interface is proportional to the resultant normal force and the coefficient of friction. Bounding loads are used for Service Levels A/B (Normal/Upset) and C/D (Emergency/Faulted). Figure 2-1 illustrates a free-body diagram of the core plate bolt to support plate joint. Applied loads acting on this friction joint include:

- Bolt preload force, including the effects of relaxation
- Dead weight force, including the effects of buoyancy
- Core plate ΔP force, including the effects of bypass flow
- Seismic forces, due to vertical and horizontal accelerations

The total preload force is calculated using the following equation:

$$F_P = F_B * N_B \quad (1)$$

Where: F_B = Preload force per bolt, lbf
 N_B = Number of core plate bolts

The dead weight force includes the weight of the core plate and the peripheral fuel bundles. The peripheral fuel bundles are the fuel bundles around the outer periphery of the core whose weight is supported by the core plate. Since these components are fully submerged in water during operation, the effect of buoyancy is taken into account. The peripheral fuel bundles are composed of several different materials, and the effect of buoyancy is included in the wet weight. The core plate is composed of a single material, and the effect of buoyancy is evaluated by applying a buoyancy factor developed with the following equation:

$$B = 1 - \rho_{\text{water}} / \rho_{\text{steel}} \quad (2)$$

Where: B = Buoyancy factor
 ρ_{water} = Density of water, lbf/ft³
 ρ_{steel} = Density of stainless steel, lbf/ft³

The dead weight force is calculated using the following equation:

$$F_{DW} = W_{CP} * B + W_{FB} * N_{FB} \quad (3)$$

Where: F_{DW} = Dead weight force, lbf
 W_{CP} = Weight of the core plate, lbf
 W_{FB} = Weight (wet) of peripheral fuel bundles, lbf
 N_{FB} = Number of peripheral fuel bundles

The net resultant vertical force acting on the core plate due to the differential pressure across the core plate is proportional to the cross-sectional area of the core plate in the flow direction.

$$F_{\Delta P} = A_{CP} * \Delta P \quad (4)$$

Where: A_{CP} = Area of core plate, in²
 ΔP = Reactor internal differential pressure (across the core plate), psi

Vertical seismic forces are calculated for Levels A/B and C/D, using a bounding Level A/B acceleration ratio and a bounding Level C/D acceleration ratio. The acceleration ratio is the ratio of the magnitude of seismic acceleration to earth's gravitational acceleration and is unit-less. Applying these ratios to the deadweight force determines the magnitude of the seismic forces. The seismic forces are cyclic and therefore act in both the positive and negative direction. For this evaluation, consideration is given to the seismic force acting in the positive y-direction; therefore, a negative sign is used in Eq. (5) to reverse the direction of the deadweight force.

$$F_{SY} = - F_{DW} * a_v \quad (5)$$

Where: a_v = Vertical seismic acceleration ratio

The vertical resultant force at the core plate to support ring interface, shown in Figure 2-1, is the sum of the applied vertical forces and is evaluated using the following equation:

$$F_R = F_{\Delta P} + F_{SY} + F_P + F_{DW} \quad (6)$$

Where: F_R = Resultant normal force, lbf

The normal force is the reaction force due to the applied resultant force and is evaluated using the following equation:

$$F_N = - F_R \quad (7)$$

Where: F_N = Normal force, lbf

The differential pressure and the seismic forces will tend to separate the bolted joint, while the preload and dead weight forces hold the bolted joint together. Thus, for there to be no slip in the bolted joint, the force due to friction must be greater than or equal to the horizontal seismic force. Bounding horizontal seismic loads are taken for Levels A/B and C/D. The horizontal friction force is evaluated using the following relation:

$$F_{SX} \leq \mu * F_N \quad (8)$$

Where: F_{SX} = Horizontal seismic force, lbf

μ = Friction coefficient

By iterating the number of core plate bolts in Eq. (1) the minimum required number of core plate bolts which satisfies Eq. (8) is determined.

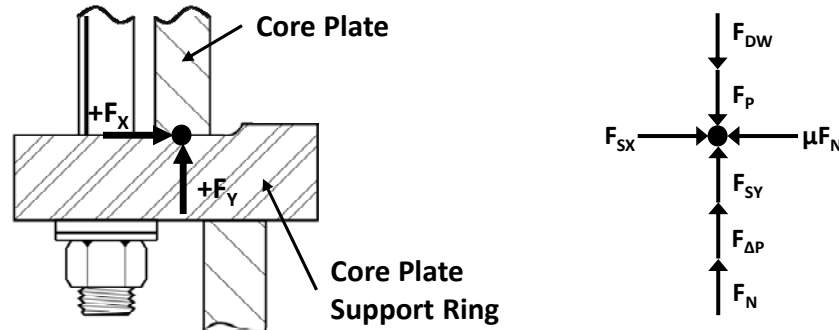


Figure 2-1: Core Plate Bolt Free-body Diagram

3.0 DESIGN INPUTS

The inputs used in this evaluation are summarized in Table 3-1 below.

Table 3-1: Design Inputs

Input	Value	Units	References
Bolt and Core Plate Material	304 SS		4, 5 (Sh. No. 1)
Preload at 54 EFPY	-12844	lbf	6
Temperature	550	°F	7
Core Plate Diameter	166	in	4, 8
Control Rod Hole Diameter	10.875	in	4, 8
No. of Fuel Holes	137		4, 8
Fuel Bundle Hole Diameter	3.5625	in	4, 8
No. of Peripheral Fuel Bundles	12		4, 8
Instrument Hole Diameter	1.863	in	4, 8
No. Instrument Holes	43		4, 8
Core Plate Weight	-10500	lbf	4, 8
Peripheral Fuel Bundle Weight (wet)	-580	lbf	4
No. of Core Plate Bolts	72		4, 8
ρ_{water} @ 550°F	45.9	lbm/ft ³	9 (pg. A-98)
ρ_{steel}	488	lbm/ft ³	9 (pg. A-90)
Coefficient of Friction	0.2		Assumed
Level A/B ΔP	29.76	psi	4
Level C/D ΔP	33	psi	4
Level A/B Vertical Acceleration Ratio	0.25		4

Table 3-1: Design Inputs (continued)

Input	Value	Units	References
Level C/D Vertical Acceleration Ratio	0.5		4
Level A/B Horizontal Force	65250	lbf	4
Level C/D Horizontal Force	87000	lbf	4

4.0 ASSUMPTIONS

The following assumptions were used in this evaluation:

1. The core plate to shroud bolted joint is assumed to be a friction-type joint, and no credit is being taken for shear in the bolts due to mechanical contact between the bolts and the core plate. This is appropriate because the bolt holes are larger than the core plate bolts [8], and unless horizontal forces greater than the initial friction force have been applied, slip is not expected to have occurred.
2. The density of stainless steel is assumed constant for the temperature range between 70°F and 550°F. This is appropriate because the volume will not change significantly in this temperature range.
3. The coefficient of static friction for Type 304 SS on Type 304 SS in the light water reactor (LWR) environment is assumed to be 0.2. The coefficient of static friction for steel on steel is reported in literature as 0.78 in the dry condition and 0.10 in the oiled condition [9, pg. 56-7]. LWR water is not expected to be as lubricating as oil; however, it is expected that the coefficient of static friction will be less than in the dry condition. The value of 0.2 is also consistent with the coefficient of static friction used in Reference [10, pg. 12], which also states that an experimentally determined coefficient closer to 0.5 was determined by GE Hitachi Nuclear Energy (GEH). Therefore, the coefficient of static friction value of 0.2 is considered conservative and appropriate for use in this evaluation.
4. The bypass flow holes surrounding the instrument holes in the core plate are assumed to be plugged. This assumption is conservative because it increases the core plate area which increases the differential pressure force, reducing the resultant normal force.
5. The mass of the peripheral fuel bundles are assumed to contribute to the vertical seismic force in the positive y-direction (up). This assumption is conservative because the peripheral fuel bundles are not coupled to the core plate, and the increased mass increases the vertical seismic force, reducing the normal force.
6. When calculating the minimum required number of core plate bolts, the remaining bolts are assumed to be evenly distributed around the core plate ensuring that eccentric loads are not applied to a small number of bolts. This is appropriate because at the bolt locations no region of the core plate is more susceptible to degradation than others. Additionally, the use of spherical washers in the bolted joint would help to ensure loading remains axial and reduce the potential for bending induced loading in the unlikely event that multiple bolts failed in close proximity creating an eccentric loading condition.

5.0 CALCULATIONS

Using the methodology described in Section 2.0 and Eq.'s (1-8), the minimum required number of core plate bolts for Levels A/B and C/D are calculated. Detailed calculations were performed in an Excel spreadsheet. Select calculations are shown in detail in this section. All calculated values are included in Appendix A.

The core plate area is calculated by subtracting the area of the holes in the core plate from the total core plate area as follows:

$$A_{CP} = \pi / 4 * (166^2 - 137 * 10.875^2 - 12 * 3.5625^2 - 43 * 1.863^2) = 8680 \text{ in}^2$$

As described in Section 2.0, by iterating the number of core plate bolts in Eq. (1) the minimum required number of core plate bolts which satisfies Eq. (8) is determined. The minimum required number of core plate bolts for Level A/B was calculated to be 45 bolts, and the Level A/B total preload force was calculated as follows:

$$F_p = -12844 * 45 = -577980 \text{ lbf}$$

The minimum required number of core plate bolts for Level C/D was calculated to be 56 bolts, and the Level C/D total preload force was calculated as follows:

$$F_p = -12844 * 56 = -719264 \text{ lbf}$$

The Service Level A/B resultant and normal forces are calculated using Eq. (6) and Eq. (7) as follows:

$$F_R = 258325 + 4118 + (-577980) + (-16472) = -332009 \text{ lbf}$$
$$F_N = 332009 \text{ lbf}$$

The Service Level C/D resultant and normal forces are calculated using Eq. (6) and Eq. (7) as follows:

$$F_R = 286449 + 8236 + (-719264) + (-16472) = -441051 \text{ lbf}$$
$$F_N = 441051 \text{ lbf}$$

6.0 RESULTS OF ANALYSIS

The results provide the minimum required number of core plate bolts and the associated frictional force at 54 EFPY. The results have conservatively been rounded up to the nearest whole number of bolts are summarized in Table 6-1.

A sensitivity analysis was performed for the peripheral fuel bundle weight by removing the peripheral fuel bundles from the dead weight calculation. Removing the deadweight of the peripheral fuel bundles significantly reduces the deadweight force and the vertical seismic forces, by almost 60%. However, since these values are so small compared to the total normal force (thousands compared to hundreds of thousands) there is no impact on the minimum required number of bolts calculated in this evaluation.

Table 6-1: Results Summary

Service Level	No. of Bolts	Friction Force (lbf)	Horizontal Force (lbf)
A/B	72	135759	65250
	45	66402	
C/D	72	129311	87000
	56	88210	

Note: Friction force values are shown as absolute values.

7.0 CONCLUSIONS

Service level C/D was the most limiting condition. The minimum number of core plate bolts required to ensure no relative horizontal displacement of the core plate is 56. The remaining core plate bolts are assumed to be evenly distributed around the core plate. These results are valid to 54 EFPY.

8.0 REFERENCES

1. James A. Fitzpatrick Nuclear Plant License Renewal Application, Amendment 9, ADAMS Accession No. ML071060390.
2. EPRI TR-107284, BWR Vessel and Internals Project, BWR Core Plate Inspection and Flaw Evaluation Guidelines (BWRVIP-25), December 1996, SI File No. BWRVIP-01-225P (**EPRI Proprietary Information**).
3. J. H. Bickford, "An Introduction to the Design and Behavior of Bolted Joints," CRC Press, Taylor & Francis Group, 3rd Edition, 1995, SI File no. 1101291.221.
4. SI Project No. 1101291, Design Input Request, Revision 4, SI File No. 1101291.201.
5. GE Document No. 21A1056, "Standard Requirements for Miscellaneous Piping and Hardware (Reactor Internals)," SI File No. 1101291.210.
6. SI Calculation No. 1101291.302, Revision 0, "Core Plate Bolt Preload Relaxation."
7. General Electric Drawing No. 729E762, Revision 2, "Reactor Thermal Cycles," SI File No. 0800846.202.
8. Sun Shipbuilding & Drydock Co. Drawing No. 42360-6, "Core Support for Core Structure," JAF MPL No. B11-0003, SI File No. 1101291.201.
9. M. R. Lindeburg, Mechanical Engineering Reference Manual, 12th Ed., Professional Publications, Inc., 2006, SI File No. 1101291.221.
10. United States Nuclear Regulatory Commission, "Safety Evaluation by the Office of Nuclear Reactor Regulation Core Plate Hold Down Bolt Inspection Plan and Analysis Entergy Nuclear Operations, Inc. Vermont Yankee Nuclear Power Station Docket No. 50-271," ADAMS Accession No. ML120760152, SI File No. 1101291.211.

APPENDIX A
CALCULATIONS

Variables

Remaining Bolts (A/B)	45
Remaining Bolts (C/D)	56

Calculations

All Bolts Preload Force	-924768	lbf
Final Preload Force (A/B)	-577980	lbf
Final Preload Force (C/D)	-719264	lbf

Control Rod Hole Area	12725.3	in ²
Peripheral Bundle Area	119.6	in ²
Instrument Hole Area	117.2	in ²
Bypass Hole Area	0.0	in ²
CP Area	8680.3	in ²

Pressure Force (A/B)	258325	lbf
per bolt	5741	lbf
Pressure Force (C/D)	286449	lbf
per bolt	5115	lbf

Density, SS (550°F)	488.0	lbm/ft ³
Buoyancy Factor	0.90594	
Deadweight Force	-16472	lbf

Vertical Seismic Force (A/B)	4118	lbf
Vertical Seismic Force (C/D)	8236	lbf

All Bolts Normal Force (A/B)	678797	lbf
All Bolts Normal Force (C/D)	646555	lbf
Final Normal Force (A/B)	332009	lbf
Final Normal Force (C/D)	441051	lbf
All Bolts Friction Force (A/B)	135759	lbf
All Bolts Friction Force (C/D)	129311	lbf
Final Friction Force (A/B)	66402	lbf
Final Friction Force (C/D)	88210	lbf

OK
OK

- | | | | | | |
|---|-----------------------------------|-------------------------------|-------------------------------|-------------------------------|------------------------------|
| <input type="checkbox"/> ANO-1 | <input type="checkbox"/> ANO-2 | <input type="checkbox"/> GGNS | <input type="checkbox"/> IP-2 | <input type="checkbox"/> IP-3 | <input type="checkbox"/> PLP |
| <input checked="" type="checkbox"/> JAF | <input type="checkbox"/> PNPS | <input type="checkbox"/> RBS | <input type="checkbox"/> VY | <input type="checkbox"/> W3 | |
| <input type="checkbox"/> NP-GGNS-3 | <input type="checkbox"/> NP-RBS-3 | | | | |

**CALCULATION
COVER PAGE**

(1) EC # 36003

(2) Page 1 of 23
26

*Rec
9/10/12*

(3) Design Basis Calc. YES NO (4) CALCULATION EC Markup

(5) Calculation No: **JAF-CALC-12-00017**

(6) Revision: **0**

(7) Title: **Minimum Required Number of Core Plate Bolts - Consideration of Aligner Brackets (SIA File No. 1101291.305 Rev 0)**

(8) Editorial
 YES NO

(9) System(s): **02-1 Reactor Vessel**

(10) Review Org (Department): **DE - Civil**

(11) Safety Class:

- Safety / Quality Related
 Augmented Quality Program
 Non-Safety Related

(12) Component/Equipment/Structure Type/Number:

02V-1

(13) Document Type: **DCAL**

(14) Keywords (Description/Topical Codes):

Core Plate Bolt

REVIEWS

(15) Name/Signature/Date
Structural Integrity Associates
Responsible Engineer

(16) Name/Signature/Date
R. Casella | R. Casella 9/10/12
 Design Verifier
 Reviewer
 Comments Attached

(17) Name/Signature/Date
G. Foster / See AS EC 36003
Supervisor/Approval
 Comments Attached

CALCULATION REFERENCE SHEET	CALCULATION NO: <u>JAF-CALC-12-00017</u> REVISION: <u>0</u>																																				
I. EC Markups Incorporated (N/A to NP calculations) N/A 1. 2. 3. 4. 5.																																					
II. Relationships:	<table border="1" style="width: 100%; border-collapse: collapse; text-align: center;"> <thead> <tr> <th style="width: 35%;">Sht</th> <th style="width: 10%;">Rev</th> <th style="width: 15%;">Input Doc</th> <th style="width: 15%;">Output Doc</th> <th style="width: 15%;">Impact Y/N</th> <th style="width: 10%;">Tracking No.</th> </tr> </thead> <tbody> <tr> <td>1. JAF-CALC-12-00013</td> <td>0</td> <td><input checked="" type="checkbox"/></td> <td><input type="checkbox"/></td> <td></td> <td></td> </tr> <tr> <td>2. JAF-CALC-12-00014</td> <td>0</td> <td><input checked="" type="checkbox"/></td> <td><input type="checkbox"/></td> <td></td> <td></td> </tr> <tr> <td>3. JAF-CALC-12-00015</td> <td>0</td> <td><input checked="" type="checkbox"/></td> <td><input type="checkbox"/></td> <td></td> <td></td> </tr> <tr> <td>4. JAF-CALC-12-00016</td> <td>0</td> <td><input checked="" type="checkbox"/></td> <td><input type="checkbox"/></td> <td></td> <td></td> </tr> <tr> <td>5.</td> <td></td> <td><input type="checkbox"/></td> <td><input type="checkbox"/></td> <td></td> <td></td> </tr> </tbody> </table>	Sht	Rev	Input Doc	Output Doc	Impact Y/N	Tracking No.	1. JAF-CALC-12-00013	0	<input checked="" type="checkbox"/>	<input type="checkbox"/>			2. JAF-CALC-12-00014	0	<input checked="" type="checkbox"/>	<input type="checkbox"/>			3. JAF-CALC-12-00015	0	<input checked="" type="checkbox"/>	<input type="checkbox"/>			4. JAF-CALC-12-00016	0	<input checked="" type="checkbox"/>	<input type="checkbox"/>			5.		<input type="checkbox"/>	<input type="checkbox"/>		
Sht	Rev	Input Doc	Output Doc	Impact Y/N	Tracking No.																																
1. JAF-CALC-12-00013	0	<input checked="" type="checkbox"/>	<input type="checkbox"/>																																		
2. JAF-CALC-12-00014	0	<input checked="" type="checkbox"/>	<input type="checkbox"/>																																		
3. JAF-CALC-12-00015	0	<input checked="" type="checkbox"/>	<input type="checkbox"/>																																		
4. JAF-CALC-12-00016	0	<input checked="" type="checkbox"/>	<input type="checkbox"/>																																		
5.		<input type="checkbox"/>	<input type="checkbox"/>																																		
III. CROSS REFERENCES: See body of calculation. 1. 2. 3. 4. 5.																																					
IV. SOFTWARE USED: Title: <u>None</u> Version/Release: _____ Disk/CD No. _____																																					
V. DISK/CDS INCLUDED: Title: <u>N/A</u> Version/Release _____ Disk/CD No. _____																																					
VI. OTHER CHANGES: None																																					

Revision	Record of Revision
0	Initial issue.



Structural Integrity Associates, Inc.®

CALCULATION PACKAGE

File No.: 1101291.305

Project No.: 1101291

Quality Program: Nuclear Commercial

PROJECT NAME:

JAF Core Plate Bolt Evaluation

CONTRACT NO.:

10340564

CLIENT:

Entergy Nuclear

PLANT:

James A. FitzPatrick Nuclear Power Plant

CALCULATION TITLE:

Minimum Required Number of Core Plate Bolts – Consideration of Aligner Brackets




Document Revision	Affected Pages	Revision Description	Project Manager Approval Signature & Date	Preparer(s) & Checker(s) Signatures & Date
0	1 - 19 A-1 - A-4	Initial Issue	 Daniel V. Sommerville 31AUG12	Responsible Engineer:  Matthew C. Walter 31AUG12 Responsible Verifier:  Harry L. Gustin 31AUG12

Table of Contents

1.0	INTRODUCTION	4
2.0	OBJECTIVE	4
3.0	METHODOLOGY	4
3.1	Energy Method	5
3.2	Stiffness Calculation	7
4.0	ASSUMPTIONS.....	8
5.0	DESIGN INPUT	9
6.0	CALCULATIONS.....	9
6.1	Stiffness Calculation.....	9
6.2	Normal Force Calculation.....	10
6.3	Stress Calculation	10
6.3.1	<i>Aligner Pin</i>	10
6.3.2	<i>Pin-to-Bracket Weld</i>	10
6.3.3	<i>Aligner Bracket</i>	11
6.3.4	<i>Bracket-to-Rim Weld</i>	11
6.3.5	<i>Limiting Force on Aligner pin bracket assembly</i>	12
6.4	Minimum Required Bolts Calculation.....	12
7.0	CONCLUSIONS	13
8.0	REFERENCES	13
	APPENDIX A ANSYS VERIFICATION.....	A-1

List of Tables

Table 1: Allowable Stress Criteria.....	15
Table 2: Stiffness Calculation.....	15
Table 3: Unit Stress Summary.....	15
Table 4: Minimum Required Bolt Calculation Comparison.....	16

List of Figures

Figure 1. Aligner Pin and Core Support Ring Interface	16
Figure 2. Aligner Pin and Bracket Assembly Locations	17
Figure 3. General View of Aligner Pin and Bracket Assembly	18
Figure 4. Dimensions of Aligner Pin and Bracket Assembly.....	18
Figure 5. Free Body Diagram of Aligner Pin and Bracket Assembly	19
Figure 6. Cross Sections Analyzed.....	19

1.0 INTRODUCTION

The James A. Fitzpatrick (JAF) nuclear power plant license renewal commitment number 23 [1, Attachment 1] states that JAF will either install core plate wedges prior to the period of extended operation or complete a plant specific analysis to develop and justify a core plate bolt inspection plan. The inspection plan must include acceptance criteria which meet the requirements of BWRVIP-25 [2].

If sufficient horizontal displacement of the core plate were to occur, the resulting misalignment could potentially prevent the control rods from inserting properly. An evaluation of the minimum number of core plate bolts required to resist horizontal displacement of the core plate, without taking credit for the load carrying capacity of the aligner pin and bracket assemblies, was performed by Structural Integrity Associates, Inc. (SI) in Reference [3].

2.0 OBJECTIVE

The objective of the calculation documented in this calculation package is to determine the minimum number of core plate bolts required to prevent lateral motion of the core plate assembly, during a seismic event, when the presence of the aligner pin and bracket assemblies is considered.

3.0 METHODOLOGY

Reference [3] provides a calculation for the minimum number of core plate bolts required to prevent horizontal displacement of the core plate assembly during a seismic event. That calculation conservatively neglects the load carrying capacity of the core plate aligner pin and bracket assemblies. These assemblies provide an additional, redundant, lateral support for the core plate. If these assemblies are considered then a more accurate calculation of the number of core plate bolts required to prevent lateral displacement of the core plate assembly can be performed. Consideration of these assemblies will result in fewer required core plate bolts.

Since the design of the aligner pin and bracket assemblies allow for a gap between the aligner pin and the core support ring it is possible that the core plate assembly would slide horizontally enough to close the gap before the aligner pin and bracket assembly were available to react the seismic load. In this case a dynamic load exists; thus, the static methods used in Reference [3] are not adequate for the present calculation. The potential for an impact loading against the aligner pin is accounted for by using an energy method which considers the kinetic energy of the core plate assembly, the elastic deformation of the aligner pin and bracket assembly, and energy lost by friction between the core plate rim and core support ring. Although plastic deformation could also occur, using a linear-elastic approach is conservative since it only considers energy absorbed up to the yield limit. This approach requires two criteria to be met:

1. All stresses must remain below the yield stress, S_y , of the material. This justifies the use of the elastic equations for spring energy.

2. ASME Code allowable stress criteria must be met for the aligner pin and bracket assemblies and AWS Code allowable stress criteria must be met for the welds. The applicable stress limits are shown in Table 1. These stress limits are conservatively applied to both Service Level A/B and Service Level C/D conditions. Service Level C/D has higher stress limits than for Service Level A/B and allows structural deformation (evaluated by plastic analysis allowed by NB-3228).

The energy method, stiffness calculations, and stress calculations are described below.

3.1 Energy Method

Considering the initial gap between the aligner pin and the core support ring the core plate assembly may accelerate from rest until the gap, x_{gap} , is closed. The aligner pin and core support ring interface is shown in Figure 1. The aligner pin and bracket assembly will then absorb energy from the impact loading contributed by the contact between the core plate assembly and the core support ring. The seismic load is the only relevant horizontal load for the core plate assembly; therefore, this is the only horizontal load considered in this analysis. Assuming the core plate starts at rest, the change in kinetic energy of the system, ΔKE , can be expressed as [6, Section 23]:

$$\Delta KE = \frac{1}{2} m_f v_f^2 - \frac{1}{2} m_i v_i^2 \quad (1)$$

Where: m_f and m_i = Final and initial mass of the system, lbm
 v_f and v_i = Final and initial velocity of the system, ft/s

Using the work-energy principle [6, Section 23], the change in kinetic energy of the system equals the work, W , performed on the system. Therefore:

$$W = \Delta KE \quad (2)$$

The work performed by, or to, the system can also be expressed as [6, Section 23]:

$$W = F \cdot x = F_{seismic} \cdot x_{gap} \quad (3)$$

The aligner pin and bracket assembly can be represented as an elastic spring (assuming only elastic deformation is allowed, which is a conservative assumption) with a stiffness, k , and displacement, δ , that counteracts the kinetic energy of the core plate. The energy in an elastic spring is [6, Section 23]:

$$\text{Energy} = \frac{1}{2} k \delta^2 \quad (4)$$

The stiffness of the aligner pin and bracket assembly, k , is calculated using classical equations and is verified by finite element analysis. The methodology for calculating stiffness is presented in Section 3.2.

In addition to the stiffness of the aligner pin and bracket assembly, the friction force acting between the core plate assembly and the core support plate, contributed by the normal force provided by the core

plate bolts, acts to resist the horizontal seismic force. Equations 3 and 4 can be rewritten for the friction force as:

$$W_{\text{friction}} = \mu \cdot F_N \cdot x_{\text{gap}} + \mu \cdot F_N \cdot \delta \quad (5)$$

Where: μ = Coefficient of kinetic friction

The total normal force contributed by all intact bolts, F_N , is calculated per Reference [3, Equation 6], using signs from Reference [3, Figure 2-1], as:

$$F_N = -(F_{\Delta P} + F_{SY} - n \cdot F_P - F_{DW}) \quad (6)$$

Where:

$F_{\Delta P}$	= Force due to differential pressure, lbf
F_{SY}	= Force due to vertical seismic loads, lbf
F_P	= Force due to bolt preload, lbf
n	= Number of intact core plate bolts
F_{DW}	= Force due to deadweight, lbf

Since the energy of the core plate due to the seismic force must be absorbed by the friction of the bolts and deformation of the bracket, Equations 3, 4, and 5 can be combined to balance the energy of the system:

$$F_{\text{seismic}} \cdot x_{\text{gap}} = \frac{1}{2} k \delta^2 + \mu \cdot F_N \cdot x_{\text{gap}} + \mu \cdot F_N \cdot \delta \quad (7)$$

Using Hooke's Law for an ideal spring, an equivalent static force, F_{eqv} , which would perform identical work as applied to the system, can be written as [6, Section 23]:

$$F_{\text{eqv}} = k \cdot \delta \quad \text{or} \quad \delta = F_{\text{eqv}} / k \quad (8)$$

Substituting Equation 8 into Equation 7 yields:

$$F_{\text{seismic}} \cdot x_{\text{gap}} = \frac{1}{2} F_{\text{eqv}}^2 / k + \mu \cdot F_N (x_{\text{gap}} + F_{\text{eqv}} / k) \quad (9)$$

Solving for the required normal force yields:

$$F_N = (F_{\text{seismic}} \cdot x_{\text{gap}} - \frac{1}{2} F_{\text{eqv}}^2 / k) / \mu (x_{\text{gap}} + F_{\text{eqv}} / k) \quad (10)$$

Equations 6 and 10 can be combined and solved to determine the number of core plate bolts required to prevent lateral displacement of the core plate assembly during a seismic event.

3.2 Stiffness Calculation

Castigliano's theorem is used to determine the stiffness of the aligner pin and bracket assembly. Castigliano's theorem is an energy method that states [7, Section 4-8]:

“When forces act on elastic systems subject to small displacements, the displacements corresponding to any force, in the direction of the force, is equal to the partial derivative of the total strain energy with respect to that force.”

This can formally be written as [7, Section 4-8]:

$$\delta_i = \partial U / \partial F_i \quad (11)$$

Where: δ_i is the displacement of the point of application of the force F_i

Through the use of calculus, and per Reference [7, Section 4-8], the following equations result for deflections in a beam:

$$\text{Axial Deflections: } \delta = (Fl)/(AE) \quad (12)$$

$$\text{Bending Deflections: } y = (Fl^3)/(3EI) \quad (13)$$

Where:

l	= the length of the section
A	= the cross-sectional area of the section
E	= the Young's modulus
I	= the moment of inertia

Using Hooke's Law (Equation 8) and solving for stiffness yields:

$$\text{Axial Stiffness: } k_{\text{axial}} = (AE)/l \quad (14)$$

$$\text{Bending Stiffness: } k_{\text{bending}} = (3EI)/(l^3) \quad (\text{cantilever beam}) \quad (15)$$

The equivalent stiffness of the system can then be calculated by treating the aligner pin and bracket assembly as a system of springs in series, with each member of the assembly contributing to a portion of the total deflection, with the equation:

$$K_{\text{eq}} = 1/(\sum 1/K) \quad (16)$$

4.0 ASSUMPTIONS

The following assumptions are made for this calculation.

1. Due to the orientation of the aligner pin assembly on the core plate rim, more than one aligner pin assembly will be loaded regardless of the direction of the earthquake loading. For this analysis, it is assumed that only one aligner pin is in contact and is in pure compression. In this scenario, two additional aligner pins would be in shear; however, the shear strength of the pins is neglected here for simplicity. This is conservative. Figure 2 shows the configuration of aligner pins and bracket assemblies per Reference [12].
2. For the aligner pin and bracket stiffness calculation, it is assumed that the welds are infinitely stiff since they are small in comparison to the overall structure and the overall stiffness is dominated by the stiffness of less stiff components (as a result of stiffnesses acting in series). The stiffness of the core plate rim is conservatively neglected. This yields a smaller deflection and therefore higher stiffness of the assembly and higher stress.
3. The length of the aligner pin beyond the weld is assumed to be 0.25 in, as shown in Figure 4. Since this is not part of the load path, the distance does not contribute to the calculations.
4. Reference [10] specifies that all bars are A-276 Type 304 stainless steel and that all plates are A-240 Type 304 stainless steel for the aligner pin and bracket assembly. Reference [13] does not provide material properties for SA-276 Type 304 stainless steel. Section II Part A of the 2002 Addenda of the ASME Code [14] gives identical chemical compositions and mechanical requirements for both SA-276 Type 304 stainless steel and SA-240 Type 304 stainless steel. Therefore, it is assumed that ASME Code Section II Part D [13] material properties are identical, and properties of SA-240 Type 304 stainless steel from Reference [13] are used for both materials.
5. The coefficient of kinetic friction is assumed to be 0.2. This is the same value that was used in the Reference [3] calculation package. Although that calculation assumes static friction and the present calculation assumes kinetic friction, Reference [16] presents an experimentally determined coefficient of friction of 0.5 for Type 304 stainless steel sliding with deoxygenated water as a lubricant. Therefore, the coefficient of kinetic friction of 0.2 is conservative and is appropriate for use in this calculation.

5.0 DESIGN INPUT

A general view of the aligner pin and bracket assembly is shown in Figure 3. Dimensions of the aligner pin and bracket assembly are obtained from References [5, 10, and 11] and are shown in Figure 4. Other design input is outlined below.

- Coefficient of kinetic friction, μ = 0.2 (see Section 4.0)
- Initial gap, x_{gap} = 0.030 in (max gap [5])
= 0.015 in. (nominal gap [5])
- Horizontal OBE seismic force on core plate, F_{seismic} = 65,250 lbf [4]
- Horizontal DBE seismic force on core plate, F_{seismic} = 87,000 lbf [4]
- Total force due to differential pressure, $F_{\Delta P}$ = 258,325 lbf for SL A/B [3, Appendix A]
= 286,449 lbf for SL C/D [3, Appendix A]
- Total force due to vertical seismic loads, F_{SY} = 4,118 lbf for SL A/B [3, Appendix A]
= 8,236 lbf for SL C/D [3, Appendix A]
- Force due to bolt preload, F_p = 12,844 lbf per bolt [3, Appendix A]
- Total force due to deadweight, F_{DW} = 16,472 lbf [3, Appendix A]
- Material type:
 - Aligner pin = A-276 Type 304 stainless steel [10]
 - Aligner bracket = A-240 Type 304 stainless steel [10]
 - Core plate rim = A-240 Type 304 stainless steel [10]
- Young's modulus (all components), E = 25,700,000 psi at 550°F [13]
- Yield strength (all components), S_y = 18,900 psi at 550°F [13]
- Ultimate tensile strength (all components), S_u = 63,400 psi at 550°F [13]
- Design stress intensity (all components), S_m = 16,950 psi at 550°F [13]

6.0 CALCULATIONS

This section presents the calculations performed for this evaluation and summarizes the relevant results. The calculations performed to determine the stiffness of the aligner pin and bracket assembly, the allowable loads acting on the assembly components, as determined by the allowable stresses, and the minimum required number of core plate bolts are documented below.

6.1 Stiffness Calculation

Figure 5 shows the free body diagram of the aligner pin and bracket assembly. Table 2 includes the details of the stiffness calculation for each component using methodology from Section 3.2. The equivalent stiffness of the aligner pin and bracket assembly is 4,100,000 lbf/in (Note: additional digits

are carried in the calculation to avoid rounding error propagation). Appendix A documents a confirmatory analysis performed, using the ANSYS [15] finite element software, to validate the results calculated using the classical methods described above.

6.2 Normal Force Calculation

The normal force is calculated using Equation 6 and loading outlined in Section 5.0 as:

Service Level A/B:

$$F_N = -(258325 + 4118 - 13051 \cdot n - 16472) = -(245971 - 12844 \cdot n) \quad (17)$$

Service Level C/D:

$$F_N = -(286449 + 8236 - 13051 \cdot n - 16472) = -(278213 - 12844 \cdot n) \quad (18)$$

Where: n = Number of intact core plate bolts

6.3 Stress Calculation

A stress analysis of the aligner pin and bracket assembly is performed to determine the limiting force which can be supported by the assembly, F_{eqv} . The stress analysis is performed using a unit load of 10,000 lbf. A ratio of the calculated stress to the allowable stress, $Stress_{calculated}/Stress_{allowable}$, is determined at each location. The core plate rim is not evaluated in this analysis since it is bounded by the bracket-to-rim weld. The following cross sections are analyzed and are shown in Figure 6:

- Aligner Pin
- Pin-to-Bracket Weld
- Aligner Bracket
- Bracket-to-Rim Weld

The location with the largest stress ratio is the limiting location. The following calculations are performed for the limiting cross sections.

6.3.1 *Aligner Pin*

$$\text{Bearing Stress: } \sigma = F/A = 10000/(\pi \cdot 1.5^2) = 1,415 \text{ psi}$$

$$\text{Stress Ratio: Elastic: } 1,415/18,900 = 0.0749$$

$$\text{Code: } 1,415/28,350 = 0.0499$$

6.3.2 *Pin-to-Bracket Weld*

$$\text{Shear Stress: } \tau = F/A$$

$$\text{Where: } A = 1.414 \cdot \pi \cdot h \cdot r \text{ [7, Table 9-1]}$$

$$\text{Therefore: } \tau = 10000/(1.414 \cdot \pi \cdot 0.25 \cdot 1.5) = 6,003 \text{ psi}$$

$$\text{Stress Ratio: Elastic: } 6,003/18,900 = 0.3176$$

$$\text{Code: } 6,003/19,020 = 0.3156$$

6.3.3 *Aligner Bracket*

$$\text{Shear Stress: } \tau = F/A = 10,000/(5 \cdot 3) = 667 \text{ psi}$$

$$\text{Stress Ratio: Elastic: } 667/18,900 = 0.0353$$

$$\text{Code: } 667/10,170 = 0.0656$$

$$\text{Bending Stress: } \sigma_{\text{bend}} = Mc/I = (10,000 \cdot 3) \cdot 1.5 / (5 \cdot 3^3 / 12) = 4,000 \text{ psi}$$

$$\text{Stress Ratio: Elastic: } 4,000/18,900 = 0.2116$$

$$\text{Code: } 4,000/28,350 = 0.1411$$

$$\text{Total stress} = \sigma_{\text{bend}} + \tau = \sqrt{667^2 + 4,000^2} = 4,055 \text{ psi}$$

$$\text{Elastic Stress Ratio: } 4,055/18,900 = 0.2146$$

6.3.4 *Bracket-to-Rim Weld*

$$\text{Shear Stress: } \tau = F/A$$

$$\text{Where: } A = 2 \cdot t_e (b+d)$$

$$\text{The throat length, } t_e, \text{ is calculated as: } t_e = \sqrt{0.5^2 + 0.75^2} = 0.9014 \text{ in (see Figure 4 for weld throat)}$$

$$\text{Therefore: } \tau = 10,000 / (2 \cdot 0.9014(5+5)) = 555 \text{ psi}$$

$$\text{Stress Ratio: Elastic: } 555/18,900 = 0.0293$$

$$\text{Code: } 555/19,020 = 0.0292$$

$$\text{Bending Stress: } \sigma_{\text{bend}} = Mc/I$$

$$\text{The Moment of Inertia, } I, \text{ is calculated as: } I = t_e (d^2/6)(3b+d)$$

$$\text{Therefore: } \sigma_{\text{bend}} = (10,000 \cdot 5.5) \cdot 2.5 / 0.9014(5^2/6)(3 \cdot 5 + 5) = 1,831 \text{ psi}$$

$$\text{Stress Ratio: Elastic: } 1,831/18,900 = 0.0969$$

$$\text{Code: } 1,831/19,020 = 0.0962$$

$$\text{Total stress} = \sigma_{\text{bend}} + \tau = 1831 + 555 = 2,386 \text{ psi}$$

$$\text{Stress Ratio: Elastic: } 2,385/18,900 = 0.1262$$

$$\text{Code: } 2,385/19,020 = 0.1254$$

6.3.5 Limiting Force on Aligner pin bracket assembly

Table 3 summarizes the results from the unit stress calculations in Sections 6.3.1 through 6.3.4. The stress ratio for shear stress at the pin to bracket weld, based on the elastic stress limit, is the highest ratio in the aligner pin bracket assembly. Therefore, the limiting equivalent force, F_{eqv} , for the system can be determined by setting the stress equal to the elastic limit of 18,900 psi and solving for the force. This yields:

$$\tau = F_{eqv}/A = F/1.414 \cdot \pi \cdot h \cdot r$$

$$F_{eqv} = 18,900 \cdot 1.414 \cdot \pi \cdot 0.25 \cdot 1.5 = 31,484 \text{ lbf}$$

This force is used as the limiting F_{eqv} in Equation 12.

6.4 Minimum Required Bolts Calculation

The normal force required by the bolts is given in Equation 10. For Service Level A/B, the normal force is determined by Equation 17, which is a function of the number of bolts, n . Combining Equation 10 and Equation 17 and solving for the number of bolts yields:

$$\begin{aligned} n &= [245971 + (F_{seismic} \cdot x_{gap} - \frac{1}{2} F_{eqv}^2/k) / \mu(x_{gap} + F_{eqv}/k)]/12844 \\ &= [245971 + (65250 \cdot 0.03 - \frac{1}{2} 31484^2/4125746) / 0.2(0.03 + 31484/4125746)]/12844 \\ &= 38.16, \text{ so 39 bolts are required} \end{aligned}$$

For Service Level C/D, combining Equation 10 and Equation 18 and solving for the number of bolts yields:

$$\begin{aligned} n &= [278213 + (F_{seismic} \cdot x_{gap} - \frac{1}{2} F_{eqv}^2/k) / \mu(x_{gap} + F_{eqv}/k)]/12844 \\ &= [278213 + (87000 \cdot 0.03 - \frac{1}{2} 31484^2/4125746) / 0.2(0.03 + 31484/4125746)]/12844 \\ &= 47.42, \text{ so 48 bolts are required} \end{aligned}$$

The calculations above assume a worst case initial gap condition of 0.030 inches between the aligner pin and core support ring, as shown in Figure 1. Since the nominal design condition includes a 0.015 inch gap and since it is equally probable for there to be a 0.000 inch gap as it is for there to be a 0.030 inch gap, additional calculations are performed to present the range of core plate bolts required to prevent lateral motion of the core plate assembly when the range of initial gap distance is considered. Further, the above calculation assumes only one aligner pin and bracket assembly support the applied load. Further insight can be obtained if two aligner pin and bracket assemblies are assumed to support the lateral load. To perform these sensitivity cases the gap size and the allowable equivalent force, F_{eqv} , are varied:

$x_{\text{gap}} = 0.000, 0.015, 0.030$ inches

$F_{\text{eqv}} = 31,484, 62,968$ lbs (62,968 is equivalent to assuming two aligner pin and bracket assemblies are in direct axial contact and equally distribute the seismic load)

Together with the original design input assumptions, a total of 6 cases are calculated and summarized in Table 4. For Service Level A/B between 7 and 39 core plate bolts are required and for Service Level C/D between 10 and 48 core plate bolts are required.

7.0 CONCLUSIONS

By taking structural credit for the aligner pin and bracket assembly, the minimum number of core plate bolts required to ensure negligible relative horizontal displacement of the core plate is between 7 and 39 for Service Level A/B and between 10 and 48 for Service Level C/D. These are comparable to the 45 bolts for Service Level A/B and 56 bolts for Service Level C/D calculated in Reference [3, Table 6-1]. The present calculation gives a lower number of required core plate bolts by taking structural credit for the core plate aligner pin bracket assembly.

8.0 REFERENCES

1. James A. Fitzpatrick License Renewal Application, Amendment 9, ADAMS Accession No. ML071060390.
2. EPRI TR-107284, BWR Vessel and Internals Project, BWR Core Plate Inspection and Flaw Evaluation Guidelines (BWRVIP-25), December 1996, SI File No. BWRVIP-01-225P (**EPRI Proprietary Information**).
3. SI Calculation No. 1101291.304, Revision 0, "Minimum Required Number of Core Plate Bolts," SI File No 1101291.304.
4. SI Project No. 1101291, Design Input Request, Revision 4, SI File No. 1101291.200.
5. JAF Drawing No 5.01-136, Revision D, "Reactor Assembly Nuclear Boiler Sh. 1," SI File No. 1101291.201.
6. M. R. Lindeburg, Mechanical Engineering Reference Manual, 12th Ed, Professional Publications, Inc., 2006.
7. R. G. Budynas and J. K. Nisbett, Mechanical Engineering Design, 8th Edition, McGraw-Hill, 2008.
8. ASME Boiler and Pressure Vessel Code, Section III, 2001 Edition with 2002 Addenda.
9. ANSI/AWS D1.1-98 Structural Welding Code – Steel.
10. FITZ Drawing No. 11825-5.10-43, Rev. 1, "Core Support for Core Structure," SI File No. 1101291.201.
11. FITZ Drawing No. 11825-5.11-31A, Rev. 2, "Aligner – Top Guide & Core Support Core Structure," SI File No. 1101291.201.

12. FITZ Drawing No. 5.10-22A, Rev. 2, “As Built Dimensions for Core Plate (MPL-B-11D003),” SI File No. NYPA-58Q-201.
13. ASME Boiler and Pressure Vessel Code, Section II, Part D, 2001 Edition with 2002 Addenda.
14. ASME Boiler and Pressure Vessel Code, Section II, Part A, 2001 Edition with 2002 Addenda.
15. ANSYS Mechanical APDL and PrepPost, Release 12.1 x64, ANSYS, Inc., November 2009.
16. US NRC, “Safety Evaluation by the Office of Nuclear Reactor Regulation Core Plate Hold Down Bolt Inspection Plan and Analysis Entergy Nuclear Operations, Inc. Vermont Yankee Power Station Docket No. 50-271,” ADAMS Accession No. ML120760152.

Table 1: Allowable Stress Criteria

Stress Type	Allowable ⁽¹⁾
Fillet Weld Shear	$0.3 S_u = 0.3(63,400) = 19,020$ psi (per [9, Table 2.3])
Base Metal Shear	$0.6 S_m = 0.6(16,950) = 10,170$ psi (per [8, NB-3227.2])
Base Metal Bearing	$1.5 S_y = 1.5(18,900) = 28,350$ psi (per [8, NB-3227.1]) (automatically satisfied by linear-elastic limit, $S_{max} < S_y$)

Note: 1. S_u = specified minimum tensile strength, S_y = specified minimum yield strength, S_m = allowable design stress intensity.

Table 2: Stiffness Calculation

Component	Axial/Bending	Stiffness Equation	E, psi	D, in	b, in	h, in	A, in ²	I, in ⁴	L, in	K, lbf/in
Pin	Axial	AE/L	25,700,000	3			7.069		5.875	30,921,293
Bracket, Vertical	Bending	$3EI/L^3$	25,700,000		5	3		11.25	5.5	5,213,373
Bracket, Horizontal	Bending	$3EI/L^3$	25,700,000		5	5		52.08	3.6875	80,086,085
Bracket, Horizontal	Axial	AE/L	25,700,000		5	5	25.00		3.6875	174,237,288
Equivalent Stiffness ($1/\Sigma(1/K)$)										4,125,746

Table 3: Unit Stress Summary

Component	Stress Type	Stress (psi)	Elastic Limit (psi)	Code Limit (psi)	Elastic Ratio	Code Ratio
Aligner Pin	Bearing	1,415	18,900	28,350	0.0749	0.0499
Aligner Pin Weld	Shear	6,003	18,900	19,020	0.3176	0.3156
Aligner Bracket	Shear	667	18,900	10,170	0.0353	0.0656
	Bending	4,000	18,900	28,350	0.2116	0.1411
	Total	4,055	18,900	N/A	0.2146	0.0000
Core Plate Rim Weld	Shear	555	18,900	19,020	0.0293	0.0292
	Bending	1,831	18,900	19,020	0.0969	0.0962
	Total	2,386	18,900	19,020	0.1262	0.1254

Table 4: Minimum Required Bolt Calculation Comparison

	# of Brackets Supporting Load	Initial Gap (in)		
		0.03	0.015	0
Service Level A/B	1	39	34	14
	2	32	26	7
Service Level C/D	1	48	43	16
	2	40	33	10

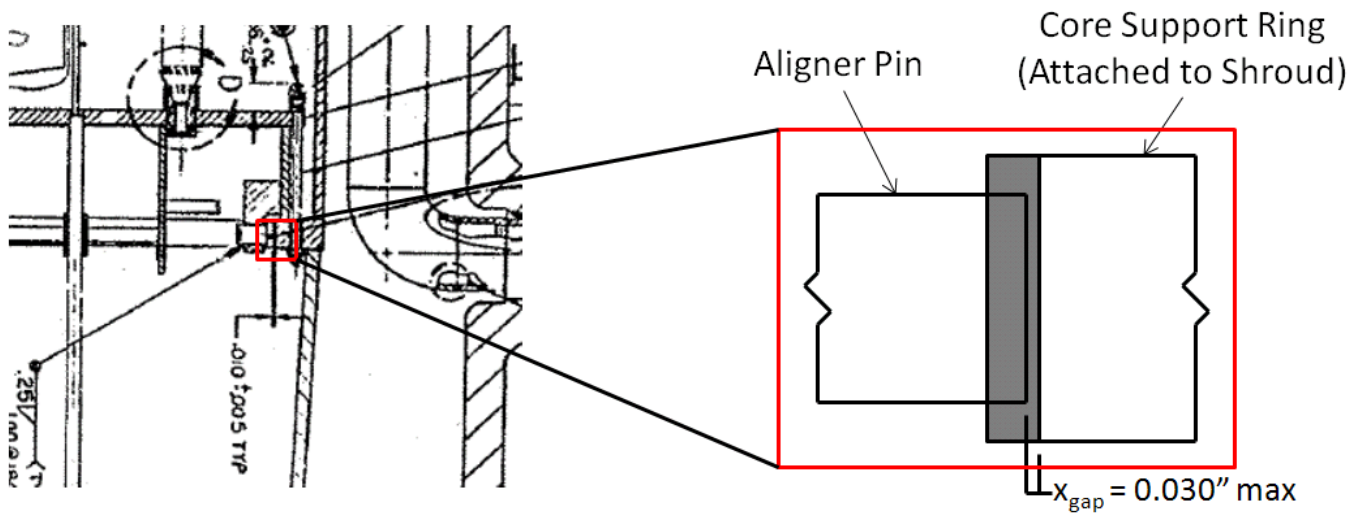


Figure 1. Aligner Pin and Core Support Ring Interface [5]

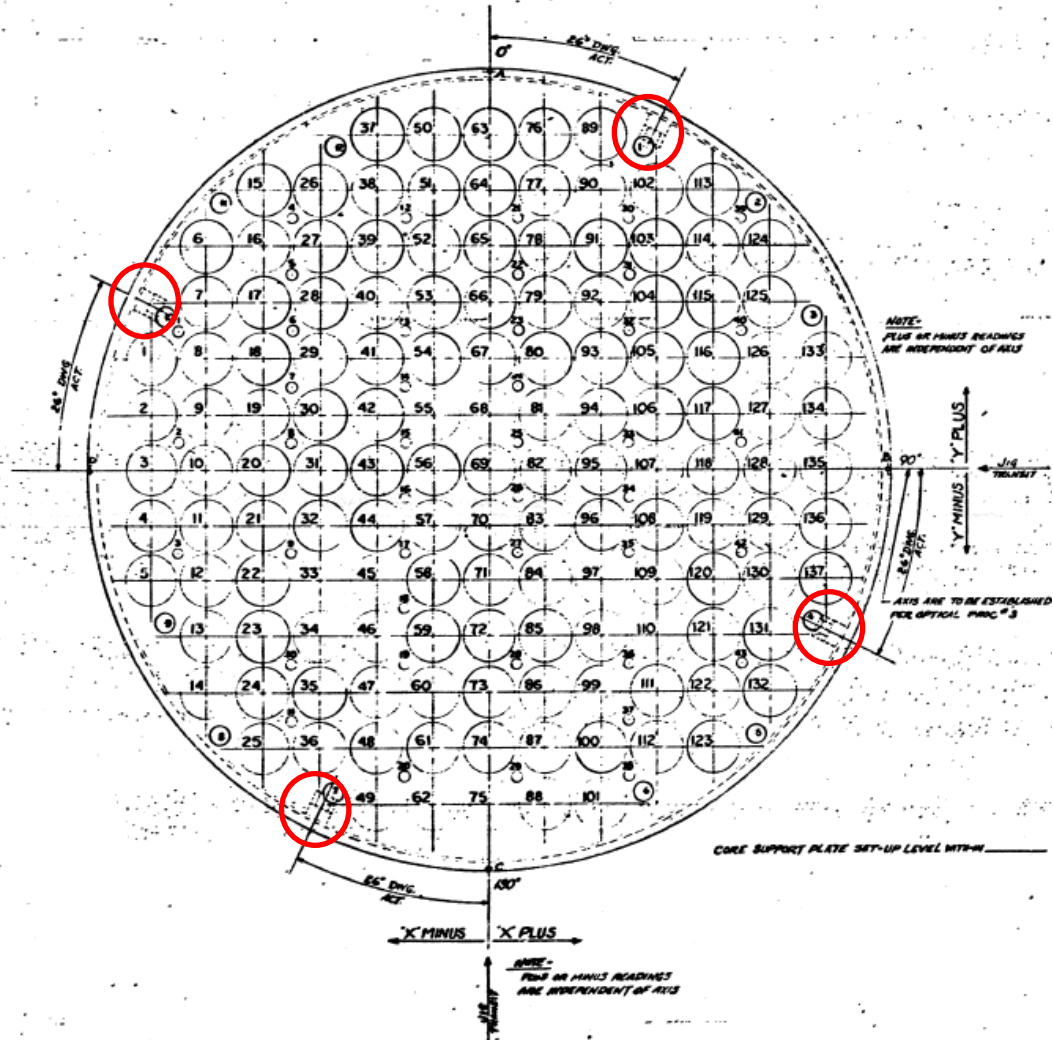


Figure 2. Aligner Pin and Bracket Assembly Locations [12]

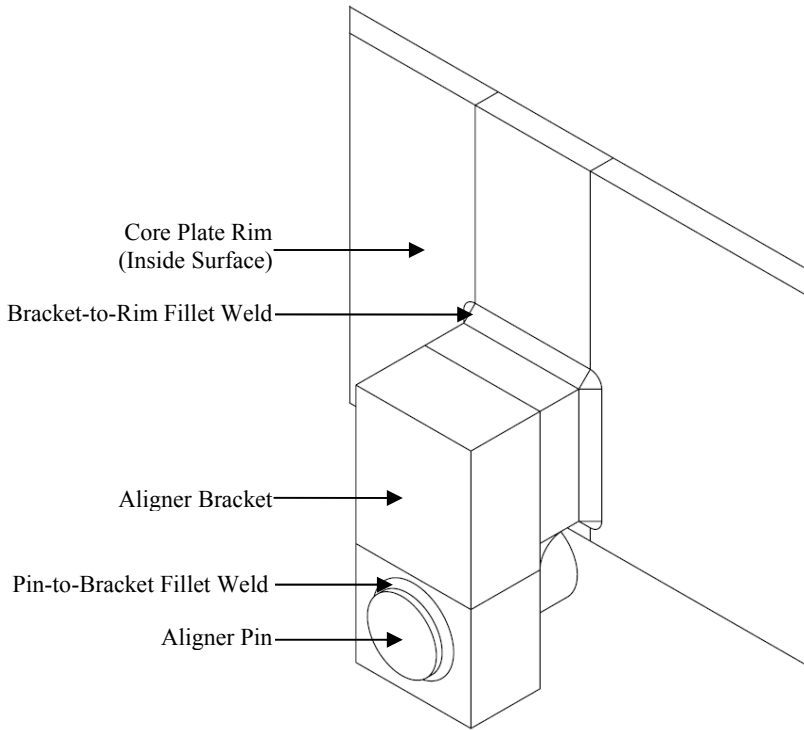


Figure 3. General View of Aligner Pin and Bracket Assembly

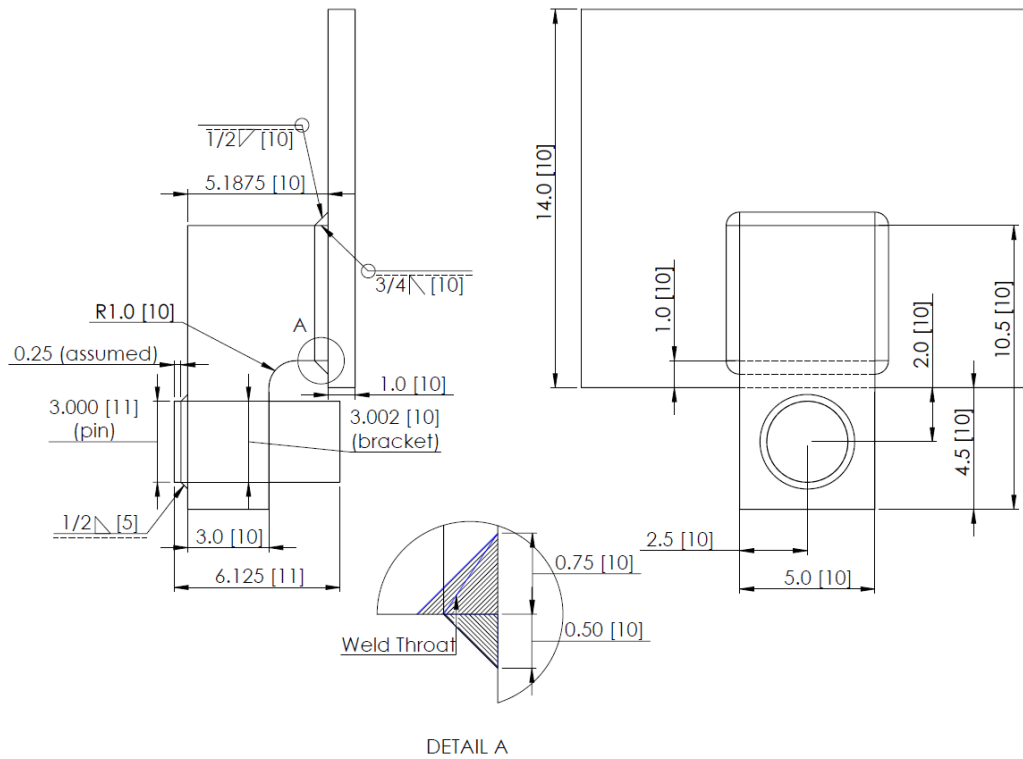


Figure 4. Dimensions of Aligner Pin and Bracket Assembly

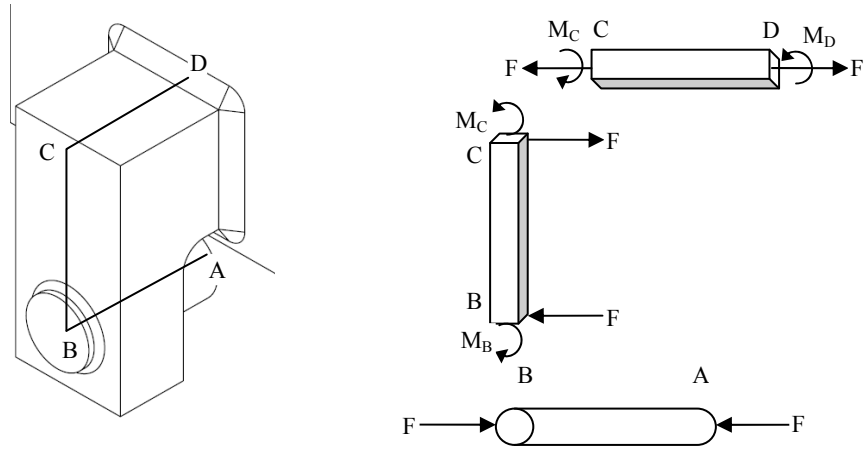


Figure 5. Free Body Diagram of Aligner Pin and Bracket Assembly

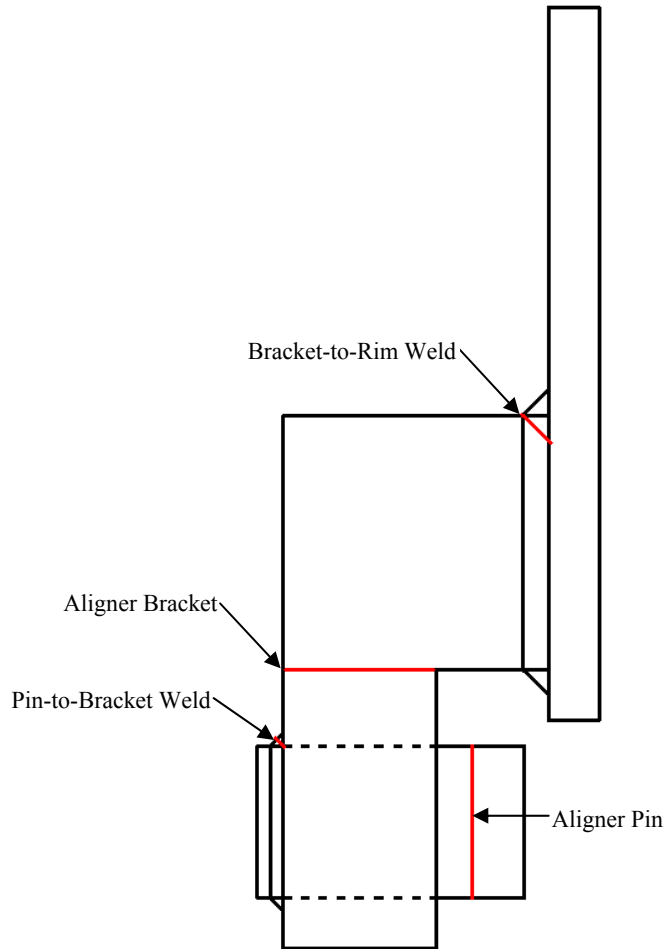


Figure 6. Cross Sections Analyzed

APPENDIX A
ANSYS VERIFICATION

The ANSYS finite element software [15] was used to verify the hand calculation methodology utilized in the calculation documented in Section 6.1 for the aligner pin and bracket assembly stiffness. Figure 3 shows the components modeled, including the core plate rim which was neglected from the hand calculation in Section 6.0. Dimensions shown in Figure 4 are used to build the model. The core plate rim is modeled as a flat plate rather than a cylindrical shell with a width of 65 inches. ANSYS SOILD285 4-node tetrahedral elements are used to build the finite element model. Material properties of Type 304 stainless steel from Section 5.0 are used.

Two different boundary conditions are considered. Figures A-1 and A-2 show the mesh and boundary conditions applied to the finite element model for both conditions evaluated. A unit pressure load of 10,000 psi was applied to the free end of the aligner pin. This corresponds to a force of 70,700 lbf. The top and bottom of the core plate rim are fixed in all degrees of freedom and the vertical faces of the rim have symmetric boundary conditions. The nodes on the free end of the aligner pin are coupled in the axial direction to simulate the contact with the core support bracket.

Figures A-3 and A-4 show the ANSYS Global Y displacement, which corresponds to the axial direction of the aligner pin, for each case considered.

Using Hooke's law (Equation 8), the equivalent stiffness of the aligner pin and bracket assembly with the core plate rim is:

$$k = F/\delta = 70,686/0.0234632 = 3,000,000 \text{ lbf/in}$$

Without the core plate rim the stiffness is:

$$k = F/\delta = 70,686/0.0136937 = 5,200,000 \text{ lbf/in}$$

The stiffness with the core plate is approximately 37% lower than the hand calculated value of 4,100,000 lbf/in from Section 6.1 and the stiffness without the core plate is 27% higher than the hand calculated value. The actual case would be somewhere between the two cases modeled in ANSYS. Since the hand calculated value is between the two ANSYS values, and close to the case without the core rim, the hand calculated value is appropriate to use.

The ANSYS files used in this calculation are listed below and are in the supporting files.

<i>Aligner.IGES:</i>	Geometry file
<i>Aligner-Pressure.INP:</i>	Input file for material properties, mesh, boundary conditions, pressure loading and solution for model with core plate rim
<i>Aligner-Pressure-No-Rim.INP:</i>	Input file for material properties, mesh, boundary conditions, pressure loading and solution for model without core plate rim

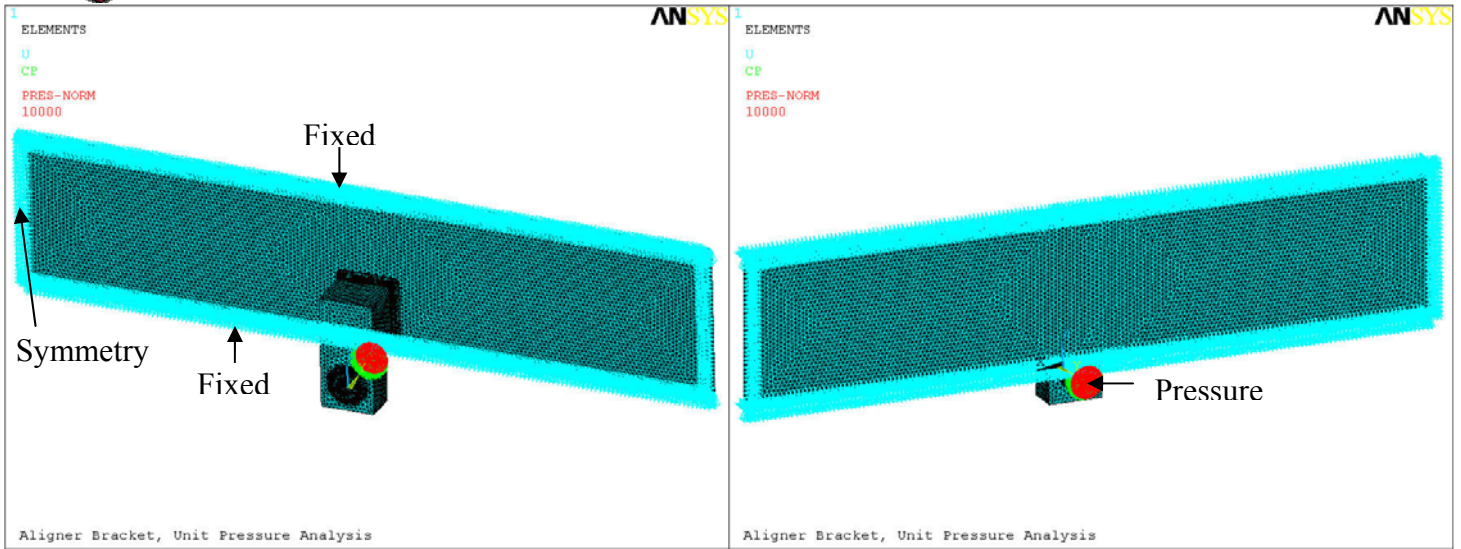


Figure A-1: Finite Element Model of Aligner Pin and Bracket Assembly with Boundary Conditions, With Core Plate Rim

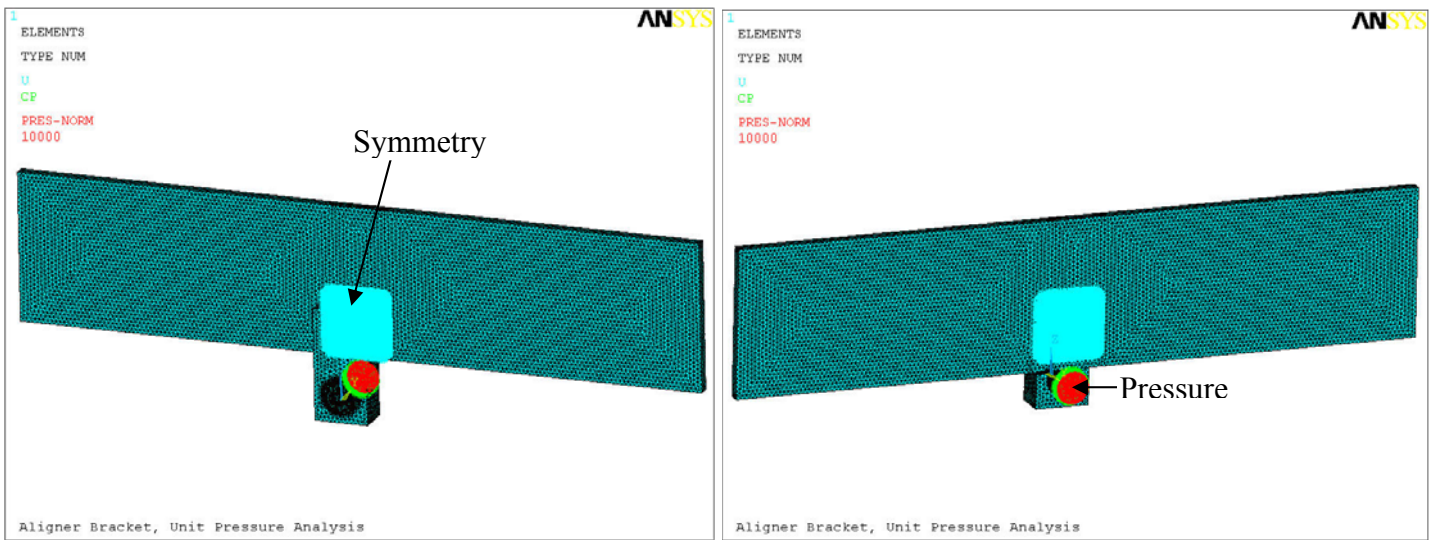


Figure A-2: Finite Element Model of Aligner Pin and Bracket Assembly with Boundary Conditions, Without Core Plate Rim

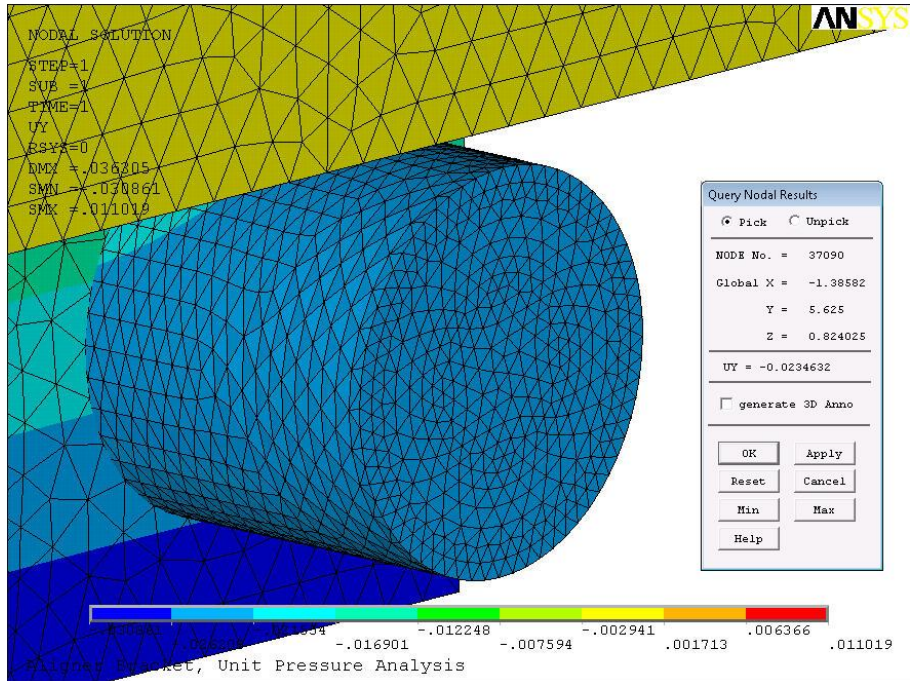


Figure A-3: Axial Displacement of Aligner Pin, With Core Plate Rim

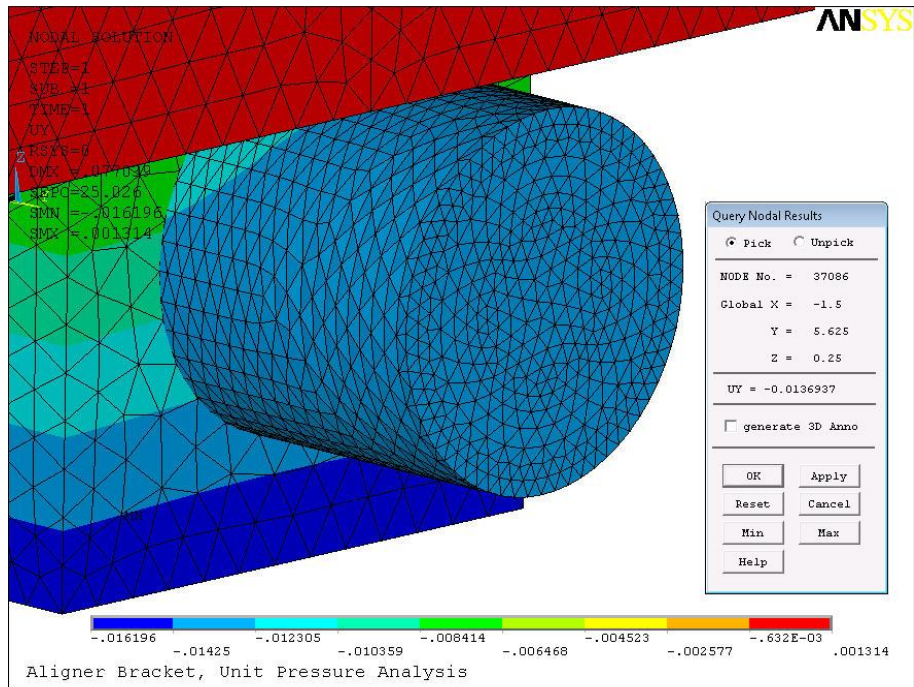


Figure A-4: Axial Displacement of Aligner Pin, Without Core Plate Rim

<input type="checkbox"/> ANO-1	<input type="checkbox"/> ANO-2	<input type="checkbox"/> GGNS	<input type="checkbox"/> IP-2	<input type="checkbox"/> IP-3	<input type="checkbox"/> PLP
<input checked="" type="checkbox"/> JAF	<input type="checkbox"/> PNPS	<input type="checkbox"/> RBS	<input type="checkbox"/> VY	<input type="checkbox"/> W3	
<input type="checkbox"/> NP-GGNS-3	<input type="checkbox"/> NP-RBS-3				
CALCULATION COVER PAGE	(1) EC # <u>36003</u>		(2) Page 1 of <u>12</u>		
(3) Design Basis Calc. <input checked="" type="checkbox"/> YES <input type="checkbox"/> NO		(4) <input checked="" type="checkbox"/> CALCULATION <input type="checkbox"/> EC Markup			
(5) Calculation No: JAF-CALC-12-00018				(6) Revision: 0	
(7) Title: Recommendations for a Core Plate Bolt Inspection Protocol (SIA File No. 1101291.306 Rev 0)				(8) Editorial <input type="checkbox"/> YES <input checked="" type="checkbox"/> NO	
(9) System(s): 02-1 Reactor Vessel		(10) Review Org (Department): DE - Civil			
(11) Safety Class: <input checked="" type="checkbox"/> Safety / Quality Related <input type="checkbox"/> Augmented Quality Program <input type="checkbox"/> Non-Safety Related		(12) Component/Equipment/Structure Type/Number:			
		02V-1			
(13) Document Type: DCAL					
(14) Keywords (Description/Topical Codes): Core Plate Bolt					
REVIEWS					
(15) Name/Signature/Date <u>Structural Integrity Associates</u> Responsible Engineer		(16) Name/Signature/Date <u>R. Casella</u> / <u>R. Casella 9/10/12</u> <input type="checkbox"/> Design Verifier <input checked="" type="checkbox"/> Reviewer <input type="checkbox"/> Comments Attached		(17) Name/Signature/Date <u>G. Foster</u> / <u>See AS EC 36003</u> Supervisor/Approval <input type="checkbox"/> Comments Attached	

CALCULATION REFERENCE SHEET	CALCULATION NO: <u>JAF-CALC-12-00018</u> REVISION: <u>0</u>																																				
I. EC Markups Incorporated (N/A to NP calculations) N/A 1. 2. 3. 4. 5.																																					
II. Relationships:	<table border="1" style="width: 100%; border-collapse: collapse; text-align: center;"> <thead> <tr> <th style="width: 35%;">Sht</th> <th style="width: 10%;">Rev</th> <th style="width: 15%;">Input Doc</th> <th style="width: 15%;">Output Doc</th> <th style="width: 15%;">Impact Y/N</th> <th style="width: 10%;">Tracking No.</th> </tr> </thead> <tbody> <tr> <td>1. JAF-CALC-12-00013</td> <td>0</td> <td><input checked="" type="checkbox"/></td> <td><input type="checkbox"/></td> <td></td> <td></td> </tr> <tr> <td>2. JAF-CALC-12-00014</td> <td>0</td> <td><input checked="" type="checkbox"/></td> <td><input type="checkbox"/></td> <td></td> <td></td> </tr> <tr> <td>3. JAF-CALC-12-00015</td> <td>0</td> <td><input checked="" type="checkbox"/></td> <td><input type="checkbox"/></td> <td></td> <td></td> </tr> <tr> <td>4. JAF-CALC-12-00016</td> <td>0</td> <td><input checked="" type="checkbox"/></td> <td><input type="checkbox"/></td> <td></td> <td></td> </tr> <tr> <td>5. JAF-CALC-12-00017</td> <td>0</td> <td><input checked="" type="checkbox"/></td> <td><input type="checkbox"/></td> <td></td> <td></td> </tr> </tbody> </table>	Sht	Rev	Input Doc	Output Doc	Impact Y/N	Tracking No.	1. JAF-CALC-12-00013	0	<input checked="" type="checkbox"/>	<input type="checkbox"/>			2. JAF-CALC-12-00014	0	<input checked="" type="checkbox"/>	<input type="checkbox"/>			3. JAF-CALC-12-00015	0	<input checked="" type="checkbox"/>	<input type="checkbox"/>			4. JAF-CALC-12-00016	0	<input checked="" type="checkbox"/>	<input type="checkbox"/>			5. JAF-CALC-12-00017	0	<input checked="" type="checkbox"/>	<input type="checkbox"/>		
Sht	Rev	Input Doc	Output Doc	Impact Y/N	Tracking No.																																
1. JAF-CALC-12-00013	0	<input checked="" type="checkbox"/>	<input type="checkbox"/>																																		
2. JAF-CALC-12-00014	0	<input checked="" type="checkbox"/>	<input type="checkbox"/>																																		
3. JAF-CALC-12-00015	0	<input checked="" type="checkbox"/>	<input type="checkbox"/>																																		
4. JAF-CALC-12-00016	0	<input checked="" type="checkbox"/>	<input type="checkbox"/>																																		
5. JAF-CALC-12-00017	0	<input checked="" type="checkbox"/>	<input type="checkbox"/>																																		
III. CROSS REFERENCES: See body of calculation. 1. 2. 3. 4. 5.																																					
IV. SOFTWARE USED: Title: <u>None</u> Version/Release: _____ Disk/CD No. _____																																					
V. DISK/CDS INCLUDED: Title: <u>N/A</u> Version/Release _____ Disk/CD No. _____																																					
VI. OTHER CHANGES: None																																					

Revision	Record of Revision
0	Initial issue.



Structural Integrity Associates, Inc.®

CALCULATION PACKAGE

File No.: 1101291.306

Project No.: 1101291

Quality Program: Nuclear Commercial

PROJECT NAME:

JAF Core Plate Bolt Evaluation

CONTRACT NO.:

10340564

CLIENT:

Entergy Nuclear

PLANT:

James A. Fitzpatrick Nuclear Power Plant

CALCULATION TITLE:

Recommendations for a Core Plate Bolt Inspection Protocol

NOTE: This document references vendor proprietary information. Such information is identified with -2xxP SI Project File numbers in the list of references. Any such references and the associated information in this document where those references are used are identified so that this information can be treated in accordance with applicable vendor proprietary agreements.




Document Revision	Affected Pages	Revision Description	Project Manager Approval Signature & Date	Preparer(s) & Checker(s) Signatures & Date
0	1 - 9	Initial Issue	 D. V. Sommerville 31AUG12	<p><u>Responsible Engineer</u></p>  C. J. Oberembt 31AUG12
				<p><u>Responsible Verifier</u></p>  T. J. Herrmann 31AUG12

Table of Contents

1.0	INTRODUCTION	3
1.1	Background.....	3
2.0	INSPECTION HISTORY	4
3.0	PLANT-SPECIFIC ANALYSIS	4
3.1	Susceptibility	4
3.2	Relaxation of Preload	5
3.3	Flaw Tolerance	5
3.4	Minimum Required Number of Bolts.....	5
4.0	INSPECTION PROTOCOL.....	6
5.0	CONCLUSIONS	8
6.0	REFERENCES	8

List of Figures

Figure 1-1:	Core Plate Bolt Assembly.....	3
-------------	-------------------------------	---

List of Tables

Table 2-1:	JAF Core Plate Bolt Inspection Summary	4
------------	--	---

1.0 INTRODUCTION

The James A. Fitzpatrick (JAF) nuclear power plant license renewal commitment number 23 [1, Attachment 1] states that JAF will either install core plate wedges prior to the period of extended operation or complete a plant-specific analysis to develop and justify a core plate bolt inspection plan. The inspection plan must include acceptance criteria which meet the requirements of BWRVIP-25 [2].

Figure 1-1 illustrates the JAF core plate bolt assembly. This document provides the recommended inspection protocol for the JAF core plate bolts.

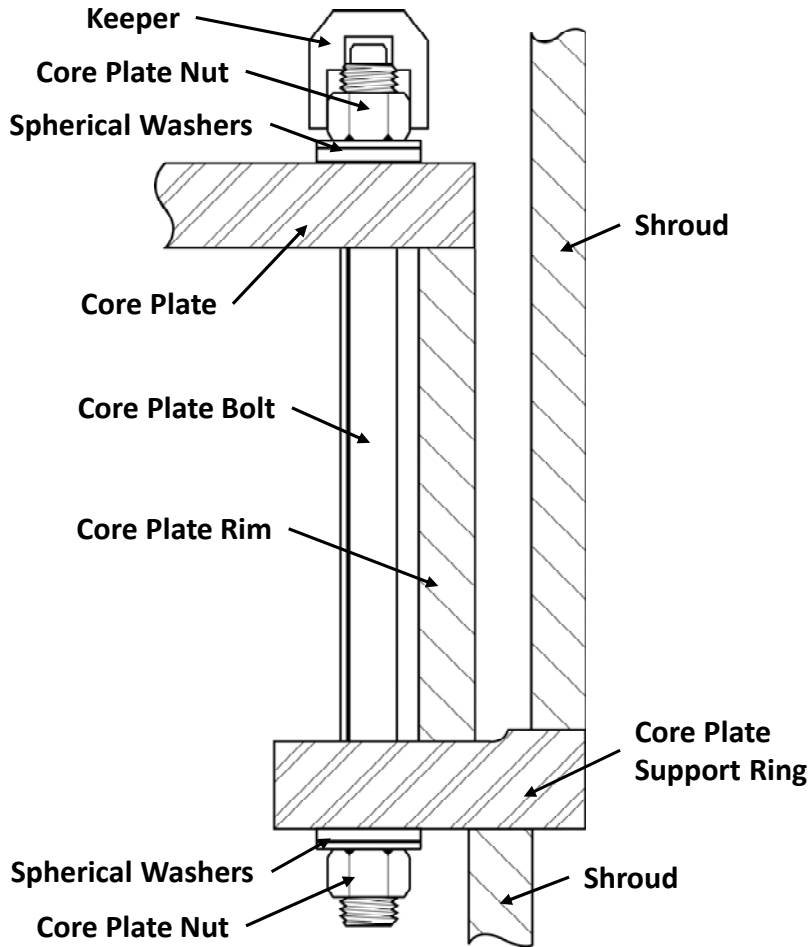


Figure 1-1: Core Plate Bolt Assembly

1.1 Background

After cracking was observed in core plate components in two Boiling Water Reactors (BWR's), inspection and evaluation guidelines were developed and presented in BWRVIP-25 [2]. The core plate bolts are identified as a critical component since these bolts ensure that no lateral displacement of the core plate occurs which could prevent control rod insertion. The guidance in BWRVIP-25 [2] recommends that one of the following options be implemented:

1. Inspect the core plate bolts.
2. Install core plate wedges.

The inspection strategies presented in BWRVIP-25 [2] require that either ultrasonic testing (UT) from the top of the bolts or enhanced VT-1 inspection from below the core plate be performed. To date there are no known techniques for performing the UT inspections on the core plate bolts.

BWRVIP-25 [2] also provides guidance that different inspection strategies may be acceptable based on the results of plant-specific analysis.

2.0 INSPECTION HISTORY

Many US plants, including JAF have inspected their core plate bolts using visual inspections from above the bolts, and no obvious signs of degradation have been found [3, 4 and 5]. A summary of the JAF inspections to date is provided in Table 2-1 below. A baseline inspection of all 72 core plate bolts was completed during refueling outage (RO) 13. While these examinations would not have been able to detect cracking in the threaded regions of the bolting, cracked keepers, rotated bolts, missing bolts or fretting wear due to bypass leakage caused by gross failures over the past 30+ years of operation would have been observable. No obvious signs of degradation have been observed. Furthermore, visual examinations performed in the US BWR fleet, including at JAF, have not found any indications of failed core plate bolts, which suggests that the operating experience has been good to date [6].

Table 2-1: JAF Core Plate Bolt Inspection Summary

Outage	No. of Bolts	Method	Results
RO11	20	VT-1	No indications requiring evaluation
RO13	72	VT-3	No indications requiring evaluation
RO18	33	VT-1	No indications requiring evaluation

3.0 PLANT-SPECIFIC ANALYSIS

Structural Integrity Associates, Inc. (SI) performed a plant specific analysis to evaluate the susceptibility of the JAF core plate bolts to known degradation mechanisms, calculate the relaxation of bolt preload over 60 years of operation, evaluate the flaw tolerance of the bolts, and calculate the minimum number of bolts required to prevent horizontal displacement. SI used conservative methods for each evaluation; these conservatisms are compounding, as described below.

Failure in this evaluation is defined as the loss of all preload. Failure could result from sufficient permanent deformation in the core plate bolts or complete separation of the cross section.

3.1 Susceptibility

SI evaluated the susceptibility of the JAF core plate bolts to relevant degradation mechanisms as documented in Reference [7]. The conclusion presented in Reference [7] is that the core plate bolts are not susceptible to irradiation assisted stress corrosion cracking (IASCC) due to low fluence, relative to the threshold value, and are not susceptible to degradation due to fatigue. Intergranular stress corrosion cracking (IGSCC) could not be completely ruled out as a possible damage mechanism. However, the probability of cracking is considered low since the material is not thermally sensitized, was purchased to a specification requiring solution annealing following cold work, has a smooth surface finish, and the environment has been mitigated with the introduction of hydrogen water chemistry (HWC) and noble metals chemical addition (NMCA) / on-line noble chemistry (OLNC) [7]. Additionally, a high purity anti-seize lubricant was used at installation and may help to provide an environmental barrier, which would be more

beneficial early in plant life when the water chemistry was most conducive to IGSCC initiation [7]. The probability of IGSCC initiation is greatly decreased after the implementation of HWC and NMCA/OLNC [7].

3.2 Relaxation of Preload

SI calculated the expected reduction in core plate bolt preload force over the 60 year life of the plant [8]. The effects of thermal relaxation, stress relaxation (primary creep) and radiation relaxation were evaluated. The effects of yielding due to the high initial preload stress and the use of the ASME Code minimum yield stress at the operating temperature were considered. The results of the reduced preload calculation were used as input in subsequent calculations.

3.3 Flaw Tolerance

SI performed a linear elastic fracture mechanics (LEFM) evaluation to determine the crack growth characteristics of the JAF core plate bolt design [9]. The LEFM evaluation included various crack locations and orientations, consistent with published data for IGSCC in threaded fasteners, to assess the flaw tolerance of the bolts. Further, the results of the LEFM evaluation were benchmarked against existing LEFM solutions for simpler configurations. The results are consistent with related information in the literature and provide additional insight for complex crack orientations and multiple crack cases. Both single and multiple circumferential flaws have been analyzed with initiation times ranging from plant startup to 30 years after startup. Time-dependent water chemistry data for reactor conductivity and electro-chemical potential (ECP) were considered. SI determined that the most important factor in crack growth is initiation time (i.e. when in plant life initiation is postulated to have occurred). If crack initiation is assumed to occur in the first 20 years of plant operation (prior to 1995) then the core plate bolt exhibits little flaw tolerance. Conversely, if crack initiation is assumed to occur after the first 20 years of plant operation (subsequent to 1995) then the core plate bolt exhibits substantially improved flaw tolerance. If single or multiple IGSCC flaws occurred in the JAF core plate bolting subsequent to 1995 then the residual life of the core plate bolting is on the order of 40-50 years [9]. If a crack had initiated early in plant life and resulted in separation or complete loss of preload, obvious signs of degradation (e.g. missing bolts, fretting wear or rotation due to bypass leakage flow, etc.) would likely be observable during visual inspections. A time sensitivity study was performed that indicates if a crack initiated after approximately 20 years of operation, the core plate bolts would reasonably be expected to have sufficient flaw tolerance to last through the period of extended operation [9].

The omission of radiation relaxation from the LEFM evaluation provided an upper bound driving force on the bolts when considering the effects of preload relaxation. The 95th percentile crack growth rates were used rather than the “best estimate” crack growth rates for all postulated flaws. A fully circumferential flaw was used rather than one or more discrete thumbnail flaws; resulting in a bounding flaw orientation. The thread form tolerance resulting in the maximum stress state was evaluated, rather than nominal dimensions. Because of these compounding conservatisms, the results of Reference [9] are considered to be a bounding assessment of the flaw tolerance of the core plate bolts.

3.4 Minimum Required Number of Bolts

SI performed hand calculations to calculate the minimum number of required core plate bolts needed to ensure that lateral displacement of the core plate would not occur during both Level A/B and Level C/D events. These evaluations included the reduced preload force developed in Reference [8]. The first evaluation conservatively ignored the contribution of the aligner pin and bracket assemblies, and calculated

the minimum number of bolts needed to ensure that the frictional force between the core plate and the support ring was sufficient to resist applied horizontal forces [10]. The limiting Level C/D conditions resulted in the highest number of required bolts; 56 bolts are required for the Level C/D condition [10].

The second evaluation considered the load carrying capacity of the aligner pin and bracket assemblies, which provide an alternate load path to limit lateral motion of the core plate [11]. The maximum allowable gap between the aligner pin and bracket (based on tolerance specifications) combined with the limiting Level C/D conditions resulted in the highest number of required bolts at 48 bolts [11]. Additionally, a sensitivity evaluation was performed for the assumed gap between the aligner pin and bracket assembly and the core support ring, which showed that if no gap was assumed the required number of bolts could be as low as 16 [11].

As discussed in Reference [10], the bolted joint was treated as a friction-type joint, and no credit was taken for mechanical contact (i.e. shear) between the bolts and the core plate. Additionally, a conservative value of 0.2 was used for the coefficient of friction between the core plate and the support ring when evaluating the minimum required number of bolts [10]. The actual coefficient of friction is expected to be closer to 0.5 based on GE test results [6]. The evaluation in Reference [11] conservatively assumed that only one aligner pin would contribute to resisting the applied horizontal forces and would be in pure compression. In this scenario, two additional aligner pins would be in shear; however, the shear strength of the pins was neglected. Elastic allowable stress limits were used in the Reference [11] evaluation; whereas, for the Level C/D condition, limiting strain in the aligner pin and bracket assembly to the elastic regime is not required (since following a Level D event, there is no expectation that the core plate assembly will need to be removed and reinstalled without significant inspections, repairs, and replacements). Consequently a plastic analysis could have been performed in which the acceptance criterion was rupture of the load carrying members in the aligner pin and bracket assembly. Consideration of plasticity and the associated increased strain energy capacity of the assembly would be expected to result in fewer required core plate bolts.

The original stress analysis performed for the core plate assembly remains applicable through 60 years of operation since the acceptance criterion for this plant specific evaluation is that there remains sufficient normal force between the core plate and core support ring such that the resulting friction force is sufficient to prevent lateral movement of the core plate assembly. This inherently requires that the cumulative remaining preload (i.e. total preload in the remaining uncracked bolts) exceeds the vertical force applied to the core plate assembly. Additionally, the use of spherical washers in the bolted joint would help to ensure loading remains axial and reduce the potential for bending induced loading in the unlikely event that multiple bolts failed in close proximity creating an eccentric loading condition.

4.0 INSPECTION PROTOCOL

There have been no obvious signs of degradation, such as cracked keepers, rotated bolts, missing bolts, or fretting wear due to bypass leakage, in the 3 previous visual inspections, including the baseline VT-3 inspection of all 72 core plate bolts [3, 4 and 5]. The JAF core plate bolts are judged to have a low susceptibility to IGSCC due to the material and manufacturing specification requirements and the coating applied at installation [7]. IGSCC cracking in the core plate bolts is unlikely, and, furthermore, simultaneous cracking in multiple bolts is even less likely, due to the random nature of the parameters that influence crack initiation times. Review of water chemistry suggests that if IGSCC initiation were to occur, it would be more likely to occur early in plant life when the water chemistry was most conducive to IGSCC [7]. If an IGSCC flaw were to have initiated early in plant life, failure (i.e. complete loss of preload) would

be expected to have occurred within a few years and signs of degradation, should have been observed during previous visual inspections. No signs of degradation have been observed during previous visual inspections at JAF. Additionally, no failed bolting has been observed in any U.S. BWR [6]. Since U.S. BWR core plate bolt design, reactor operation, and environment are similar, the absence of fleet experience of cracking is a good indicator of resistance to degradation in general.

Since 1995 JAF water chemistry is mitigating which suggests that IGSCC initiation will not occur since that time and into the future as long as effective HWC and NMCA/OLNC continues. In the unlikely event that a flaw were to have initiated later in plant life, the bolts are much more flaw tolerant due to favorable water chemistry and the flaw would not be expected to grow to a size which would result in failure of the bolt during the period of extended operation.

The JAF core plate bolt design provides for at least 22% excess capacity (number of bolts required) when considering the relaxation of bolt preload over the 60 year life of the plant, limiting Level C/D load conditions, a conservative coefficient of friction, and not accounting for the aligner pin and bracket assemblies [10]. If credit for the aligner pin and bracket assemblies were taken, the margin would increase to at least 33% [11]. Even if 16 (or likely more) of the existing 72 bolts exhibited IGSCC and failure in the period of extended operation, the joint would retain sufficient bolting capacity to prevent lateral movement of the core plate assembly. This would ensure the ability to insert the control rod drives (CRDs) and safely shut down the plant in a design basis seismic event.

GE test data shows that the CRDs can be inserted with core plate misalignment on the order of 0.5 inches or more [12]; whereas, the present analyses [7, 8, 9, 10, 11] did not allow any displacement (with the exception of the small elastic displacement considered in the aligner pin and bracket assembly on the order of thousands of an inch). For the core plate assembly to displace this much the assembly would have to experience substantial plastic deformation which would absorb significant energy. Therefore, there is further inherent margin in the system's ability to ensure CRD insertion which is also not being credited.

Consequently, considering the conservative evaluation used it can be reasonably concluded that the core plate bolts have a low susceptibility to IGSCC and are flaw tolerant. Further, the core plate assembly bolted joint design has demonstrated that the design includes more bolts than are necessary to prevent lateral movement of the core plate assembly, and the core plate assembly includes redundant load paths through the aligner pins and brackets. Finally, multiple visual inspections, including a 100% baseline inspection of the bolts, have been performed which identified no signs of degradation. The observed lack of degradation is consistent with industry-wide experience [6].

For these reasons, no further inspections are required for the JAF core plate bolts during the period of extended operation.

Additionally, this inspection protocol is supported by BWRVIP-25 [2, Section 3.2]. This section states that there may be plant-specific situations, such as required inspection locations that are shown to have been solution annealed, where a plant-specific evaluation would specify no inspection is required. Currently the core plate bolts are the only required inspection location per BWRVIP-25 [2], and the JAF core plate bolts were procured to a purchase specification requiring solution annealing after cold working processes [13].

5.0 CONCLUSIONS

This evaluation supports the following conclusions:

1. No obvious signs of degradation have been observed during the 3 previous visual inspections of the JAF core plate bolts.
2. The JAF core plate bolts have a low susceptibility to IGSCC, and initiation is unlikely based on the material and manufacturing specification requirements.
3. If IGSCC initiation had occurred early in plant life when plant water chemistry was most conducive of IGSCC, failures would be expected to have occurred and obvious signs of degradation (e.g. missing bolts, fretting wear or rotation due to bypass leakage flow, etc.) should have been observed during previous inspections.
4. If IGSCC initiation were to occur later in plant life, after the implementation of HWC and NMCA/OLNC, the core plate bolts have substantially improved flaw tolerance.
5. The JAF core plate design provides at least 22% excess number of bolts, even when considering the relaxation of bolt preload over the 60 year plant life; thus, ensuring the ability to insert the control rod drives (CRDs) and safely shut down the plant in a design basis seismic event. This excess capacity doesn't credit the aligner pins which would further increase margin.
6. Based on this plant specific evaluation, no further inspections of the JAF core plate bolts are required.

6.0 REFERENCES

1. James A. Fitzpatrick Nuclear Plant License Renewal Application, Amendment 9, ADAMS Accession No. ML071060390.
2. EPRI TR-107284, BWR Vessel and Internals Project, BWR Core Plate Inspection and Flaw Evaluation Guidelines (BWRVIP-25), December 1996, SI File No. BWRVIP-01-225P (**EPRI Proprietary Information**).
3. SI Project No. 1101291, Design Input Request, Revision 4, SI File No. 1101291.200.
4. James A. Fitzpatrick ICD No. JAF-ICD-03-00014, Revision 0, "JAF-IVVI Program-Technical Justification, Alternate Technique for Inspection of Vessel Internals Core Plate Rim Hold-down Bolts (BWRVIP-25)," SI File No. 1101291.204.
5. James A. Fitzpatrick Program Section No. SEP-RVI-004, Revision 0, Appendix F, "Core Plate," SI File No. 1101291.204.
6. NRC SER, "Safety Evaluation by the Office of Nuclear Reactor Regulation Core Plate Hold Down Bolt Inspection Plan and Analysis Entergy Nuclear Operations, Inc. Vermont Yankee Nuclear Power Station Docket No. 50-271," ADAMS Accession No. ML120760152, SI File No. 1101291.211.
7. SI Calculation No. 1101291.301, Revision 0, "Core Plate Bolt Degradation Susceptibility Evaluation."
8. SI Calculation No. 1101291.302, Revision 0, "Core Plate Bolt Preload Relaxation."
9. SI Calculation No. 1101291.303, Revision 0, "Core Plate Bolt Fracture Mechanics Evaluation."

10. SI Calculation No. 1101291.304, Revision 0, “Minimum Required Number of Core Plate Bolts.”
11. SI Calculation No. 1101291.305, Revision 0, “Minimum Required Number of Core Plate Bolts – Consideration of Aligner Brackets.”
12. GE Document No. NEDC-32406, “Final Test CRD Performance Evaluation Testing with Driveline Misalignment,” SI File No. 1101291.206.
13. GE Document No. 21A1056, “Standard Requirements for Miscellaneous Piping and Hardware (Reactor Internals),” SI File No. 1101291.210.

Engineering Report No. JAF-RPT-12-00006 Rev 0
Page 1 of 25



**ENTERGY NUCLEAR
Engineering Report Cover Sheet**

Engineering Report Title:

James A. FitzPatrick Core Support Plate Rim Bolt Fluence Evaluation at End of Cycle 20, 32 EFPY and 54 EFPY

Engineering Report Type:

New Revision Cancelled Superseded
Superseded by: _____

Applicable Site(s)

IP1 IP2 IP3 JAF PNPS VY WPO
ANO1 ANO2 ECH GGNS RBS WF3 PLP

EC No. 36003

Report Origin: Entergy Vendor
Vendor Document No.: ENT-JAF-001-R-001

Quality-Related: Yes No

Prepared by: Transware Date: _____
Responsible Engineer (Print Name/Sign)

Design Verified: R. Casella / *R Casella* Date: 6/20/12
Design Verifier (if required) (Print Name/Sign)

Reviewed by: *WJR* Date: _____
Reviewer (Print Name/Sign)

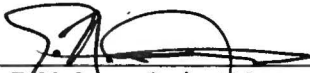
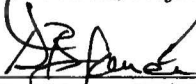

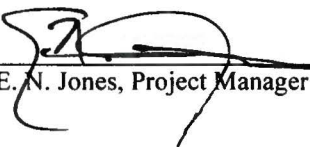
Approved by: G. Foster / *See AS EC 36003* Date: _____
Supervisor / Manager (Print Name/Sign)

JAMES A. FITZPATRICK CORE SUPPORT PLATE RIM BOLT FLUENCE EVALUATION AT END OF CYCLE 20, 32 EFPY AND 54 EFPY

Document Number: ENT-JAF-001-R-001
Revision 0

Preparing Organization:

TransWare Enterprises Inc.
1565 Mediterranean Drive
Sycamore, Illinois 60178

Prepared By:	 E. N. Jones, Project Manager	<u>6/12/2012</u> Date
Reviewed By:	 D. R. Jones, Project Engineer	<u>6/12/2012</u> Date
Reviewed By:	 V. K. Jones, QA Specialist	<u>6/12/2012</u> Date
Approved By:	 E. N. Jones, Project Manager	<u>6/12/2012</u> Date

Prepared For:

Entergy Nuclear Operations, Inc.
Entergy Nuclear FitzPatrick, LLC
268 Lake Road
Lycoming, NY 13093

Rick Casella, Entergy Representative

Controlled Copy Number: _____

DISCLAIMER OF WARRANTIES AND LIMITATION OF LIABILITIES

THE INFORMATION CONTAINED IN THIS REPORT IS BELIEVED BY TRANSWARE ENTERPRISES INC. TO BE AN ACCURATE AND TRUE REPRESENTATION OF THE FACTS KNOWN, OBTAINED OR PROVIDED TO TRANSWARE ENTERPRISES INC. AT THE TIME THIS REPORT WAS PREPARED. THE USE OF THIS INFORMATION BY ANYONE OTHER THAN THE CUSTOMER OR FOR ANY PURPOSE OTHER THAN THAT FOR WHICH IT IS INTENDED, IS NOT AUTHORIZED; AND WITH RESPECT TO ANY UNAUTHORIZED USE, TRANSWARE ENTERPRISES INC. MAKES NO REPRESENTATION OR WARRANTY AND ASSUMES NO LIABILITY AS TO THE COMPLETENESS, ACCURACY OR USEFULNESS OF THE INFORMATION CONTAINED IN THIS DOCUMENT. IN NO EVENT SHALL TRANSWARE ENTERPRISES INC. BE LIABLE FOR ANY LOSS OF PROFIT OR ANY OTHER COMMERCIAL DAMAGE, INCLUDING BUT NOT LIMITED TO SPECIAL, CONSEQUENTIAL OR OTHER DAMAGES.

QUALITY REQUIREMENTS

This document has been prepared in accordance with the requirements of 10CFR50 Appendix B, 10CFR21, and TransWare Enterprises Inc.'s 10CFR50 Appendix B quality assurance program.

ACKNOWLEDGMENTS

TransWare Enterprises Inc. wishes to acknowledge the following Entergy engineer who contributed to this project: Ms. Kornelia Szwarc for providing the reactor operating history and fuels data for the project. TransWare also wishes to acknowledge Mr. Rick Casella of Entergy Nuclear FitzPatrick, LLC for his overall support and management of this project.

CONTENTS

1	Introduction	1-1
2	Summary of Results	2-1
3	Description of the Reactor System and Calculation Methodology	3-1
3.1	Reactor System Mechanical Design Inputs.....	3-1
3.2	Reactor Operating Data Inputs.....	3-2
3.2.1	Power History Data.....	3-2
3.2.2	Reactor State-Point Data.....	3-3
3.2.2.1	Beginning of Operation through Cycle 17 State Points	3-3
3.2.2.2	Projected Operation through End of Design Life State Points....	3-5
3.2.3	Core Loading Pattern	3-5
4	Core Support Plate Rim Bolt Uncertainty Analysis	4-1
5	Calculated Neutron Fluence for Core Support Plate Rim Bolts	5-1
6	References.....	6-1

LIST OF FIGURES

Figure 3-1 Axial View of JAF Core Support Plate Rim Bolt 3-2

LIST OF TABLES

Table 2-1	Bounding Neutron Fluence for Energy >1.0 MeV for JAF Core Support Plate Rim Bolts at the Rim Bolt Surface	2-1
Table 2-2	Bounding Neutron Fluence for Energy >0.1 MeV for JAF Core Support Plate Rim Bolts Along the Rim Bolt Centerline Axis	2-1
Table 3-1	Number of State-point Data Files for Each Cycle in JAF	3-4
Table 3-2	Summary of the JAF Core Loading Pattern	3-6
Table 4-1	CSP Rim Bolt Fluence Uncertainty and Bias	4-2
Table 5-1	Bounding >1.0 MeV Neutron Fluence for JAF Core Support Plate Rim Bolts at the Rim Bolt Surface	5-1
Table 5-2	Bounding >0.1 MeV Neutron Fluence Axial Profile for JAF Core Support Plate Rim Bolts at Bolt Centerline Axis	5-2

1

INTRODUCTION

This report presents the results of the core support plate (“CSP”) rim bolt fluence evaluation performed for the James A. FitzPatrick Nuclear Power Station (“JAF”). Bounding peak bolt fluence was calculated for energy >1.0 MeV at three time periods: end of cycle (“EOC”) 20, 32 effective full power years (“EFPY”) and 54 EFPY. This bounding peak fluence value shall be used to support irradiation-assisted stress corrosion cracking (“IASCC”) studies. This evaluation also includes a bounding axial fluence profile for the bounding CSP rim bolt for energy >0.1 MeV to support fluence-induced relaxation studies.

The fluence values presented in this report were calculated using the RAMA Fluence Methodology [1]. The RAMA Fluence Methodology (hereinafter referred to as the Methodology) has been developed for the Electric Power Research Institute, Inc. (EPRI) and the Boiling Water Reactor Vessel and Internals Project (BWRVIP) for the purpose of calculating neutron fluence in Boiling Water Reactor (BWR) components. The Methodology has been approved by the U. S. Nuclear Regulatory Commission [2] for application in accordance with U. S. Regulatory Guide 1.190 [3]. Benchmark testing has been performed using the Methodology for several surveillance capsule and reactor pressure vessel fluence evaluations. Results of these benchmark efforts show that the Methodology accurately predicts fluence in the RPV and surveillance capsule components of BWRs. Benchmark testing has also been performed using the Methodology to perform fluence evaluations on other internal reactor components such as the top guide and shroud [4]. At this time, the Methodology as applied in this report provides the best available tool for estimating neutron fluence in reactor pressure vessel internal components in and beyond the core beltline region.

The information and associated evaluations provided in this report have been performed in accordance with the requirements of 10CFR50 Appendix B.

2

SUMMARY OF RESULTS

This section provides a summary of the results of the CSP rim bolt fluence evaluation for the JAF reactor. The primary purpose of this evaluation is to determine the bounding neutron fluence for energy range >1.0 MeV and the axial fluence profile over the height of the bolt for energy range >0.1 MeV. Fluence was calculated at the EOC 20 at 27.7 EFPY and projected to 32 and 54 EFPY. Section 5 contains complete fluence results for the CSP rim bolt.

Table 2-1 summarizes the fluence determined for the bounding CSP rim bolt location for energy >1.0 MeV. The bounding fluence is $1.93\text{E}+20$ n/cm² at 54 EFPY for energy >1.0 MeV.

Table 2-2 summarizes the axial fluence determined for the bounding CSP rim bolt location through the bolt centerline axis for energy >0.1 MeV. The bounding average axial fluence for the CSP rim bolts is $3.84\text{E}+19$ n/cm² at 54 EFPY for energy >0.1 MeV.

Table 2-1
Bounding Neutron Fluence for Energy >1.0 MeV for JAF Core Support Plate Rim Bolts at the Rim Bolt Surface

	EOC 20 (27.7 EFPY) Fluence (n/cm ²)	32 EFPY Fluence (n/cm ²)	54 EFPY Fluence (n/cm ²)
Bounding Bolt Location	1.25E+20	1.36E+20	1.93E+20

Table 2-2
Bounding Neutron Fluence for Energy >0.1 MeV for JAF Core Support Plate Rim Bolts Along the Rim Bolt Centerline Axis

Bolt Elevation	EOC 20 (27.7 EFPY) Fluence (n/cm ²)	32 EFPY Fluence (n/cm ²)	54 EFPY Fluence (n/cm ²)
Top of Bolt	1.78E+20	1.96E+20	2.88E+20
Bottom of Bolt	1.17E+17	1.29E+17	1.89E+17
Average	2.38E+19	2.61E+19	3.84E+19

3

DESCRIPTION OF THE REACTOR SYSTEM AND CALCULATION METHODOLOGY

This section describes the JAF fluence model used to determine the bounding CSP rim bolt fluence presented in this report. The fluence model is based on the RAMA fluence model used in a previous fluence evaluation performed in 2007 [5]. The current evaluation incorporates additional operating data covering the cycles that have transpired since the previous evaluation.

3.1 Reactor System Mechanical Design Inputs

The JAF reactor is modeled with the RAMA Fluence Methodology and is described in detail in the previous evaluation [5]. The CSP rim bolts were not explicitly included in the model. The fluence results were edited from the inlet water regions, core support plate, and shroud flange components that the bolt would pass through. Additionally, the effect of not explicitly modeling the bolt was included in the analytical uncertainty evaluation that was performed and is documented in Section 4.

The CSP rim bolts are positioned near the outer edge of the core support plate at regular intervals of 5 degrees, starting at 2.5 degrees. There are 72 bolts in entirety. The bolts extend from about 3.5 inches above the core support plate to about 2.25 inches below the lower shroud flange. This corresponds to upper and lower elevations of 203.10 inches (515.87 cm) and 177.40 inches (450.59 cm). The bolts are positioned at a radius of 85 inches (215.9 cm) from the center of the CSP and have a diameter of 1.125 inches (2.86 cm). Figure 3-1 illustrates the axial configuration of the bolt as well as the internal components it passes through.

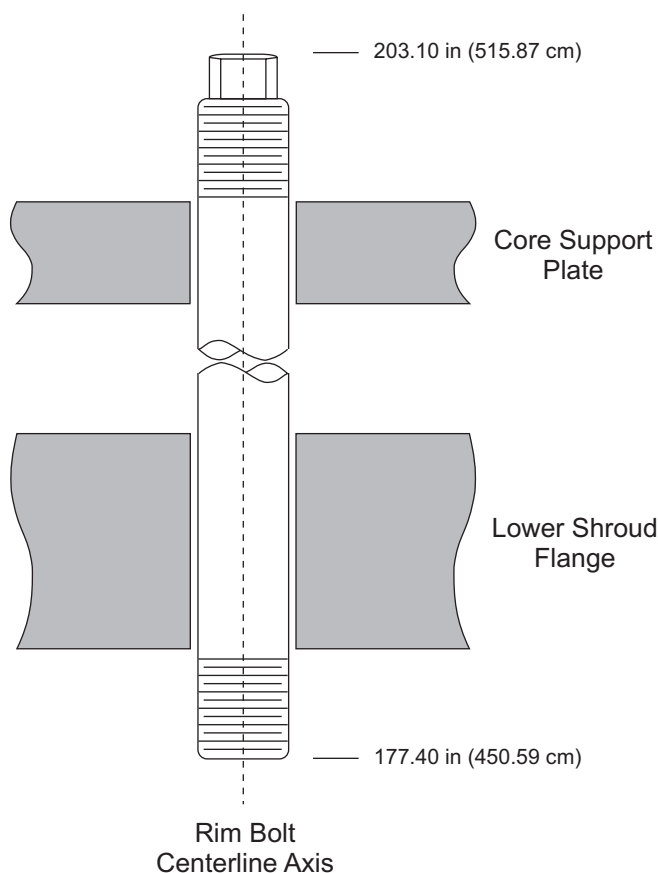


Figure 3-1
Axial View of JAF Core Support Plate Rim Bolt

3.2 Reactor Operating Data Inputs

An accurate evaluation of fluence in the reactor requires an accurate accounting of the reactor operating history. The primary reactor operating parameters that affect neutron fluence evaluations for BWR's include the reactor power level, core power distribution, core void fraction distribution (or equivalently, water density distribution), and fuel material distribution.

3.2.1 Power History Data

The reactor power history used in the JAF component fluence evaluation was based on daily power history information for operating cycles 1 through 17 [5], cycle energy productions for cycles 18 through 19, projected energy production for cycle 20, and a projected equilibrium cycle for cycle 21 and beyond [6]. The daily power values represent step changes in power on a daily basis and are assumed to be representative of the power over the entire day. The shutdowns were primarily due to the refueling outages between cycles. The power history data accounts for the reactor shutdown periods. The cycle energy productions for cycles 18 and higher were provided in terms of full power days. Table 3-1 provides the accumulated effective full power years of power generation at the end of each cycle in this fluence evaluation.

The rated thermal power output of JAF for operating cycles 1 through 12 is specified as 2436 MWt. A power uprate was achieved in cycle 13 raising the rated thermal power output to 2536 MWt. The power level 2536 MWt is used for projection purposes to the end of JAF's operating life.

3.2.2 Reactor State-Point Data

Reactor operating data for the JAF component fluence evaluation was provided as state-point data files for operating cycles 1 through 17 [5]. The state-point files provide a best-available representation of the operating conditions of the unit over the operating lifetime of the reactor. The data files include three-dimensional data arrays that describe the fuel materials, moderator materials, and the relative power distribution in the core region.

A separate neutron transport calculation was performed for each of the available state points. The calculated neutron flux for each state point was combined with the appropriate power history data described in Section 3.2.1 in order to predict the neutron fluence in the reactor internal components.

3.2.2.1 Beginning of Operation through Cycle 17 State Points

A total of 206 state-point data files were used to represent the 17 reported operating cycles of JAF. Table 3-1 shows the number of state points used for each cycle in this fluence evaluation.

**Table 3-1
Number of State-point Data Files for Each Cycle in JAF**

Cycle Number	Number of State Point Data Files	Rated Thermal Power MWt ²	Accumulated Effective Full Power Years (EFPY)
1	11	2436	1.3
2	7	2436	2.0
3	10	2436	2.8
4	10	2436	3.8
5	7	2436	4.9
6	10	2436	6.0
7	10	2436	7.4
8	13	2436	8.5
9	12	2436	9.7
10	10	2436	10.6
11	13	2436	12.0
12	15	2436	13.4
13	15	2536	15.1
14	15	2536	16.7
15	15	2536	18.6
16	17	2536	20.4
17	16	2536	22.2
18	See note 1	2536	24.0
19	See note 1	2536	25.9
20	See note 1	2536	27.7
21	See note 1	2536	29.5
>21	See note 1	2536	32.0/54.0

- 1) Complete operating data for cycles 18 and beyond was not available at the time of the analysis. Projected fluence was based on peripheral fuel bundle relative power densities, which were provided for cycles 18 through 21. The power densities for cycle 21 were used to project to 32 and 54 EFPY.
- 2) The rated thermal power level is provided for each cycle. Actual power levels were used in modeling the plant's operation during each cycle.

3.2.2.2 Projected Operation through End of Design Life State Points

For fluence predictions to EOC 20, 32 EFPY and 54 EFPY, the neutron flux in the CSP rim bolt regions was adjusted based on comparisons between the relative power densities for the peripheral fuel bundles nearest to the bolt, provided for cycles 18 through 21 [6], and the power densities obtained from the state points used to model cycles 16 and 17.

The reactor is licensed at a thermal power level of 2536 MWt for cycles beyond operating cycle 13. Therefore, fluence projections based on EFPY values use 2536 MWt as the basis for determining the amount of energy produced during one EFPY.

The projection of fluence to the end of the reactor licensed lifetime employs certain assumptions that can change. For example, if future reactor cycles deviate from the equilibrium cycle assumed in this analysis, then evaluations using the projected fluence may be inaccurate. Deviations from equilibrium cycle conditions can be incurred as the result of, for example, power uprates, new fuel designs, and revised heat balances. It is recommended that each future operating cycle be evaluated for potential impact on the projected fluence presented in this report and that the fluence analysis be updated accordingly.

3.2.3 Core Loading Pattern

It is common in BWRs that more than one fuel assembly design will be loaded in the reactor core in any given operating cycle. For fluence evaluations, it is important to account for the fuel assembly designs that are loaded in the core in order to accurately represent the neutron source distribution at the core boundaries (i.e., peripheral fuel locations, the top fuel nodes, and the bottom fuel nodes).

Six different fuel assembly designs are used in the reactor during cycles 1 through 17. Table 3-2 provides a summary of the fuel designs loaded in the reactor core for these operating cycles. The cycle core loading patterns are used to identify the fuel assembly designs in each cycle and their location in the core loading pattern. For each cycle, appropriate fuel assembly models are used to build the reactor core region of the JAF RAMA fluence model.

The additional cycles evaluated in this report continue to utilize a General Electric (“GE”) 10x10 fuel assembly design with cycle 21 representing a complete transition to the next generation GE 10x10 fuel assembly design (GNF2).

**Table 3-2
Summary of the JAF Core Loading Pattern**

Cycle	General Electric (GE) 7x7 Fuel Assembly Designs	General Electric (GE) 8x8 Fuel Assembly Designs	Westinghouse 8x8 Fuel Assembly Designs	General Electric (GE) 9x9 Fuel Assembly Designs	Framatome ANP 10x10 Fuel Assembly Designs	General Electric (GE) 10x10 Fuel Assembly Designs	Dominant Peripheral Fuel Design in the RAMA Model
1	560						GE 7x7
2	428	132					GE 7x7
3	292	268					GE 7x7
4	132	428					GE 7x7
5		560					GE 8x8
6		560					GE 8x8
7		560					GE 8x8
8		556	4				GE 8x8
9		556	4				GE 8x8
10		552	4	4			GE 8x8
11		404		156			GE 8x8
12		200		356	4		GE 8x8
13		12		352	4	192	GE 9x9
14				174	4	382	GE 9x9
15						560	GE 10x10
16						560	GE 10x10
17						560	GE 10x10
>17						560	GE 10x10

4

CORE SUPPORT PLATE RIM BOLT UNCERTAINTY ANALYSIS

This section presents the analytical uncertainty analysis and bias determination for the JAF core support plate rim bolt fluence evaluation. Since there are no activity measurements available for the rim bolts, the uncertainty is based solely on an analytic uncertainty factor developed in this section that represents the overall uncertainty (1σ) and bias in the CSP rim bolt fluence for this analysis. The method implemented for determining the uncertainty and bias for fluence is described in the RAMA Theory Manual [1].

The calculational models used for fluence analyses are comprised of numerous analytical parameters that have associated uncertainties in their values. The uncertainty in these parameters needs to be tested for its contribution to the overall fluence uncertainty.

The uncertainty values for the geometry parameters are based upon manufacturing tolerances in the dimensional data used to construct the plant geometry model. The uncertainty values for the material parameters are based upon uncertainties in the material densities for the water and nuclear fuel materials and the compositional makeup of typical steel materials.

The uncertainty values for the fission source parameters are based upon uncertainties in the fuel exposure and power factors for the fuel assemblies loaded on the core periphery. The transport method used in the fluence analysis employs a fission source calculation that accounts for the relative contributions of the uranium and plutonium fissile isotopes in the fuel and the relative power density of the fuel in the reactor. Both fission source parameters are derived directly from information calculated by three-dimensional core simulator codes. The uncertainty values for the nuclear cross-section parameters are based upon uncertainties in the number densities for the predominant nuclides that make up the reactor materials.

The uncertainty parameters for the fluence model inputs are based upon geometry meshing and numerical integration parameters used in the neutron flux transport calculation. The process for determining the geometry meshing and numerical integration parameters involves an exhaustive sensitivity study that is described in the RAMA Procedures Manual [7].

The results presented in this section and shown in Table 4-1 show that the uncertainty for the JAF core support plate rim bolt fluence evaluation is 27.0% for energy >1.0 MeV and 31.1% for energy >0.1 MeV. The bias values are determined to be -45.1% for energy >1.0 MeV and -51.7% for energy >0.1 MeV. The negative bias values indicate that the bounding fluence values reported in Section 5 would be adjusted down by the respective bias amount to determine the bias-adjusted fluence values. Thus, the as-calculated values are conservative and determined to be bounding.

Table 4-1
CSP Rim Bolt Fluence Uncertainty and Bias

Energy Range	Uncertainty (1σ)	Bias
>1.0 MeV	27.0%	-45.1%
>0.1 MeV	31.1%	-51.7%

5

CALCULATED NEUTRON FLUENCE FOR CORE SUPPORT PLATE RIM BOLTS

This section presents the bounding neutron fluence results for the JAF core support plate rim bolts. Two sets of fluence values are presented. The first is the bounding rim bolt fluence for the surface of the bolt closest to the reactor core and is determined for energy >1.0 MeV. The second is an axial fluence profile for the bounding bolt location through the centerline axis over the entire height of the bolt and is determined for energy >0.1 MeV. Bounding rim bolt fluence is calculated at three time periods: EOC 20, 32 EFPY and 54 EFPY.

The bounding rim bolt is determined to reside at the 42.5-degree location in the NNE octant fluence model and corresponds to the symmetric bolts located at 47.5, 132.5, 137.5, 222.5, 227.5, 312.5, and 317.5 degrees. The rim bolt has a height of about 25.7 inches, extending from approximately 177.40 inches to 203.10 inches relative to vessel zero. Figure 3-1 in Section 3 provides an illustration of the rim bolt relative to the components it intersects.

Table 5-1 summarizes the bounding fluence determined for the rim bolts for energy >1.0 MeV for the three time periods. The bounding fluence is determined to be 1.93E+20 n/cm² at 54 EFPY for energy >1.0 MeV. Table 5-2 summarizes the bounding axial fluence profiles determined for the rim bolts for energy >0.1 MeV for the three time periods.

It was shown in Section 4 that the as-calculated fluence values reported here are conservative and, therefore, represent the bounding values for the JAF core support plate rim bolts. No adjustments have been made to these values to account for the biases reported in Section 4.

Table 5-1
Bounding >1.0 MeV Neutron Fluence for JAF Core Support Plate Rim Bolts at the Rim Bolt Surface

	Fluence (n/cm ²) at EOC 20	Fluence (n/cm ²) at 32 EFPY	Fluence (n/cm ²) at 54 EFPY
Bounding Core Support Plate Rim Bolt	1.25E+20	1.36E+20	1.93E+20

Table 5-2
Bounding >0.1 MeV Neutron Fluence Axial Profile for JAF Core Support Plate Rim Bolts at Bolt Centerline Axis

Distance from the Top of Bolt (in)	Fluence (n/cm ²) at EOC 20	Fluence (n/cm ²) at 32 EFPY	Fluence (n/cm ²) at 54 EFPY
0.0	1.78E+20	1.96E+20	2.88E+20
0.4	1.58E+20	1.74E+20	2.56E+20
0.8	1.41E+20	1.55E+20	2.27E+20
1.2	1.25E+20	1.37E+20	2.01E+20
1.6	1.11E+20	1.22E+20	1.79E+20
2.0	9.82E+19	1.08E+20	1.59E+20
2.4	8.72E+19	9.59E+19	1.41E+20
2.8	7.74E+19	8.51E+19	1.25E+20
3.2	6.87E+19	7.55E+19	1.11E+20
3.6	6.42E+19	7.06E+19	1.04E+20
4.0	5.61E+19	6.17E+19	9.06E+19
4.3	4.90E+19	5.39E+19	7.92E+19
4.7	4.28E+19	4.71E+19	6.92E+19
5.1	3.74E+19	4.12E+19	6.05E+19
5.5	3.27E+19	3.60E+19	5.28E+19
5.9	2.64E+19	2.90E+19	4.25E+19
6.3	2.35E+19	2.58E+19	3.79E+19
6.7	2.09E+19	2.30E+19	3.37E+19
7.1	1.86E+19	2.05E+19	3.01E+19
7.5	1.66E+19	1.82E+19	2.68E+19
7.9	1.48E+19	1.62E+19	2.38E+19
8.3	1.31E+19	1.45E+19	2.12E+19
8.7	1.17E+19	1.29E+19	1.89E+19
9.1	1.04E+19	1.15E+19	1.68E+19
9.5	9.29E+18	1.02E+19	1.50E+19
9.9	8.27E+18	9.10E+18	1.34E+19

Table 5-2
Bounding >0.1 MeV Neutron Fluence Axial Profile for JAF Core Support Plate Rim Bolts at Bolt Centerline Axis (continued)

Distance from the Top of Bolt (in)	Fluence (n/cm ²) at EOC 20	Fluence (n/cm ²) at 32 EFPY	Fluence (n/cm ²) at 54 EFPY
10.3	7.37E+18	8.10E+18	1.19E+19
10.7	6.56E+18	7.22E+18	1.06E+19
11.1	5.84E+18	6.43E+18	9.43E+18
11.5	5.20E+18	5.72E+18	8.40E+18
11.9	4.63E+18	5.10E+18	7.48E+18
12.3	4.13E+18	4.54E+18	6.66E+18
12.7	3.68E+18	4.04E+18	5.93E+18
13.0	3.27E+18	3.60E+18	5.28E+18
13.4	2.91E+18	3.21E+18	4.71E+18
13.8	2.60E+18	2.86E+18	4.19E+18
14.2	2.31E+18	2.54E+18	3.73E+18
14.6	2.06E+18	2.26E+18	3.32E+18
15.0	1.83E+18	2.02E+18	2.96E+18
15.4	1.63E+18	1.80E+18	2.64E+18
15.8	1.45E+18	1.60E+18	2.35E+18
16.2	1.30E+18	1.42E+18	2.09E+18
16.6	1.15E+18	1.27E+18	1.86E+18
17.0	1.03E+18	1.13E+18	1.66E+18
17.4	9.15E+17	1.01E+18	1.48E+18
17.8	8.15E+17	8.96E+17	1.32E+18
18.2	7.26E+17	7.98E+17	1.17E+18
18.6	6.46E+17	7.11E+17	1.04E+18
19.0	5.75E+17	6.33E+17	9.29E+17
19.4	5.13E+17	5.64E+17	8.27E+17
19.8	7.18E+17	7.90E+17	1.16E+18
20.2	6.36E+17	7.00E+17	1.03E+18

Table 5-2
Bounding >0.1 MeV Neutron Fluence Axial Profile for JAF Core Support Plate Rim Bolts at Bolt Centerline Axis (continued)

Distance from the Top of Bolt (in)	Fluence (n/cm ²) at EOC 20	Fluence (n/cm ²) at 32 EFPY	Fluence (n/cm ²) at 54 EFPY
20.6	5.64E+17	6.20E+17	9.10E+17
21.0	5.00E+17	5.50E+17	8.07E+17
21.4	4.43E+17	4.87E+17	7.15E+17
21.7	3.93E+17	4.32E+17	6.34E+17
22.1	3.48E+17	3.83E+17	5.62E+17
22.5	3.08E+17	3.39E+17	4.98E+17
22.9	2.73E+17	3.01E+17	4.41E+17
23.3	2.42E+17	2.66E+17	3.91E+17
23.7	2.15E+17	2.36E+17	3.47E+17
24.1	1.90E+17	2.09E+17	3.07E+17
24.5	1.69E+17	1.85E+17	2.72E+17
24.9	1.49E+17	1.64E+17	2.41E+17
25.3	1.32E+17	1.46E+17	2.14E+17
25.7	1.17E+17	1.29E+17	1.89E+17
Average	2.38E+19	2.61E+19	3.84E+19

6

REFERENCES

1. *BWRVIP-114: BWR Vessel Internals Project, RAMA Fluence Methodology Theory Manual*, EPRI, Palo Alto, CA: 2003. 1003660.
2. Letter from William H. Bateman (U. S. NRC) to Bill Eaton (BWRVIP), “Safety Evaluation of Proprietary EPRI Reports BWRVIP-114, -115, -117, and -121 and TWE-PSE-001-R-001,” dated May 13, 2005.
3. *Calculational and Dosimetry Methods for Determining Pressure Vessel Neutron Fluence*, Nuclear Regulatory Commission Regulatory Guide 1.190, March 2001.
4. *BWRVIP-145: BWR Vessel and Internals Project, Evaluation of Susquehanna Unit 2 Top Guide and Core Shroud Material Samples Using RAMA Fluence Methodology*, EPRI, Palo Alto, CA: 2005. 1011694.
5. “James A. FitzPatrick Core Shroud, Top Guide and Core Support Plate Fluence Evaluation at End of Cycle 17 and 54 EFPY,” TransWare Enterprises Inc., ENT-FLU-002-R-002, Rev. 0, November 2007.
6. Email from Kornelia Szwarc (Entergy) to Dean Jones (TransWare), “RE: JAF - Fluence Levels at Core Plate Bolts,” dated March 28, 2012 at 7:43:16 UTC.
7. *BWRVIP-121: BWR Vessel Internals Project, RAMA Fluence Methodology Procedures Manual*, EPRI, Palo Alto, CA: 2003. 100806.